"FUNCTIONAL ANALYSIS OF PROLYL HYDROXYLASE X IN DRUG RESISTANCE"

By Meenal Moudgil

A Thesis Submitted to

The Faculty of Graduate Studies

In Partial Fulfillment of the Requirements for the Degree of

MASTER OF SCIENCE

Department of Biochemistry and Medical Genetics

University of Manitoba

Winnipeg, Manitoba, Canada

February, 2012

TABLE OF CONTENTS

ACKNOWLEDGEMENTS

This thesis culminates my second innings as a student. While this innings has been extremely enjoyable, educational and enlightening, it surely was demanding as well. This thesis is the result of untiring efforts of many people who I must recognize and acknowledge here.

The contribution and cooperation of my family has been enormous thoughout my life especially during my studies. My father's inspiration has been my inner strength for my transition from a school teacher to a research student and my mother has always been the guiding star for me to pursue higher studies. My husband Sanjay's unwavering support and encouragement helped me to smoothly walk through my journey as a graduate student. My mother and father-in-law's enormous love and encouragements enabled me to resume my graduate studies after the birth of my second daughter and helped me to balance my responsibilities and commitments as a mother and a graduate student. My sister and brother-in-law's moral support and valuable suggestions gave me strength throughout my studies. My lovely nieces', nephew's, and two daughters' - Shradha, Garima, Aaditya, Nishthha and Srishta - love and cooperation during my studies have been immaculate and un-matching.

I am thankful to all the past and present members of Dr. Mowat's lab especially Shannon, Caroline, Ray, Rachelle, Yuan, Shauna, Heather, Wan, Kofi, Cordula and Sabbir, who had made the lab a very friendly place to work and for their guidance, assistance and suggestions; Arju, Cecile, Don, Ellice, Jan, Ludger, Mary, Molly, Nikki and Vineeta for always lending their help with a friendly smile; Dr. Luke for his technical guidance that

helped me tremendously to learn about retroviral work and Zoanne Nugent for her suggestions regarding the statistical analysis of my data.

My special thanks to Sabbir for his constructive suggestions, technical guidance and constant support; Soma and Sanat's for their contributions as great friends who helped me throughout my studies and encouraged me to develop a positive attitude; Ms. Tuntun Sarkar for her moral support and advice throughout my studies; and Dr. Etienne Leygue for his valuable suggestions to improve the presentations for the departmental seminars.

My sincere thanks to my advisory committee members - Dr. G. Hicks, Dr. R.D. Gietz, and Dr. J. Dodd; for their positive and valuable feedback, suggestions and directions that helped me develop outstanding analytical and research skills.

I thank the Canadian Institute of Health and Research for providing me with funding and Manitoba Institute of Cell Biology for providing me the wonderful research facilities and a platform to pursue my research.

I deeply thank and acknowledge my supervisor Dr. M. Mowat for being such a wonderful mentor. His technical guidance has helped me to proceed with my project and to perform sequential and thoughtful experiments. I acknowledge him for giving me the flexibility and freedom to time and design experiments and to guide me through the work to proceed logically.

Finally, I offer my earnest gratitude to the great Master Parmahansa Yogananda Ji for his blessings and divine teachings that always helped me to overcome challenges during my studies.

ABSTRACT

A novel gene, named as the *PHDX* gene, had been previously identified while screening genes for their involvement in resistance to the chemotherapeutic drug etoposide and to hydrogen peroxide, using the methodology of retrovirus promoter trap mutagenesis. This study was undertaken for the purpose of testing whether the loss of *PHDX* gene is responsible for drug resistance in CHO-E-126 cell line which was created from Chinese hamster ovary cells having a retroviral receptor and selected for etoposide resistance. The *PHDX* gene resides on mouse chromosome 11 and has homology with the prolyl hydroxylase gene family. We hypothesized that the inactivation of the *PHDX* gene by promoter trap mutagenesis will confer resistance to etoposide and hydrogen peroxide in the E-126 cell line. In addition, the alteration of the cellular hydroxyproline levels by the loss of the gene might influence the drug response through the production of oxygen free radicals. To study the involvement of the *PHDX* gene in etoposide and hydrogen peroxide induced drug-resistance, we used two experimental approaches to modulate the function of the gene in cells. First, we silenced the expression of this gene by RNA interference (RNAi) through stable and transient knockdown experiments in the parental Chinese hamster ovary (CHO-K1) cells, and second, we overexpressed the gene in CHO-Cl-22 and CHO-E-126 cells. We assessed the effect of the knockdown by RT-PCR. The effect of etoposide and hydrogen peroxide was determined by the clonogenic crystal violet staining assay and the MTT assay. Through our siRNAi knockdown studies, we were able to demonstrate the involvement of the gene in drug resistance. We were unable to show that the overexpression of the gene was capable of reverting to the drug sensitive phenotype.

LIST OF TABLES

LIST OF FIGURES

LIST OF ABBREVIATIONS

ADP	Adenosine diphosphate
AEBSF	[4-(2-aminoethyl) benzenesulfonyl fluoride]
AT	ataxia telangiectasia
ATP	Adenosine triphosphate
α-MEM	alpha minimum essential medium
Apaf-F	apoptotic protease factor- 1
ATCC	American type culture collection
BH	B cell lymphoma-2 Homolgy
β-ME	Beta mercaptoethanol
cDNA	complementary deoxyribo nucleic acid
CHO	chinese hamster ovary
CO_2	carbon dioxide
Cyt C	Cytochrome C
CVS	crystal violet staining
dd H_2O	deionized distilled water
DMEM	Dulbecco's modified eagle's medium
DMSO	dimethyl sulphoxide
DNA	deoxyribo nucleic acid
DS	double stranded
DSB	double stranded breaks
DTT	dithiothreitol
EDTA	ethylenediamine tetra acetic acid
EGF	epidermal growth factor
EGLN	egg laying defective nine
ER	endoplasmic reticulum
ES	embryonic stem
FBS	fetal bovine serum
Fe^{+2}	iron
GAPDH	glyceraldehyde phosphate
gDNA	genomic deoxyribo nucleic acid
GSP	gene specific primer
HGPRT	hypoxanthine guanine phosphoribosyl transferase
HIF	hypoxia inducible factor

HRE	hypoxia response element
HSP	heat shock protein
H_2O	water
H_2O_2	hydrogen peroxide
IC_{50}	inhibitory concentration of 50 %
IAP	inhibitor of apoptosis
JNK	c-Jun N-terminal kinase - 1
K1PHDX	Chinese hamster prolyl hydroxylase X
KOAC	potassium acetate
LTR	long terminal repeat
miRNA	micro ribonucleic acid
miRNP	micro ribonucleic acid protein
MMR	mismatch repair
mRNA	messanger ribonucleic acid
MOMP	mitochondrial outer membrane permeabilization
mPHDX	mouse prolyl hydroxylase X
MPT	mitochondrial permeable pore
MTT	methyl thiazol tetrazolium
NADPH	nicotinamide adenine dinucleotide phosphate
NPT	neophosphotransferase
nt	nucleotide
OD	optical density
O_2	oxygen
PARP	poly ADP ribose polymerase
PBS	phosphate bufered saline
PCR	polymerase chain reaction
PDGF	platelet derived growth factor
PHD	prolyl hydroxylase domain
PK	protein kinase
PML	promyelocytic leukemia
PMSF	phenyl methyane sulfonyl fluoride
Poly A	poly adenine
PS	phosphatidyl serine
PSTs	promoter-proximal sequence tags
PTGS	post-transcriptional gene silencing
PUMA	P53 upregulated modulator of apoptosis
PVDF	poly vinylidene fluoride
RACE	rapid amplification of cDNA ends

RB	retinoblastoma
RIPA	radio immuno precipitation assay
RISC	RNA induced silencing complex
RNA	ribonucleic acid
ROS	reactive oxygen species
RT-PCR	reverse transcription - polymerase chain reaction
SA	splice acceptor
SDS	sodium dodecyl sulphate
siRNAi	small interfering RNA interference
shRNAi	short hairpin RNA interference
tBid	truncated bid
TBS	tris-buffered saline
TBST	tris-buffered saline tween
TM	transmembrane
TNF	tumour necrosis factor
TOPO - II	topoisomerase-II
TRAIL	TNF-related apoptosis inducing ligand
UTR	untranslated region
UV	ultra violet

CHAPTER 1 - LITERATURE REVIEW AND BACKGROUND INFORMATION

1.1 Introduction

In previous studies from our laboratory, a prolyl hydroxylase gene was identified through insertional mutagenesis of the Chinese hamster ovary cell line, with a retroviral receptor gene (CHO-K1-Cl-22). A number of cell lines were created by infecting CHO-K1-Cl-22 cells with the U3NeoSV1 promoter trap retrovirus with the goal to identify genes involved in programmed cell-death. Various clones were selected for etoposide resistance.One of the etoposide resistant clones named CHO-E-126 showed cross resistance to hydrogen peroxide and had integration of the retrovirus into a novel prolyl hydroxylase gene named as *1110031I02Rik* in the mouse. We named this prolyl hydroxylase gene as *PHDX*. The mouse homolog maps chromosome 11.

In this thesis, I will discuss the functional analysis of the *PHDX* gene and test its possible role in drug resistance. The experimental strategies I took to test its role in drug resistance include knock down of the *PHDX* gene using small interfering RNA interference (siRNAi) technology. In addition, experiments were carried out to introduce the normal *PHDX* gene into CHO-E-126 and CHO-Cl-22 cells to observe the effects of this gene's response to etoposide and hydrogen peroxide.

1.2 Prolyl Hydroxylases

Prolyl hydroxylases are responsible for post-translational hydroxylation of proline leading to various inter and intracellular signalling cascades (Myllyharju, 2003). Prolyl

hydroxylases are involved in the post-translational alteration of proline to form hydroxyproline. Collagen prolyl 4-hydroxylases are found in the lumen of endoplasmic reticulum (ER) and are involved in the hydroxylation of proline in collagen and the other proteins having collagen like domains responsible for the biosynthesis of collagen (Kivirikko and Myllyharju, 1998; Kivirikko and Pihlajaniemi, 1998; Myllyharju and Kivirikko, 2001). The vertebrate collagen prolyl hydroxylase has two isoenzymes called Type I and Type II (Annunen *et al.*, 1997; Helaakoski *et al.*, 1995). Type I is the chief form present in most cell-types and tissues but Type II amounts to 30 % of the total P4H activity (Myllyharju, 2003). Besides hydroxylation of proline, these enzymes act as molecular chaperons during collagen synthesis. Also, they have a pivotal role in extra cellular matrix formation and normal metazoan development (Winter and Page, 2000).

Of late, other prolyl hydroxylases have been found in the cytoplasm, and have been shown to regulate the transcription of hypoxia inducible factor (HIF)-1α (Bruick and McKnight, 2001; Epstein *et al.*, 2001). Three different mammalian genes related to the family of HIF prolyl hydroxylases, called Egl-nine (EGLN) have been described, which share highly conserved domains. These include EGL-9 (protein responsible for normal egg-laying in *C. elegans*), the three human orthologues - EGLN1(a.k.a. prolyl hydroxylase domain (PHD2) or HIF prolyl hydroxylase (HPH2)), EGLN2 (a.k.a. PHD1 or HPH3), EGLN3 (a.k.a. PHD3 or HPH1) (Freeman *et al.*, 2003)).

SM-20 is a protein found in rat and its overexpression is responsible for cell death in sympathetic neurons deprived of nerve growth factor (Straub *et al.*, 2003). *SM-20* and *EGLN3* genes have a high degree of (98-100 %) sequence similarity (Freeman *et al.*, 2003).

In over-expression studies, it has been demonstrated that EGLN3 levels affect the stability of HIF-1α protein under both normoxic and hypoxic conditions indicating that PHD3 may contribute in a feedback loop controlling HIF-1α activity (Cioffi *et al.*, 2003). Also, it has been recently observed in mice that inhibition of prolyl hydroxylase, via inducible nitric oxide synthase, results in the improvement of postischemic renal injury due to stabilization of HIF (Zhang *et al.*, 2011). The overexpression of SM-20 (causing cell death in nerve cells) and inhibition of prolyl hydroxylase (causing improvement in ischemic renal tissue) suggest both anti and pro apoptotic function of prolyl hydroxylases.

In normoxia, prolyl hydroxylase proteins catalyze the production of hydroxyproline from proline by using oxygen and 2-oxoglutarate as co-substrates along with Fe^{2+} and ascorbate. The other by product of the reaction is succinate (Berra *et al.*, 2006). Prolyl hydroxylation creates a binding site for a ubiquitin ligase complex containing the von Hippel-Lindau (VHL) tumor suppressor protein (Kaelin, 2005) which leads to rapid degradation of hypoxia inducible factor (HIF-1α) (Berra *et al.*, 2003). During hypoxia HIF-1α complex is stabilized in the nucleus and dimerizes with HIF-1β subunit, leading to the transcription of its target genes (Bruick and McKnight, 2001; Ivan *et al.*, 2001; Jaakkola *et al.*, 2001). HIF regulates the expression of more than a hundred genes (Zhang *et al.*, 2011) including the transcription of genes which lead to various tumorigenic processes like angiogenesis, erythropoisis, vasodilation and glycolysis (Berra *et al.*, 2006) (**Figure 1**).

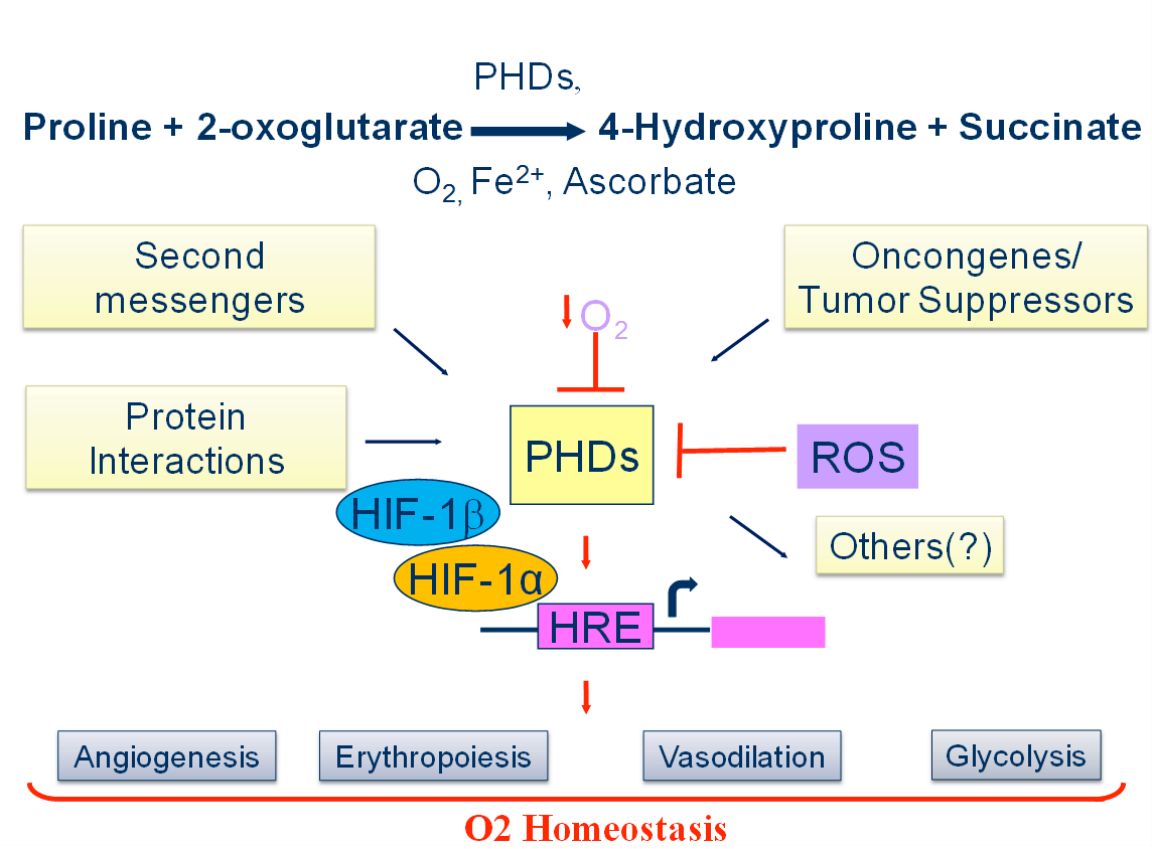

Figure 1: Interactions of Prolyl-hydroxylase domain (PHD)

Diagrammatic representation of prolyl-hydroxylase domain's role related to various interactions upon different types of stimuli through changes in HIF-1α stability.

Modified from Macmillan Publishers Ltd:[EMBO] (Berra *et al.*, 2006)

1.3 Prolyl Hydroxylases and Reactive Oxygen Species (ROS)

The oxidation of hydroxyproline by hydroxyproline oxidase is documented to participate in response to cytotoxic stress through the activation of the p53 pathway leading to apoptosis (Cooper *et al.*, 2008). Hydroxyproline-induced production of ROS was observed in LoVo and RKO cells after treatemnt with adriamycin (Cooper *et al.*, 2008). Since both adriamycin and etoposide are toposisomerase inhibitors and their mechanism of action is similar (Theard *et al.*, 2001), it is possible that treatment with etoposide might also lead to ROS production through hydroxyproline. Also, treatment with both etoposide and hydrogen peroxide has been reported to increase the intracellular peroxide levels rapidly and hence the generation of reactive oxygen species (ROS) (Gorman *et al.*, 1997).

Of importance is that prolyl hydroxylases are inhibited by reactive oxygen species (ROS) (Berra *et al.*, 2006). Therefore as a result of excessive ROS production, increased hydroxyproline levels need to be checked through inhibition of prolyl hydroxylases by creating a negative feedback loop mechanism in the cells. However ROS has been implicated as a second messenger in multiple signalling pathways (Apel and Hirt, 2004) leading to programmed cell death by damaging DNA, lipids and mitochondria in a p53 dependent manner (Sordet *et al.*, 2003). Therefore, ROS can also play an important role in apoptosis by regulating the activity of certain enzymes involved in the cell death pathways (Garcia-Ruiz *et al.*, 1997; Kruman *et al.*, 1997).

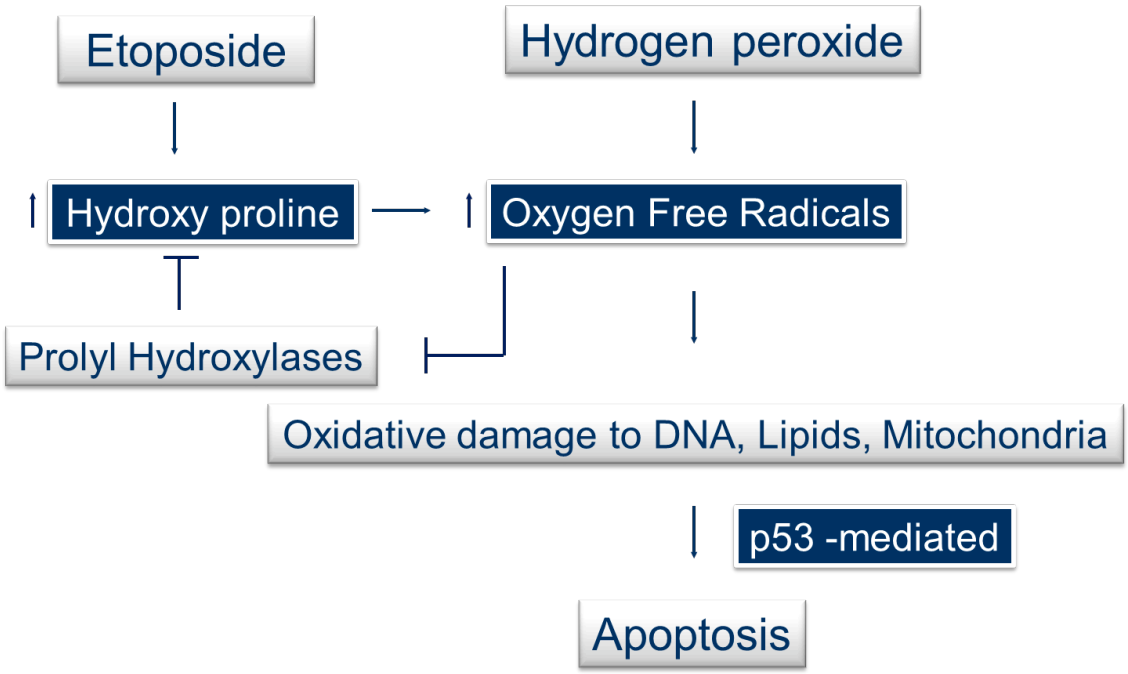

Figure 2: Model to depict negative feed back loop mechanism through inhibition of Prolyl Hydroxylases by ROS generated through Etoposide and Hydrogen Peroxide.

(Berra *et al.*, 2006; Cooper *et al.*, 2008; Foyer and Noctor, 2005; Gorman *et al.*, 1997; Sablina *et al.*, 2005; Theard *et al.*, 2001)

1.4 Mutagenesis and Gene Trapping

CHO-E-126 cells were created through retroviral mutagenesis. Mutagenesis is a technique used to alter the genomic sequence of a gene in such a way that it changes the genetic message carried by that gene (Zuryn *et al.*, 2010). The genomic sequences can be changed randomly or specifically. Initially mutagenesis strategies were induced through either chemicals or radiation e.g. X-Rays, UV rays. The prime limitation of this approach was that it was hard to study the function of a particular gene since this strategy lacked the required specificity to target a particular gene. The frequency of these mutations is relatively high when compared to other strategies but this affects more than one gene and thus functional analysis is difficult (Stanford *et al.*, 2001). With the advancement of various molecular biology techniques, it was possible to generate mutations through both random and site-directed mutagenesis (Keon *et al.*, 2003; Stanford *et al.*, 2001).

Gene targeting and gene trapping are such molecular tools exploited to study the function of a gene. Gene targeting is a mutagenesis technique which utilizes homologous recombination to specifically target a gene after the DNA is introduced into ES cells (Abuin *et al.*, 2007). Gene trapping is a random mutagenesis approach which leads to transcriptional disruption of the endogenous gene function as a result of an insertion of foreign DNA (Wilson *et al.*, 1989). Gene trapping leads to random mutagenesis but gene targeting enables the knockout of specific genes (Guan *et al.*, 2010). Gene targeting is quite robust and was established to produce knockout mice using homologous recombination in embryonic stem (ES) cells to make transgenic mice and is quite laborious and time-consuming. In order to

randomly disrupt gene function in mice, an alternative strategy gene trapping is used (Araki *et al.*, 2009).

Gene-trap mutagenesis leads to random generation of loss-of-function mutations. A gene-trap vector encompasses a splice acceptor site immediately upstream of a promoterless reporter (Gossler *et al.*, 1989). When an endogenous *cis*-acting promoter and enhancer elements of the trapped gene become transcriptionally active, a fusion transcript of the reporter and trapped gene is created resulting in mutation of the trapped gene (Stanford *et al.*, 2001; Wilson *et al.*, 1989). The efficiency of gene traps per vector as compared to promoter trap vectors increases at least 50-fold because the relative size of introns is more than the size of exons (Stanford *et al.*, 2001; Zuryn *et al.*, 2010). The chief pitfall of using gene trap vectors is that since the insertion is intronic, alternative splicing can sometimes occur. This can result in low levels of wild type transcripts resulting in hypomorphic expression (McClive *et al.*, 1998). However the main benefit of gene trap mutagenesis is that a particular gene trapping vector can be utilized to mutate thousands of genes in ES cells (Wiles *et al.*, 2000; Zambrowicz *et al.*, 1998). Gene trapping vectors usually lack important transcriptional elements for instance enhancers (O'Kane and Gehring, 1987), promoters (Hicks *et al.*, 1997) or polyadenylation (poly(A)) sites (Niwa *et al.*, 1993), making them transcriptionally active only when inserted into an endogenous gene near the promoter (Abuin *et al.*, 2007).

Enhancer trap vectors generally comprise a basal promoter with a minimal activity immediately upstream of the reporter gene. Insertion of the enhancer trap vector close to the enhancer of trapped gene leads to the transcriptional activation of the reporter gene when the

trapped gene gets activated (Jao *et al.*, 2008). The major drawback with the enhancer trapping is that enhancers can act over large distances and this makes the isolation of a particular gene quite challenging. As a result, the basic goal to achieve loss of function mutations gets immensely affected. Promoter trap vectors are intended for the expression of reporter gene along with that of the trapped gene (Friedrich and Soriano, 1991; Gossler *et al.*, 1989). These vectors overcome the distance problem as associated with the enhancer trap constructs but at the same time unlike enhancer trap vectors, they have at least 200 fold lesser capacity to show reporter gene activity (Friedrich and Soriano, 1991; Stanford *et al.*, 2001). Gene Trap or poly (A) trap vectors have a reporter gene with a splice acceptor (SA) site at the 5' end and poly (A) signal at 3' end. These vectors exploit the promoter of target gene after integrating within the intron of that gene leading to the formation of a fusion transcript containing 5' sequence of the gene with the reporter gene (Gossler *et al.*, 1989).

Besides containing a reporter gene, these vectors also contain a selectable marker (Hubbard *et al.*, 1994), leading to the identification of the clones with viral integration (Stanford *et al.*, 2001). The fusion transcripts can be identified through rapid amplification of cDNA ends (RACE) (Frohman *et al.*, 1988) and the information regarding the exact location of insertion can be obtained by inverse genomic PCR (Silver and Keerikatte, 1989).

A new generation of retroviral vectors exploits the use of conditional control of gene expression. The temporal and spatial control of gene expression is achieved by either transcriptional transactivation or DNA recombination through tetracycline-controlled transactivator or regulatory system. (Lewandoski, 2001). To introduce site-specific DNA recombination to manipulate gene expression, Cre and Flp recombinase sytems are used (Jao

et al., 2008). Cre and Flp, the site specific recombinases, bind to and recombine specific sequences of DNA known as loxP or Frt sites, respectively (Hutcheson and Kardon, 2009) Cre/loxP or Flp/FRT systema facilitate the insetion and/or excision of sequences flanked by loxP sites into the host genome thereby acting as an efficient vehicle to insert or delete genes (Hutcheson and Kardon, 2009; Maury *et al.*, 2011).

1.5 U3NeoSV1 Promoter Trap

The U3NeoSV1 promoter trap retrovirus was used previously in the laboratory for mutagenesis studies in Chinese hamster ovary cells. The construct was originally generated to disrupt gene function in mouse ES cells and a library was created for large scale functional studies (Hicks *et al.*, 1997). The promoter trap was designed in such a way that it contained a promoterless neomycin resistant gene in the U3 region of the long terminal repeat and utilized the promoter of the gene therefore resulting in the neomycin resistance when the targeting vector inserted into the gene by disrupting its cellular expression (Chang *et al.*, 1993; Withers-Ward *et al.*, 1994).

The vector has a pBR322 plasmid origin of replication, an ampicillin resistance gene, BamH1 and EcoR1 restriction sites which enables the isolation and cloning of provirus and flanking viral sequences directly in *Escherichia coli* (Hicks *et al.*, 1995). In addition, it contains *lac* operator *(lac* O) sequence which allows partial purification of the flanking sequence fragments by binding to the *lac* repressor protein (Gossen *et al.*, 1993; Pathak and Temin, 1990). The presence of cryptic 3' splice site 28 nucleotides downstream of neophosphotransferase (NPT) gene facilitates trapping when the vector integrates into intronic regions resulting in aminoglycoside analogue G418 resistance thereby disrupting the

targeted gene (Hicks *et al.*, 1997). The intronic insertion might result in a hypomorphic expression (Roshon *et al.*, 2003) because of the disruption of endogenous gene function. Most of the time, gene entrapment vectors would disrupt the gene in such a way that it could splice in-frame with NPT coding sequence, and polyadenylation and 3' end formation arise predominantly in the 5' long terminal repeat (LTR) of the U3 gene trap vector (Osipovich *et al.*, 2004). The region next to provirus is sequenced by using Neo specific primer which creates a tag for the mutated gene and is unique for each and every disrupted gene. These sequence specific tags are designated as 'promoter-proximal sequence tags' or PSTs and allow the identification of the disrupted gene (Hicks *et al.*, 1997).

1.6 Mechanics of Apoptosis

Apoptosis is derived from a Greek word which means "falling leaves" - contextually referring to "de-adhesiveness" of the apoptotic cells from its vicinity after death. It was first coined by Kerr, Wyllie and Currie (Mevorach, 2003). Apoptosis has an essential place in development and maintenance of homeostasis. It is a highly conserved process from nematodes to humans (Hengartner and Horvitz, 1994a). Apoptosis was found in the developmental studies of the hermaphrodite flatwarm *C. elegans*. Henngartner and Horvits found that out of 1090 cells generated, 131 underwent programmed cell death which made it an excellent model to study apoptosis (Hengartner and Horvitz, 1994b).

Apoptosis, also known as programmed cell death is a dynamic and physiological process of cell death. The cell itself triggers a cascade of events by implementing its own demise following its own body disposal (Oltvai and Korsmeyer, 1994)The onset of apoptosis

is marked by a trigger, which could be endogenous regulatory proteins and hormones, xenobiotic chemicals, oxidative stress, anoxia or radiation (Corcoran *et al.*, 1994).

Apoptosis is an ATP dependent and genetically regulated process involved in discrete changes in nuclear, mitochondrial and cytoplasmic membranes (Kam and Ferch, 2000). It starts with the detachment of a cell from its extracellular matrix and adjacent cells through the loss of microvilli and desmosomes (Wyllie, 1997) leading to chromatin condensation, cell shrinkage followed by nuclear fragmentation and formation of membrane bound apoptotic bodies (Stewart, 1994) which are engulfed by phagocytes in the neighborhood thereby leaving no trace of the apoptotic cells (Kam and Ferch, 2000).

Apoptosis is controlled by two specific but converging pathways the extrinsic, controlled by death receptors and the intrinsic, which is controlled through mitochondrial mediated pathways (Ekoff and Nilsson, 2011). These independent pathways still involve certain crosstalk (Strasser *et al.*, 1995). In the extrinsic pathway, upon the binding of death receptors such as Fas/CD95R or TRAIL (TNF receptor family) by their ligands lead to the activation of initiator caspases 8 or 10, which further activate the effector caspases 3 or 7 or by cleavage of Bid into truncated bid (tBid). The translocation of tBid to mitochondria causes a loss of mitochondrial membrane potential and release of cytochrome C and activation of effector caspases, thereby activating the mitochondrial intrinsic pathway (crosstalk). The intrinsic pathway responds to the stress factors which originate inside the cell such as DNA damage or growth factor withdrawal (Cory and Adams, 2002; Green and Reed, 1998).

The key players of both extrinsic and intrinsic pathways are caspases and their activities are controlled by the Inhibitor of Apoptosis (IAP) family proteins. The IAPs regulate and impede the proteolytic cleavage activities of caspases (Salvesen and Duckett, 2002). The IAPs are further regulated by mitochondrial proteins, Smac/DIABLO, released during apoptosis (Shiozaki and Shi, 2004).

The Bcl-2 family of proteins plays a pivotal role in the mitochondrial apoptotic pathway. The balance of pro and anti-apoptotic Bcl-2 family members determines the outcome of the pathway leading to mitochondrial outer membrane permeabilisation (MOMP) and ultimately forming the apoptosome consisting of cytochorme c, apoptotic protease factor 1 (Apaf-1) and adenosine triphosphate (ATP). These apoptosomes activate the initiator caspase 9 which further induce the effector caspases 3 or 7 resulting in to apoptosis (Adams and Cory, 2001). The balance between cell-survival and cell-death is maintained by Bcl-2 family members of proteins which are both pro and anti-apoptotic in nature. These members have at least one or up to maximum of four Bcl-2 homolgy (BH) domains (Ekoff and Nilsson, 2011). Bcl-2, Bcl-XL, Bcl-w, A1/Bfl-1 and Mcl-1 are the anti-apoptotic members which contain up to four BH domains (BH1-4) and a transmembrane (TM) domain. The pro-apoptotic members are categorized into two sub-categories *viz.* BH3 only domain proteins and the protiens containing BH1, BH2, BH3 and a transmembrane domain. Bcl-XS, Bad, Bid, Bim, Bmf, Puma (p53 upregulated modulator of apoptosis) and Noxa belong to the former sub-category while Bax, Bak and Bok belong to the latter sub-category of pro-apoptotic proteins (Adams and Cory, 2001; Huang and Strasser, 2000). Balance between different members and the interaction among different categories of Bcl-2 proteins

determines the decision of the cell to survive or undergo apoptosis (Ekoff and Nilsson, 2011).

Besides proto-oncogene *Bcl-2*, the tumor suppressor *p53* is another very important gene related to the regulation of apoptosis. Sometimes when apoptosis is repressed by *Bcl-2*, it is induced by *p53* (Kam and Ferch, 2000). Overexpression of *p53* is reported to activate apoptosis (Yonish-Rouach *et al.*, 1991). Disruption of *p53* (-/-) in the mice, made the mice thymocytes resistant to etoposide and radiation, which otherwise showed normal apoptosis when treated with glucocorticoids (Clarke *et al.*, 1993). It has been reported that *p53* induces Bcl-2 homology region three (BH3) containing gene *puma* (Jeffers *et al.*, 2003). *Puma* can trigger mitochondria dependent apoptosis through interaction with Bax protein. The p53 protein is implicated in cell-death induced by cytotoxic drugs in response to DNA damage. Cell-lines having mutations in *p53* expression were found to show resistance when exposed to cytotoxic drugs (Harris and Hollstein, 1993). Therefore loss of *p53* function is related to the failure of the cells to apoptose and thus there is emergence of drug resistant cancer cells (Horvitz *et al.*, 1994). Apoptosis may also be induced independently of *p53* (Stewart, 1994). It has been revealed that *bcl-2* represses apoptosis induction by adenovirus E1A (dependent on functional *p53*) proposing a downstream effect of *bcl-2* on *p53* dependent cell death (Chiou *et al.*, 1994). Therefore *bcl-2* and *p53* may respectively be considered as negative and positive regulators of cell death. Last but not the least is *c-myc* oncogene which is responsible for cell proliferation (Evan and Littlewood, 1993). c-Myc upon dimerization with another protein called Max is reported to act as a potent inducer of apoptosis (Amati *et al.*, 1993).

1.7 Etoposide - the topoisomerase poison - and Apoptosis

In an attempt to identify genes that may alter the apoptotic response, the cell-lines resistant to a very potent antineoplastic drug etoposide ($C_{29}H_{32}O_{13}$) a.k.a. VP-16 **(Figure 3)** were created. This chemotherapeutic drug is a topoisomerase poison that induces apoptosis by damaging the DNA (Mizumoto *et al.*, 1994). Unlike other cytotoxic drugs which have a tendency to cause necrosis at higher doses, etoposide is reported to cause apoptosis at low concentrations (Marks and Fox, 1991).

Etoposide is derived from podophyllotoxin, a toxin found in American Mayapple and contains a hindered phenolic ring, a vital structure for antineoplastic activity (Loike and Horwitz, 1976; Slevin, 1991). The drug is implicated in causing DNA breaks either through interaction with DNA-topoisomerase II complexes or reactive oxygen species (Slevin, 1991). Etoposide does not bind to DNA but interacts with topoisomerase II stoichiometrically (Tanaka *et al.*, 2007). This means that the drug interaction occurs in such a way that each molecule of etoposide comes in contact with a single molecule of ATP- bound topoisomerase II, consequently stabilizing only a single-stranded break (Bromberg *et al.*, 2003; Vilain *et al.*, 2003). Therefore, single or double stranded breaks formation is based on the molar ratio between covalently bound etoposide and topoisomerase II (Montecucco and Biamonti, 2007). Topoisomerase II (Topo II) is involved in controlling the topology of DNA in an ATP mediated process by undergoing a conformational change, resulting in resolving double stranded knots in the DNA during replication (Montecucco and Biamonti, 2007). This enzyme catalyzes the formation of transient covalently bonded TopoII-DNA

cleavage complexes (Wang, 1996). It has been shown that treatment with epipodophyllotoxins results in the stabilization of these cleavage complexes (Beck *et al.*, 1999). This increase the percentage of these complexes, which are highly toxic for the cell (Chaudhary and Roninson, 1993; Koike *et al.*, 1996). The mode of action assumes that there are collisions involved between the cleavage complexes and the progression of replication forks, thereby converting cleavage complexes into irreversible double strand DNA breaks (DSBs) (D'Arpa *et al.*, 1990; Zhang *et al.*, 1990). Repair enzymes recognize these DSBs as lethal lesions and triggers a cascade of events involved in cell-cycle check points and the activation of *p53*, leading to apoptosis **(Figure 4)** (Beck *et al.*, 1999).

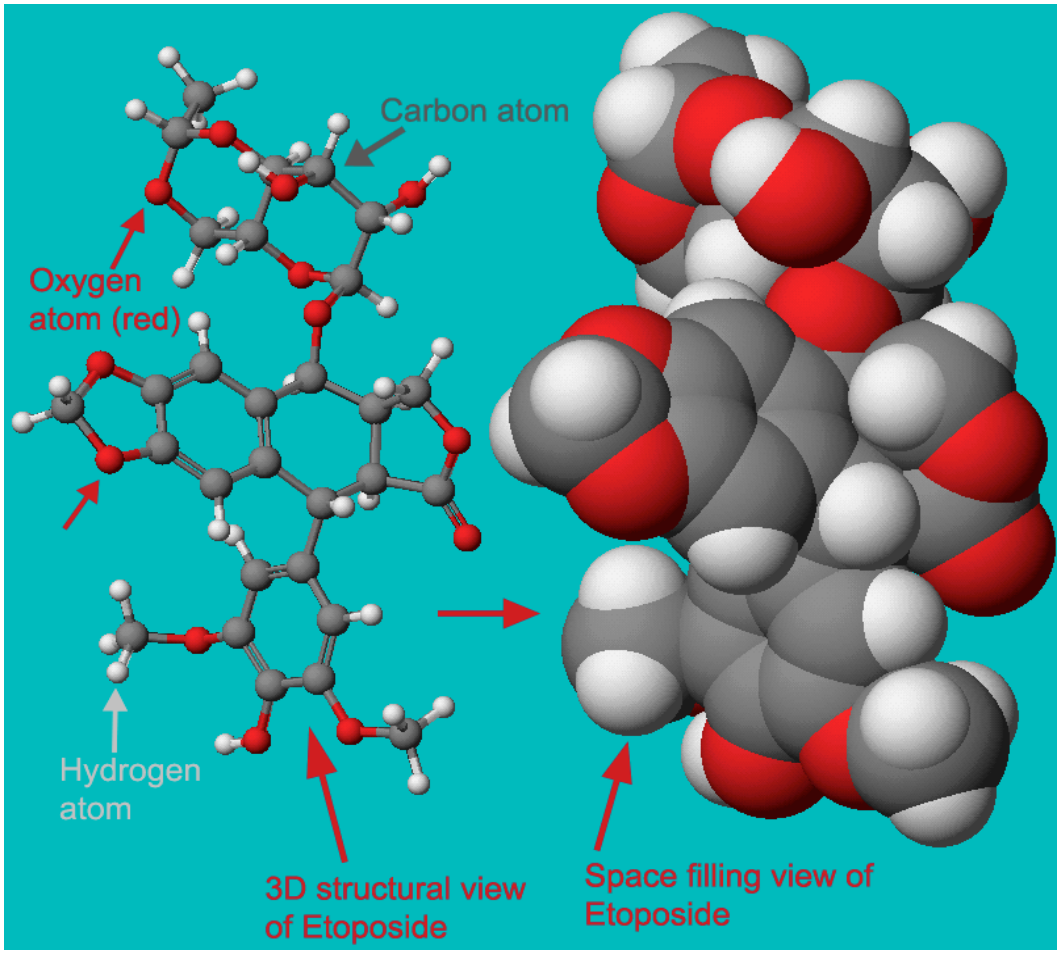

Figure 3: 3-D Structural and Space filling view of Etoposide

(Created by using the software Scigress Explorer Ultra version 7.7.0.47, 2008, Fujitsu Limited)

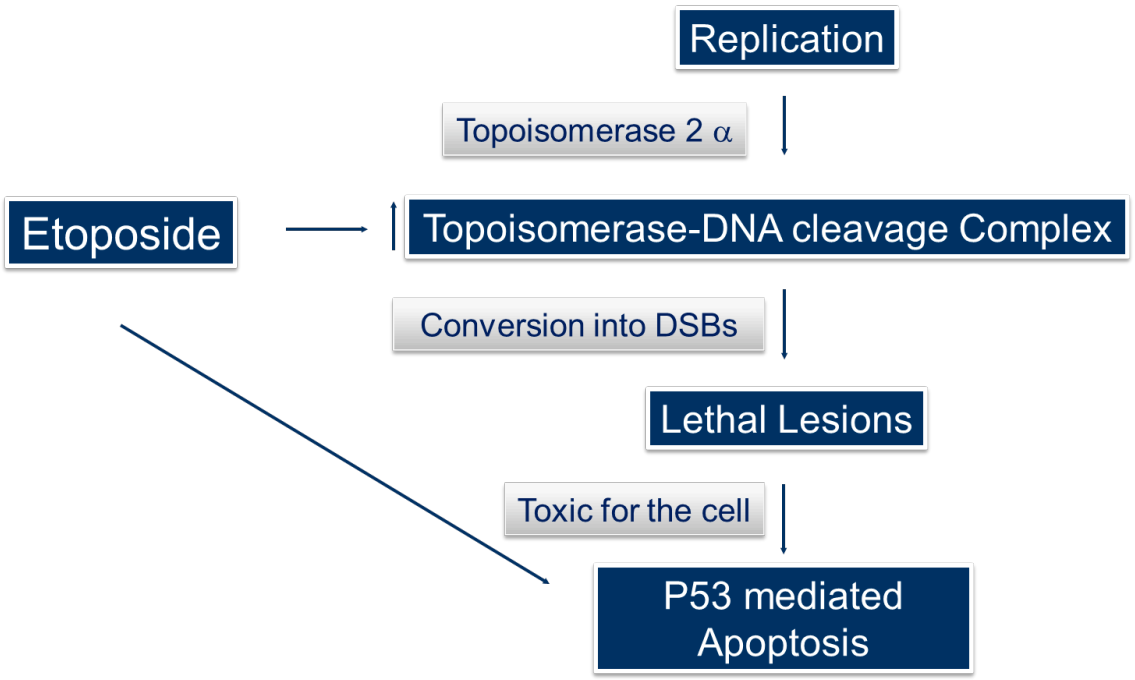

Figure 4: Diagrammatic representation of the role of topoisomerase II α and effect of etoposide.

During DNA damage after etoposide treatment, the DNA damage response is manifested through various signalling pathways. DNA-PK (protein kinase) and ATM (ataxia telangiectasia mutated) are activated by double strand breaks, in order to repair these newly formed cytotoxic lesions (Jackson, 1996; Keith and Schreiber, 1995; Zakian, 1995). Poly(ADP-ribose) polymerase (PARP) is also observed to be activated which acts as a catalyst to transfer ADP-ribose units from NAD^+ to protein linked chains of poly(ADP-ribose) (Realini and Althaus, 1992). This leads to chromatin remodelling by removing histones and interacting with repair complexes (de Murcia *et al.*, 1986).

1.8 Other Mechanisms of killing by Etoposide

Other mechanisms of action of etoposide, besides the inhibition of topoisomerase, may be important for its cytotoxic effects (van Maanen *et al.*, 1988). DNA damage through etoposide is found to be dependent on the presence of a hydroxyl group at the C-4' of the dimethoxyphenol ring (E-ring) (Loike and Horwitz, 1976). The oxidative transformations in the E-ring leads to the formation of products which can cause DNA damage (van Maanen *et al.*, 1988). On the other hand hypersensitivity shown by human ataxia telangiectasia (AT) fibroblasts to etoposide treatment is caused by the production of free radicals rather than the inhibition of topoisomerase II (van Maanen *et al.*, 1988).

Etoposide is strong lipid antioxidant and has been found to prevent the externalization of phosphatidaylserine (PS) in HL 60 cells. The PS externalization provides the signal to the macrophages to engulf the apoptotic cell thus eliminating the PS-dependent signalling (Tyurina *et al.*, 2004).

Etoposide treatment is known to increase the endogenous ceramide levels thereby activating the cermaide signalling pathway (Toman *et al.*, 2002). Etoposide induced apoptosis has been reported in human glioma cells through the generation of ROS by stimulating the p53 pathway. It was observed that production of ROS caused the activation of neutral sphingomyelinase followed by the generation of ceramide (Sawada *et al.*, 2001)

1.9 Mechanisms of Resistance to Etoposide

One of the major problems with chemotherapy is that after certain period of time cancer cells become resistant to treatment, which results in disease relapse. One of the mechanisms by which cancer cells develop resistance to the cytotoxic agents is through the modification of apoptotic pathway. It has been observed that low-etoposide resistant $MeWo_{Eto01}$ cells depicted reduced but noticeable apoptotic activities as compared to high-etoposide resistant $MeWo_{Eto1}$ cells which did not reveal any of the events related to apoptosis (Helmbach *et al.*, 2002). The study in low-etoposide resistant cells showed a marked decrease in the release of cytochrome c which was found to be absent in high-etoposide resitant cells suggesting the alteration of intrinsic apoptotic pathway. Hsp27 is also found to inhibit caspase 9 in apoptosis induction by etoposide (Helmbach *et al.*, 2002) suggesting that Hsp27 has its effect on apoptosome by inhibiting the activity of procaspase 9 downstream of cytochrome c release (Garrido *et al.*, 1999). The high expression of Hsp70 and Hsp27 is correlated with metastatic breast endometrial or gastric cancer having poor prognosis (Maehara *et al.*, 2000; Munster *et al.*, 2001; Wataba *et al.*, 2001). Hence the inhibition of

capspase 9 not the cytochrome c release in etoposide resistant cells might be a possible mechanism of drug resistance (Helmbach *et al.*, 2002).

The etoposide resistance has also been observed in L929 fibroblasts stably transfected with Akt kinase gene (Karpinich *et al.*, 2002). Akt, a serine-threonine kinase, is responsible for the phosphorylation of pro-apoptotic protein Bad. (Datta *et al.*, 1997). The phosphorylation of Bad prevents its binding to anti-apoptotic protein Bcl-X. Consequently, Bcl-X is able to bind to pro-apoptotic protein Bax thereby preventing the translocation of Bax to mitochondria membranes and thus blocking the downstream apoptotic pathway. In the fibroblasts with Akt overexpression, the translocation of pro-apoptotic protein Bax to mitochondria and subsequent release of cytochrome c, which are important processes during apoptosis, were not detected suggesting the involvement of Akt in etoposide resistance (Karpinich *et al.*, 2002).

The modulation of topoisomerase expression and activity can be the crucial factors in resistance to topoisomerase inhibitors. At least a 10-fold decrease in activity of topoisomerase has been observed in etoposide resistant melanoma cells suggesting the contribution of decreased enzymatic activity to drug resistant phenotype (Lage *et al.*, 2000). The change in topoisomerase activity could be attributed to reduction of nuclear content of both the isoform of topo II (Lage *et al.*, 2000), mutations in topo II encoded genes (Danks *et al.*, 1993) and changes in the catalytic activity of the enzyme through phosphorylation (Takano *et al.*, 1991).

A significant decrease in the nuclear content of DNA mismatch repair (MMR) proteins in human melanoma cells is associated with resistance to antineoplastic agents

etoposide, cisplatin, vindesine and fotemustine (Lage *et al.*, 1999). The defects in MMR system can be associated directly with cell cycle check points and apoptosis induction in response to DNA repair (Fink *et al.*, 1998). Since these proteins detect DNA damage in response to interaction of etoposide with topoisomerase II that lead to the transduction of apoptotic signals (Aebi *et al.*, 1997).

1.10 Hydrogen Peroxide, reactive oxygen species (ROS), and Cell Death

Hydrogen peroxide is considered as a reactive oxygen species because it is a very strong oxidizing agent and could be detrimental for the cells at higher concentration (Droge, 2002). The peroxisomes in the cells produce the enzyme catalase peroxidase which deals with the reactive oxygen species by breaking down low concentration of hydrogen peroxide into harmless water (H_2O) and oxygen (O_2) (Corpas *et al.*, 2001). Catalase peroxidase is also found in the cytosol or mitochondria. Besides catalase, the other major enzymes involved in the breakdown of hydrogen peroxide are glutathione peroxidase and thioredoxin peroxidase (peroxiredoxins). To detoxify the effects of hydrogen peroxide, there is a tight regulation of antioxidant enzymes and signalling pathways in sensing the free radicals (Veal *et al.*, 2007).

Hydrogen peroxide itself is generated in the cells through NADPH (nicotinamide adenine dinucleotide phosphate) oxidase dependent and independent mechanisms (Veal *et al.*, 2007). The growth factors and cytokines such as PDGF (platelet derived growth factor), EGF (epidermal growth factor), insulin, angiotensin II, and TNFα (tumor necrosis factor alpha) are stimulated because of the production of hydrogen peroxide by NAPDH oxidases (Geiszt and Leto, 2004; Park *et al.*, 2004). However, the generation of hydrogen peroxide

might induce diverse biological responses *viz.* stimulation of cell proliferation (Foreman *et al.*, 2003; Geiszt and Leto, 2004), differentiation (Li *et al.*, 2006; Sauer *et al.*, 2000), migration (Ushio-Fukai, 2006), or apoptosis (Cai, 2005; Gechev and Hille, 2005) depending on the level of hydrogen peroxide in the cells. The mechanism/s underlying the concentration dependence response is still unclear (Veal *et al.*, 2007). In fact higher concentration of intracellular hydrogen peroxide leads to oxidative stress by reducing antioxidant capacity (Veal *et al.*, 2007) and promotes apoptosis in a p53 mediated manner (Sablina *et al.*, 2005).

Increased cellular concentration of hydrogen peroxide is related to various aspects of carcinogenesis for example DNA damage, mutations and genetic instability (Henle and Linn, 1997; Hunt *et al.*, 1998; Imlay and Linn, 1988; Jackson and Loeb, 2000; Park *et al.*, 2005; Pericone *et al.*, 2002), which can be attributed to the activation of HIF-1α (Lopez-Lazaro, 2007). The activation of HIF-1α is directly associated with resistance to apoptosis, invasion/metastasis, angiogenesis and immortalization (Lopez-Lazaro, 2006; Nishi *et al.*, 2004; Semenza, 2003; Semenza, 2006). It has recently been observed that hydrogen peroxide is present in abundance in cancer cells and is considered to play a dual role for malignant transformation of cells or senitizing cancer cells (Lopez-Lazaro, 2007). The cancer cells are found to be more susceptible to hydrogen peroxide induced cell killing as compared to normal cells. Therefore it is feasible that augmenting the cellular levels of hydrogen peroxide by exploiting hydrogen peroxide generating systems such as etoposide can be a significant approach for the improvement of clinically beneficial anticancer strategies (Lopez-Lazaro, 2007).

1.11 Functional Genomics approaches

Functional genomics entail to study the biological function of genes by exploiting various molecular biology techniques such as knocking out the gene (for example insertional mutagenesis, generation of knockout mice) or by silencing gene expression through RNA interference technology (for example shRNAi, siRNAi) (Keon *et al.*, 2003). The generation of knockout mice to study gene function is quite labour and cost intensive (Sliva and Schnierle, 2010). Moreover a number of *in vivo* gene knock-out experiments are unsuccessful in determining the function of genes because of lethality during early stages of embryonic development (Karagiannis and El Osta, 2004). Therefore an alternative choice available to determine the function of a gene involves the utilization of RNA interference technology. It has been proven as an effective tool to study the function of a gene in a quite rapid and cost effective manner (Dykxhoorn *et al.*, 2003).

RNA interference (RNAi) technology is used to limit the level of transcript either by stimulating sequence specific RNA degradation or by inhibiting translation through the exogenous application of double stranded (ds) RNA (Agrawal *et al.*, 2003). This is also known as post-transcriptional gene silencing (PTGS). The two step mechanistic model for RNAi involves the binding of RNA nucleases (for example Dicer) to dsRNA followed by its cleavage into distinct 21-25 nucleotide RNA fragments (siRNA) with 3' overhang of two nucleotides in an ATP dependent manner; in the next step, there is an incorporation of the antisense strand of double stranded siRNA into multinucleate complex, RISC (RNA induced silencing complex), which degrades the homologous single stranded mRNA by pairing with it and cutting it in the middle of the duplex region **(Figure 5a and b)** (Agrawal *et al.*, 2003).

Gene silencing through siRNA can also trigger promoter gene methylation and chromatin condensation (Ross *et al.*, 2007).

siRNA synthesis can be done *in vitro* or through vectors that are capable of making *de novo* intracellular siRNA (Donze and Picard, 2002; Yang *et al.*, 2002; Yu *et al.*, 2002). The siRNA expression vectors could be either viral based or non-viral based systems which allow siRNAs to be expressed as fold back stem- loop structures (short hairpin) (Agrawal *et al.*, 2003). These expression vectors have the shRNA sequence between a polymerase III promoter and a thymidine transcription termination site. After transcription, the stem-loop structure with 3' UU overhang is generated and eventually processed intracellularly thereby converting shRNA molecules into approximately 21-nt long effector siRNA molecules (Karagiannis and El Osta, 2004). *In vitro* siRNA delivery through cytoplasm is transient in nature and the knock down effect lasts roughly for a week in dividing cells and for several weeks in resting cells (Bartlett and Davis, 2006; Bartlett and Davis, 2007) while nuclear delivery of gene expression cassettes that express short hairpin RNA (shRNA) which are processed in the cell to produce siRNA lead to stable down regulation of the gene (Sliva and Schnierle, 2010).

The micro RNAs (miRNAs), 19 to 24-nt non coding single stranded segments, are processed *in vivo* by Dicer from approximately 70-nt stem-loop structures to produce approximately 22-nt miRNAs (Lee *et al.*, 1993). These single stranded segments are then incorporated with miRNA-protein (miRNP) complex leading to transcriptional and translational repression **(Figure 5c)** (Agrawal *et al.*, 2003). The stem loop structure of naturally occurring pre-miRNA hairpins with a double stranded stem of approximately 23-25

bp and a loop region of approximately 5-nt is similar to the distinct structure of shRNA (Lapierre *et al.*, 2011b). In contrast to siRNA, miRNAs primarily lead to translational repression due to imperfect pairing to their target mRNA (Sliva and Schnierle, 2010).

It has recently been observed that to trigger RNAi system, the dsRNA motif required is identified by the RNAi associated proteins and the guide strand is needed as a cofactor to aid the mRNA binding co-factor in the RISC's Argonaute catalytic protein (Lapierre *et al.*, 2011a). The activated RISC then unwinds the double stranded siRNA and targets mRNA by using siRNA as a guide resulting into the nucleolytic degradation of the target sequence leading to a loss of gene expression (Meister and Tuschl, 2004; Zamore *et al.*, 2000).

RNA interference technology is powerful tool for manipulation of gene expression but it can produce off target effects besides selective silencing of target genes (Hannon, 2002; Zamore *et al.*, 2000). The double strandard RNA longer than 29-30 nucleotides can elicit interferon response but this can be avoided by keeping the length of dsRNA to 21-nt (Rao *et al.*, 2009a). Sometimes the non-specific effects of siRNA are observed leading to the suppression of non-target genes because of the cross-hybridization of the transcripts containing the regions of partial homology with the siRNA sequence (Persengiev *et al.*, 2004). In addition to the cross hybridization between siRNA and non-targeted genes, siRNAs can occasionally bind to several cellular proteins because of sequence similarities. This is called aptamer effect and leads to the altered function of endogenous proteins (Semizarov *et al.*, 2003). The concentration dependent non-specific effects of siRNA have also been observed. The high concentration of siRNA can give non-specific effects but the knock down gets affected if the concentration of siRNA is lowered (Persengiev *et al.*, 2004)The

translational repression of untargeted genes can also occur through the initiation of miRNA mechanism due to the formation of duplexes between the bulging loops and the siRNA sequences (Doench *et al.*, 2003).

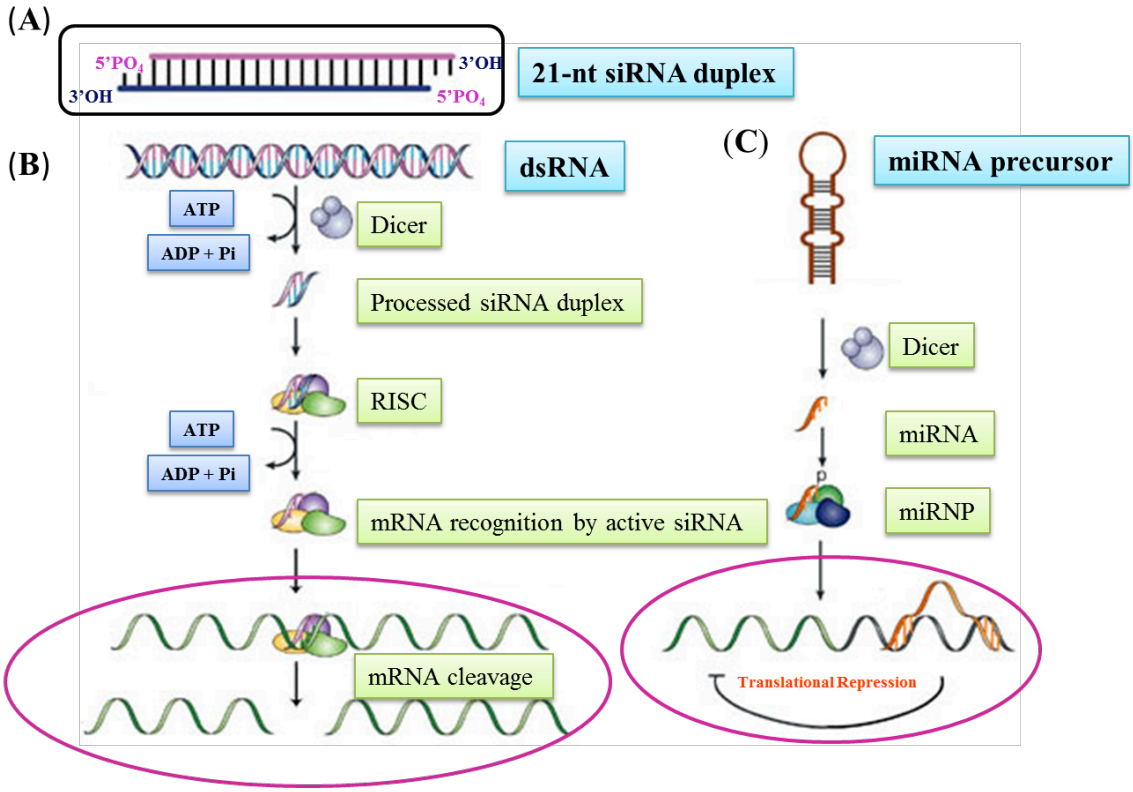

Figure 5: Pathway to depict the processing of siRNA and miRNA

A: siRNA with 5'phosphate 19 bp long duplex region with 3' hydroxyl termini having two unpaired nucleotide overhangs.

B: The siRNA Pathway involves the cleavage of dsRNA by RNAse III, Dicer, in an ATP dependent reaction and finally the incorporation of siRNA with RNA-inducing silencing complex (RISC) to target sequence specific cleavage of mRNA.

C: The miRNA Pathway involves the cleavage of approximately 70-nt hairpin miRNA precursor into approximately 22-nt miRNA by Dicer. The single stranded miRNA are incorporated into a miRNA-protein complex (miRNP) with partial sequence complementarity to target mRNA resulting into translational repression.

Modified from Macmillan Publishers Ltd:[Molecular Cell Biology] (Dykxhoorn *et al.*, 2003)

1.12 Previous work regarding the creation and characterization of CHO-E-126 cells and shRNA Knock down of *PHDX* gene

To learn more about the apoptotic machinery, the U3NeoSV1 promoter trap retrovirus (a kind gift from Dr. Earl Ruley – Vanderbilt University **(Figure 6),** was used to infect Chinese Hamster Ovary cells with a transfected ecotropic retroviral receptor gene CHO-Cl-22 (Hubbard *et al.*, 1994) to create a library of mutated cells. Dr. Jeannick Cizeau then selected this library of cells for etoposide resistant clones. The screening for retrovirally infected cells for etoposide resistance resulted in the isolation of 45 clones at a ratio of nine resistant colonies per 10^4 infected cells plated. Parallel experiments with uninfected CHO cells resulted in few etoposide resistant colonies (around single colony per million cells).

CHO-E-126, one of etoposide resistant clones used in this study, also showed resistance to hydrogen peroxide. Hydrogen peroxide generates reactive oxygen species, which affects numerous cellular functions by causing DNA damage, lipid peroxidation (damage to cell membrane), proteins' damage through oxidation (Foyer and Noctor, 2005), and mitochondrial damage through mitochondrial permeability pore (MPT) leading to loss of membrane potential and ATP depletion (Nieminen *et al.*, 1997) and ultimately leading to apoptosis.

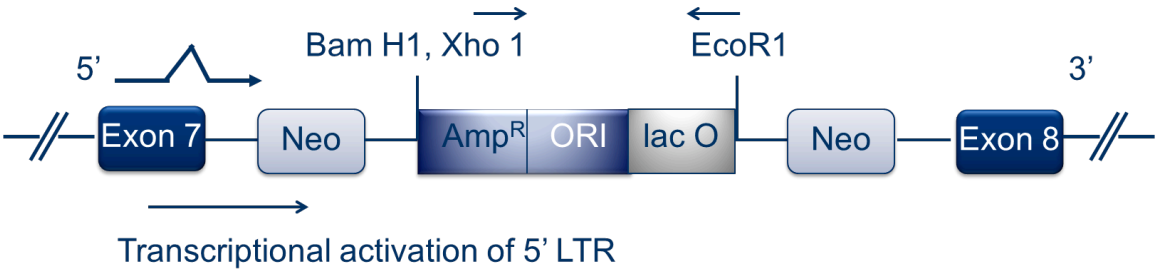

Figure 6:U3Neo SV1 Promoter Trap Integration between Exon 7 & 8 of Mm *PHDX*

Modified from Elsevier Ltd:[Methods in Enzymology] (Hicks *et al.*, 1995)

The site of viral integration and sequences flanking the provirus were determined by inverse PCR and 5'RACE (rapid amplification of cDNA ends) experiments by Kofi Chapman in the laboratory. The southern blot analysis found that there was a single virus integration (Nyaho JKC, 2003). The sequence analysis confirmed that the virus interrupted a novel gene which shares homology with a novel gene *1110031I02Rik* found on mouse Chromosome 11 that has a prolyl hydroxylase domain; therefore we name this novel prolyl hydroxylase gene *PHDX*.

The parental CHO-K1 cells were chosen for this project because these cells are functionally hemizygous at approximately 20% of loci due to silencing of one allele by DNA methylation (Holliday and Ho, 1990) and therefore a substantial fraction of active genes exist only in a single copy (Siminovitch, 1976). Therefore because of this allelic exclusion, sometimes a single mutational event is enough to abrogate the gene function.

1.13 Rationale, Hypothesis and Approach of the current study

The aim of this study was to test the role of *PHDX*, a novel proly hydroxylase gene, in drug resistance. In our laboratory, the etoposide and hydrogen peroxide resistant cell line CHO-E-126 was previously characterized and shown that the integration of a promoter trap retrovirus was into the novel prolyl hydroxylase gene (Nyaho JKC, 2003). Since this disruption resulted in the reduced expression of *PHDX* gene, it was hypothesized that this gene might be involved in drug resistance. In addition, the alteration of the cellular hydroxyproline levels by the loss of the gene might influence the drug response through the production of oxygen free radicals.To address this question, we utilized two experimental

approaches. First we used the RNA interference technology to knock down *PHDX* gene. Secondly we also overexpressed the gene to determine its involvement in resistance to Etoposide and hydrogen peroxide.

CHAPTER 2 - MATERIALS AND METHODS

2.1 Cell Lines

The cell-lines used in the study were:

CHO-K1 were obtained from ATCC (American Type Culture Collection, Manassas, VA- ATCC # CCL-61)

CHO-Cl-22 (Hubbard *et al.*, 1994)

CHO-E-126 (created by Dr. Jeanik Cizeau)

Phoenix Eco cells (obtained from Dr. Geoff Hicks laboratory -Nolan Lab - http://www.stanford.edu/group/nolan/MTAs/mtas.html) (DiCiommo *et al.*, 2004)

NIH 3T3 human fibroblast (obtained from Dr. Kirk Mcmanus Laboratory - ATCC American Type Culture Collection, Manassas, VA- ATCC # 1658^{TM}) (Jainchill *et al.*, 1969)

2.2 Cell culture conditions

The cells were grown in a humidified atmosphere with 5% carbon-di-oxide (CO_2) at 37 $^{\circ}$C. All cells except for Phoenix Eco cells were grown in alpha-Minimum Essential Medium (α-MEM, Invitrogen, Burlington, Ontario), supplemented with 3.7g/L sodium bicarbonate, 100µg/ml Streptomycin, 100U/ml Penicillin G along with 10% of Fetal Bovine Serum (FBS, Sigma-Aldrich, St.Louis, MO). Pheonix Eco cells were grown in Dulbecco's Modified Eagle's Medium (DMEM, Invitrogen, Burlington, Ontario) supplemented with 10% Fetal Bovine Serum, 1% Penicillin-Streptomycin (Gibco, Grand Island, NY), 1%

Glutamine (Gibco, Grand Island, NY) and 1% Sodium Pyruvate (Gibco, Grand Island, NY).

2.3 Primer Design

All primers were designed using the Gene-Fisher-version 2 software (Bielefeld University Bioinformatics Service, Bielefeld, Germany) and synthesized by Eurofin mwg/operon (Huntsville, AL).

2.4 Primers

Table 1: List of Primers

Primer Name	Primer Basis	Primer Sequence 5' --→ 3'
Neo1	U3NeoSV1 Neomycin Resistance Gene	CCATCTTGTTCAATCATGCGAAACGATCC
Amp1	U3NeoSV1 Neomycin Resistance Gene	GCCGAGCGCAGAAGTGGTCCTG
pBABE F	Immediate 5' end of *PHDX* gene	CCCCGAGTTTGGTGGCTCTCG
cDNA R	Immediate 3' end of *PHDX* gene	TAAGGCACATTGAGCAGCAG
Neo R2	U3NeoSV1 Neomycin Resistance Gene	GAACTGTTCGCCAGGCTCAAGG
cDNA L	Immediate 5' end of *PHDX* gene	GCGACCAGTACCAAGAAGGA
cDNA R	Immediate 3' end of *PHDX* gene	TAAGGCACATTGAGCAGCAG
GAPDH GSP1	Mouse *GAPDH* gene	GAAGTCGCAGGAGACAACCTGGTCCT
GAPDH GSP2	Mouse *GAPDH* gene	TGGCAAGTTCAAAGGCACAGTCAAGG
Forward FF	Immediate 5' end of *PHDX* gene	ATGGCGCCTCAGCGGAGG

Reverse RR	Immediate 3' end of *PHDX* gene	TCACGTGAGTACTGGGTCCTC
FF BAMKOZ	Immediate 5' end of *PHDX* gene	CATGGGATCCACCATGGCGCCT CAGCGGAGG
RR SAL1	Immediate 3' end of *PHDX* gene	CAGTGTCGACTCACGTGAGTAC TGGGTCCTC
pBabe F	5' end of pBABE puro vector sequence	CCCCGAGTTTGGTGGCTCTCG
pBabe R	3' end of pBABE puro vector sequence	GGAAGGAGCCTGTTACCCGAG
PHDXRe-6bF	Exon 8 of *PHDX* gene	CTATCGGATTACTTAGAGGACTT CG
PHDXRe-6R	Exon 9 of *PHDX* gene	TTGCAGGTGAAAGCGATGGTGA TG

2.5 Total RNA Isolation

Cells were grown in 150 mm cell culture dishes (Nunclon, Roskilde, Denmark) and total RNA was isolated from the cells using RNeasy® Mini Kit (Qiagen, Mississauga ON) and resuspended in 30 µl of RNase-free water. The concentration of total RNA was determined in the Ultrospect 3000 UV/visible spectrophotometer (Pharmacia Biotech, Piscataway, NJ).

2.6 cDNA Synthesis

The total RNA (1-5 µg) was mixed with, 3µg/µl OligodT Primers (Invitrogen, Burlington, Ontario) and 2.5mM dNTP mix (TaKaRa Bio Inc., Otsu, Shiga, Japan) and brought to a volume of 12 µl. The mixture was heated at 65 °C for 5 minutes, chilled on ice and cDNA synthesis mix containing 5X first strand buffer and 0.1M DTT (Invitrogen, Burlington, ON) to a volume of 8 µl was added to it and heated at 25 °C for 2 minutes. Then 200 units of Superscript II™ reverse transcriptase (Invitrogen, Burlington, Ontario) was added to the mixture and heated at 25 °C for 10 minutes, 42 °C for 50 minutes and 70 °C for 15 minutes.

2.7 Plasmid DNA Preparation by Phenol-Chloroform Extraction

Plasmids were prepared by the method of Sambrook and Russel as detailed below (Sambrook and Russell, 2001). The overnight culture of transformed *E. coli* in 250 ml LB medium with antibiotics was pelleted in a 500 ml centrifuge bottle at 6000 rpm for 15 minutes at 4 °C in Beckman J-2 MC (JA-10 Rotor). The pellet was resuspended in 10 ml ice

cold 50 mM Tris-Cl pH 8.0, mixed and the contents transferred in 50 ml BD Falcon tube (VWR, Mississauga, ON) and kept on ice. To lyse the cells, 1.25ml of freshly prepared Lysozyme (20 mg/ml in 50 mM Tris-Cl pH 8.0) was added, mixed on vortex, and incubated on ice for 10 minutes. Then 1.25 ml of 250 mM ethylenediamine tetra acetic acid (EDTA) pH 8.0 mixed and incubated on ice for 5 minutes. After that 125µl of RNAseA (10 µg/ml) was mixed with the cocktail and incubated on ice for 10 minutes. Then 0.5 ml of 1% Sodium dodecyl sulfate (SDS) was mixed carefully by inverting the tube upside down gently. The contents were centrifuged at 8000 rpm in JA-10 rotor for 30 minutes at 4 °C. The supernatant was taken and 800 µl of 5 M Potassium acetate (KOAc) was added to it. Then an equal volume of Phenol: isoButanol (1:1) solution was mixed with it. The contents were spun at 3500 rpm for 10 minutes. Cake formation took place at the interphase. The bottom aqueous layer was taken by puncturing the cake and extracted with equal volume of phenol followed by Chloroform and iso amyl alcohol at a ratio of 24 to 1 respectively for the complete removal of cellular debris. Isopropanol (0.7 volume) was incubated with the extracted liquid for 15 minutes at room temperature in order to precipitate the DNA. The contents were then centrifuged at maximum speed for 15 minutes. Then 70 % ethanol was added to the pellet and the contents were spun at full speed for 10 minutes. The pellet was air-dried and dissolved in TE buffer (10 mM Tris-Cl and 1 mM EDTA) pH-8.0.

2.8 Examination of Etoposide and Hydrogen Peroxide (H_2O_2) resistance using Crystal Violet Staining Assay

The crystal violet staining colonogenic assay protocol used in this study was

described by Saintigny *et al.* (Saintigny *et al.*, 2002). Cells were plated at a concentration of 1 X 10^3 cells per 2ml of medium per well in quadruplet in six-well plates (Nunclon, Roskilde, Denmark). Cell number was determined using Beckmann Coulter Counter. Cells were allowed to adhere overnight. After 24 hours after seeding, the media was aspirated and the cells were treated with variable concentrations of etoposide freshly prepared in dimethy sulphoxide (DMSO) (Sigma-Aldrich, St. Louis, MO) or H_2O_2(Sigma-Aldrich, St. Louis, MO) diluted in media. During etoposide treatment, the first well was left untreated, the second well was treated with DMSO only (1μM) in media and the rest of the wells were treated with 50 nM, 100 nM, 500 nM and 1 μM of etoposide in media.

For H_2O_2 treatment in crystal violet staining assay (Saintigny *et al.*, 2002), the first well used as a control was left untreated and rest of the wells were treated with variable concentrations of H_2O_2 (diluted in media) *viz.* 75, 100, 125, 150 and 175 μM. The cells were incubated for 48 hours and the drug containing media was replaced with 2.0 ml fresh media per well after washing each well with 1.0 ml of phosphate buffered saline (1X PBS). The cells were allowed to recover from the effect of etoposide or H_2O_2 with a change of media every other day until the untreated cells reached confluency (approximately one week). After one week, the media was aspirated from each well followed by single wash with 1.0 ml of 1 X PBS. The cells were stained with 1.0 ml of 0.5% aqueous crystal violet stain. Plates were returned to the incubator at 37 $^{\circ}$C with 5% CO_2 for one hour. Crystal Violet stain was removed by pipetting and the plates were gently rinsed with two changes of deionized distilled water (dd H_2O) in order to wash away the unbound stain. The plates were allowed to dry overnight. To dissolve the stain, 1.0 ml of 0.1% acetic acid in 50% ethanol was added to

each well. Two hundred µl from each well in triplicate was transferred into 96 well plates (Nunclon, Roskilde, Denmark). The optical density (OD) was determined at 540 nm using Titertek Multiskan MCC/340. Graphical representation and assembling of the data was done using the software Origin Lab 8.5. The statistical analysis was done by using GraphPad Prism 5 software.

2.9 Examination of Etoposide and Hydrogen Peroxide (H_2O_2) resistance using 3-(4,5-Dimethylthiazol-2-yl)-2,5-diphenyltetrazolium bromide (MTT) Assay

Cells were plated at a concentration of 3 X 10^3 cells per 100µl of medium per well in 96 well plates. Cell number was determined using Beckmann Coulter Counter. After 24 hours of seeding, the media was aspirated and the cells were treated with variable concentrations of etoposide freshly prepared in dimethy sulphoxide (DMSO)/H_2O_2 diluted in media. For etoposide treatment the first column (Wells A-H) was left blank and cells were left untreated in the second column. Cells in the third column (Wells A-H) were treated with DMSO (250 µM), the vehicle control and rest of the columns(Wells A-H) were treated with variable concentrations of etoposide *viz.* 25, 50, 75, 100, 150, 200 and 250 µM per column. The different concentrations of H_2O_2 used were 50, 100, 200, 300, 400, 500 and 600 µM per column while using untreated cells in one of the columns as a control.

The cells were treated with etoposide or H_2O_2 for 48 hours at 37 $^\circ$C with 5% CO_2 and again incubated with 10 µl of MTT Formazan [1-(4,5-Dimethylthiazol-2-yl)-3,5-diphenylformazan (Sigma-Aldrich, St. Louis, MO - 5 mg/ml in 1 X PBS) per well for four hours in order to allow the formation of formazan crystals (Mosmann, 1983). To sediment

formazan crystals, plates were centrifuged for 10 minutes at 2000 rotations per minute (rpm) in a Beckman Coulter Allegra 25R Centrifuge. The media was removed by flicking the plates gently over absorbent pads and the crystals were dissolved in 100 µl of spectral grade DMSO by shaking on a minishaker. The optical density was determined at 540 nm using Titertek Multiskan MCC/340 Microplate Reader. Graphical representation and assembling of the data was done using the software Origin Lab 8. The statistical analysis was done using GraphPad Prism 5 software.

2.10 Statistical Analysis of Results

The results of cytotoxic assays were analyzed using the Non-linear Regression program in the Graph Pad Prsim 5 software. Mean IC_{50} values were calculated using Graph Pad Prism 5 software and pValues were calculated by comparing Mean IC_{50} values with the Mean IC_{50} values from the control cell-line using the Student's t-Test in GraphPad Prism 5 (Motulsky HJ, 2007). The results of real time RT-PCR were analyzed using one way analysis of variance (ANOVA) followed by Dunnett's post-hoc test for the comparison of cell-lines by using GraphPad Prism 5 software (Motuslky HJ, 2007).

2.11 Sequencing Verification

2.11.1 Genomic DNA (gDNA) Extraction, PCR Amplification and Product Visualization

CHO Cl-22 and CHO E-126 cells were grown under standard conditions. Genomic DNA was extracted from these cells using GenElute^{TM} Mammalian Genomic DNA Miniprep

Kit (Sigma-Aldrich, St. Louis, MO). DNA was quantified using the Ultrospect 3000 UV/visible spectrophotometer (Pharmacia Biotech, Piscataway, NJ). The genomic DNA (0.2 µg) was placed in 100 mM Tris-HCl (pH-8.3), 2.5 mM dNTP mixture (TaKaRa Bio Inc., Otsu, Shiga, Japan), 5 units/µl TaKaRa HS Taq (TaKaRa Bio Inc., Otsu, Shiga, Japan) with forward primer Neo1 and reverse primer Amp1 (10 µM), and was brought to a final volume of 50 µl. The samples were heated to 94 ºC for one minute and then subjected to 35 cycles of 94 ºC for 20 seconds, 65 ºC for 30 seconds and 72 ºC for two minutes. A final extension at 72 ºC took place for 15 seconds. The amplified products were visualized on 1 % agarose gel containing 0.4 µg/ml ethidium bromide.

2.11.2 PCR Amplification of E-126 cDNA to detect *Neo-PHDX* Fusion and Product Visualization

The cDNA from CHO Cl-22 and CHO E-126 (0.5 µg each) cells was amplified with 10X reaction buffer, 2.5mM dNTP mix, 5 units/µl TaKaRa Taq (TaKaRa Bio Inc., Otsu, Shiga, Japan) along with 10 µM cDNA L and NeoR2 primers and brought to a final volume of 25 µl. The samples were heated to 94 °C for one minute and then underwent 35 cycles of 94 °C for 20 seconds, 65 °C for 30 seconds and 72 °C for 2 minutes. The final extension was done at 72 °C for 15 minutes. After amplification, the products were separated and visualized on a 1% agarose gel containing 0.4 µg/ml of ethidium bromide. The band was excised and DNA was purified for sequencing by using Gel-Extraction kit (Qiagen, Mississauga ON).

The primers used to sequence 300 ng of E-126 cDNA were forward primer pBABE F and reverse primer Neo R2. The samples were sent to Robarts Research Institute, London Ontario for sequencing.

2.12 Western Immunoblot Analysis of Neophosphotransferase-*PHDX* Fusion Protein

2.12.1 Cell-Lysate Preparation

CHO-K1 and CHO E-126 cells were grown in 150 mm cell-culture dishes (Nunclon, Roskilde, Denmark), media was aspirated and cells were washed twice with ice-cold 1XPBS. The cells were gently scraped with ice-cold 1 X PBS and centrifuged (Damon-IEC DPR-6000) at 1000 rpm for five minutes. The pellet was washed with PBS and the cells were resuspended in Radio Immuno Precipitation Assay (RIPA) lysis buffer. RIPA buffer is composed of 150 mM Sodium Chloride, 1.0 % Nonidet P-40, 0.5 % Sodium deoxycholate, 0.1 % SDS, 50 mM Tris-Cl pH 8.0 contained SigmaFast^{TM} protease inhibitor cocktail [4-(2-aminoethyl) benzenesulfonyl fluoride (AEBSF), E-64, bestatin, leupeptin, aprotinin, and EDTA,(Sigma-Aldrich, St. Lois, MO)] and 1 mM phenylmethanesulfonylfluoride (PMSF). The cells were left on ice for 20 minutes, sonicated 3X for 4-5 seconds and left on the shaker at 4 $^{\circ}$C for 10 minutes. The cellular debris was removed by centrifugation at 13000 rpm (Sorvall Legeng Micro 21 Centrifuge, ThermoScientific, South Logan, Utah) for 10 minutes. The protein quantification was done by using BCA protein assay on a Spectramax 190 at a wave length of 590 nm, and the standard curve was obtained using SOFTmax Pro 3.1.2 software. The samples were stored at -80 $^{\circ}$C.

2.12.2 Gel-Electrophoresis and Protein Transfer

The total protein samples from CHO-K1 and CHO E-126 (50 μg each) containing 6X loading buffer (150 mM Tris-Cl pH 6.8, 30 % glycerol, 12 % SDS, 1.7M β-Mercepethalnol

and 0.1 % Bromophenol blue) were denatured at 95°C for 10 minutes and loaded onto 10 % SDS-polyacrylamide gel (Laemmli stacking and resolving gel). The samples were separated at 100 V by electrophoresis in running buffer (25 mM Tris, 192 mM glycine and 0.1 % w/v SDS). Separated protein was transferred from the gel to an Immobilon-P Polyvinylidene fluoride (PVDF) hydrophobic membrane (Millipore, Bedford, MA) for two hours at 100 V in transfer buffer (25 mM Tris, 192 mM and 20 % Methanol, pH 8.3).

2.12.3 Immunodetection

The samples transferred to membranes were prepared for immunodetection. The membrane was blocked overnight at 4 °C with 5% skim milk powder dissolved in TBST Buffer (20 mM Tris, 137 mM NaCl, 0.1 % Tween 20). The membrane was washed twice briefly in TBST. The membrane was incubated over night with Anti-Neophosphotransferase II polyclonal antibody (Cat. # 06-747, Cedarlane, Hornby, Ontario) in 1 % skim milk powder in TBST (1:1000 dilution) at 4 °C overnight with agitation. The next day the membrane was washed twice briefly in TBST followed by 3 X 15 minutes washes in the wash buffer with agitation at room temperature. The membrane was then incubated with goat anti-rabbit IgG-HRP antibody (Cat. # sc-2004, Santa Cruz Biotechnology, Santa Cruz, CA) in 1 % skim milk powder (1:5000 dilution) for one hour at room temperature with agitation. The detection was done using the ECL Plus Western blotting reagents (GE Healthcare, Buckinghamshire, UK after washing the membrane as previously described after primary antibody incubation. The blots were scanned on the Storm 840 PhosphorImager Scanner (Molecular Dynamics, Inc, Sunnyvale, CA) using the blue fluorescence/chemifluorescence mode, 100 microns, PMT 8V.

2.12.4 Stripping and Re-probing

The membrane was washed briefly, submerged in stripping buffer (100 mM β-Mercepethalnol, 2 % SDS, 62.5 mM Tris-cl pH 6.7) and incubated at 50 °C for 30 minutes with occasional shaking. The membrane was ready for blocking and probing again after washing it 2 X 10 minutes in the wash buffer. After stripping, the membrane was blotted again with GAPDH rabbit polyclonal IgG antibody (Cat. # sc-25778, Sigma-Aldrich, St. Louis, MO) in 1% skim milk powder in TBST (1:1000 dilution) at room temperature for two hours with agitation. Then the membrane was washed again and incubated with goat anti-rabbit IgG-HRP antibody (Cat. # sc-2004, Santa Cruz Biotechnology, Santa Cruz, CA) in 1 % skim milk powder (1:5000 dilution) for one hour at room temperature with agitation. The detection was done using the ECL Plus Western blotting reagents (GE Healthcare, Buckinghamshire, UK after washing the membrane as previously described for primary antibody incubation.

2.13 Gene Silencing of *PHDX* in Chinese Hamster Ovary Cells by using small interfering RNA interference (siRNAi) Technology

2.13.1 siRNA

Two individual sets of 21 bp duplexes of siRNA were used to silence the function of *PHDX*. A pool of four individual double strandard (ds) siRNAs *viz.* **Mm_1110031I02Rik_1 FlexiTube siRNA**, **Mm_1110031I02Rik_2 FlexiTube siRNA**, **Mm_1110031I02Rik_3 FlexiTube siRNA,** and **Mm_1110031I02Rik_4 FlexiTube siRNA** were targeted against *PHDX* a.k.a. *Mm_1110031I02Rik* gene at four different regions of the coding sequence.

Mm_1110031I02Rik_1, target DNA sequence: 5’ CTGGTCGAGTCTCATTCTTTA 3’

Mm_1110031I02Rik_2, target DNA sequence: 5’TCGCGAATAAATAGCACAGAA 3’

Mm_1110031I02Rik_3, target DNA sequence: 5’CACCATCGCTTTCACCTGCAA 3’

Mm_1110031I02Rik_4, target DNA sequence: 5’GCGGAGCAGATTCGCAGAATA 3’

The scrambled control siRNA called All Star –ve Control with 3’modification Alexa fluor 488 along with a pool of individual double stranded siRNA were obtained from Qiagen, Mississauga Ont. along with a pool of four siRNAs.

All Star –ve Ctrl (Scrambled Control) AF 488:

Target DNA sequence: 5’ CAGGGTATCGACGATTACAAA 3’

Sense: 5’ GGGUAUCGACGAUUACAAAUU 3’

Antisense: 5’UUUGUAAUCGUCGAUACCCUG 3’

Another siRNA utilized for gene silencing was designed using Ambion’s siRNA target finder (Ambion, Austin, Texas, USA). The siRNA was designed by targeting 3’ untranslated (UTR) region of *PHDX*. Out of the three siRNA designed, one was chosen based on the highest score for the effectiveness of siRNA knock down (Elbashir *et al.*, 2001).

3’UTR PHDX:

Target DNA sequence: 5’ AATGTGCCTTATGAATTATCC 3’

Sense: 5’ UGUGCCUUAUGAAUUAUCCTT 3’

Antisense: 5’ GGAUAAUUCAUAAGGCACATT 3’

The sequence designed targeting 3’UTR was synthesized by **Eurofins MWG Operon (**Huntsville, AL).

2.13.2 Transfection of CHO-K1 cells with siRNA

CHO-K1 cells were seeded at a density of 1 X 10^5 cells per well containing α-MEM supplemented with 10 % FBS with antibiotics 24 hours prior to transfection with siRNA. The next day, media from the cells was replaced with α-MEM supplemented with 5% FBS with antibiotics. Lullaby (OZ Biosciences, Marseille, France) transfection reagent was used for siRNA delivery into CHO-K1 cells. Both siRNA and Lullaby were diluted in serum and antibiotic free α-MEM and incubated for five minutes at room temperature. After five minutes, diluted siRNA was mixed gently with diluted Lullaby transfection reagent by flicking the tube gently and incubated for another twenty five minutes in order to form complexes. The complexes were added drop-wise with gentle swirling of the plate. The final concentration of siRNA per well was kept as 100 nM for each scrambled control, pooled as well as 3’UTR PHDX siRNAs. The cells were treated with siRNA for 48 hours but the complexes were removed from the cells after 24 hours by replacing the media with α-MEM supplemented with 10% FBS containing antibiotics. Then the cells were harvested for total RNA isolation.

2.13.3 RNA isolation and cDNA Synthesis

Total RNA was isolated from CHO-K1, mock transfected CHO-K1, CHO-K1 cells treated with scrambled control siRNA, Pooled siRNA and 3'UTR PHDX siRNA using RNeasy®Mini Kit (Qiagen, Mississauga, Ontario). Total RNA was resuspended in 30 µl of RNase-free water and quantified spectrophotometrically. One-5 µg each of total RNA was mixed with, 0.5 µg/µl OligodT Primers (Invitrogen, Burlinton, Ontario) and 2.5 mM dNTP mix (TaKaRa Biomedicals) and brought to a volume of 14.5 µl with dd H_2O. The mixture was heated at 65 °C for 5 minutes, quickly chilled on ice and cDNA synthesis mix containing 5 X RT buffer, Riblock RNAse Inhibitor and 200 units of Maxima® Reverse Transcriptase (Fermentas, Burlington, Ontario) to make a volume of 20 µl, was added to it and heated at 50 °C for 30 minutes and 85 °C for 5 minutes.

2.13.4 Multiplex PCR and Product Visualization

Gene expression for siRNA knock down experiments was determined by multiplex PCR using GAPDH as a control. cDNA equivalent to 300 ng of RNA was amplified with 10 X reaction buffer, 2.5mM dNTP mix, 5 units/µl TaKaRa Taq(TaKaRa Bio Inc., Otsu, Shiga, Japan) along with 10 µM Forward FF and Reverse RR primers and 10 µM GAPDH GSP1 and GAPDH GSP2 primers. The PCR mix was brought to a final volume of 25 µl. The samples were heated to 94 °C for one minute and then underwent 40 cycles of 94 °C for 15 seconds, 65 °C for 30 seconds and 72 °C for 1.15 minutes. The final extension was done at 72 °C for 10 minutes. After amplification, the products were separated and visualized on a 1% agarose gel containing 0.4 µg/ml of Ethidium Bromide.

2.14 Construction of pBABE Puro/*PHDX* cDNA Vectors

2.14.1 Total RNA Isolation and Amplification of *PHDX* cDNA

CHO-K1 cells were grown in 150 mm cell culture dishes and total RNA was isolated from the cells using RNeasy® Mini Kit (Qiagen, Mississauga Ont.) and resuspended in 30 µl of RNase-free water. The concentration of total RNA was determined spectrophotometically.

Five µg total RNA isolated from CHO-K1 cells was used to prepare cDNA by using Superscript II™ reverse transcriptase (Invitrogen, Burlington, Ontario) was added to the mixture and heated at 25 °C for 10 minutes, 42 °C for 50 minutes and 70 °C for 15 minutes.

2.14.2 Preparation of mouse *PHDX* (m*PHDX*) cDNA

The m*PHDX* cDNA was obtained from IMAGE Mouse cDNA clone (catalogue # EMM1002-22333, Open Biosystems, Huntsville, AL). The cDNA was amplified using proof reading Platinum® *pfx* DNA polymerase (Invitrogen, Burlington, ON). Following denaturaion at 94 °C for 2 minute, 2 µl of cDNA was subjected to 35 cycles of 94 °C for 15 seconds, 55 °C for 30 seconds, and 68 °C for 1.20 minutes. A final extension was done at 68 °C for 10 minutes.

2.14.3 Purification of m*PHDX* and CHO-K1 *PHDX* cDNA

The amplified *PHDX* cDNA from mouse was gel purified by Gel extraction Kit (Qiagen, Mississauga Ont.). The PCR amplified cDNA from Chinese hamster ovary cells was purified using PCR Purification Kit (Qiagen, Mississauga Ont.). The DNA was eluted in 30 µl of Elution Buffer and quantified spectrophotometrically.

2.14.4 Addition of Restriction sites

To add restriction sites BamH1 at 5' end and Sal1 at 3' end, the cDNA from both mouse and chinese hamster ovary cells was amplified again with primers FFBAMKOZ (containing BamH1 and kozak sequence) and RR SAL1 (containing Sal1), obtained from Eurofins MWG Operon **(**Huntsville, AL), using proof reading Platinum® *pfx* DNA Polymerase as mentioned before.

2.14.5 Restriction Digestion of *PHDX* cDNA and pBABE puro Vector

The *PHDX* cDNA from both mouse and Chinese hamster ovary cells and pBABE puro vector (obtained from Addgene, Cambridge, MA) underwent digestion with BamH1 and Sal1. Each of 50 µl DNA was combined with 5 µl each BamH1and Sal1 (New England Biolabs), 10 µl of restriction enzyme buffer (New England Buffer 3), 1 µl of 100 X BSA (10 mg/ml), 29 µl ddH_2O, mixed and incubated at 37 ºC for four hours and heat inactivated Sal1 at 65 ºC for 20 minutes. DNA from both mouse and CHO-K1 was purified using PCR Purification Kit (Qiagen, Mississauga Ont.) and eluted in 30 µl Elution Buffer.

2.14.6 Ligation of *PHDX* cDNA with pBABE Puro Vector

Digested and PCR purified 6 : 1 molar ratio of *PHDX* cDNA and pBABE puro DNA respectively was mixed with 2 µl 5 X Ligase Buffer and 1 µl T4 DNA Ligase (New England Biolabs – 400 U/ul, Ipswich, MA). The mixture was incubated overnight at 4 ºC

2.14.7 Transformation of pBABE puro/*PHDX* Constructs

The ligated vectors were transformed into chemically competent DH5α E. coli. Each of the 5µl ligated DNA (2.5-5 ng/µl) was mixed gently with 50 µl of competent cells by

gently flicking the tubes. The mixture was incubated for 20 minutes and transferred to 42 ºC water bath for 50 seconds and again incubated on ice for 2 minutes. 500 µl of SOC was added to the mixture and the tubes were incubated for 1.5 hours at 37 ºC with shaking. Fifty µl each of the transformation mixture was spread on LB plates with 100 mg/ml Ampicillin.

2.14.8 Sequence Verification of mouse *PHDX* (m*PHDX*) and Chinese hamster *PHDX* (K1*PHDX*) Contructs

The DNA was prepared from ampicillin resistant cells by Phenol-Chloroform extraction as mentioned before and the constructs with *PHDX* inserts were sequenced using pBabe F and pBabe R primers.Three hundred ng of DNA samples were sent for sequencing to Eurofin mwg/operon (Huntsville, AL).

2.14.9 Transfection of Phoenix Eco cells with pBABE Puro contructs

pBABE Puro empty vector and both the constructs were transfected in to Phoenix Eco retrovirus packaging cell line (DiCiommo *et al.*, 2004) (by using Lipofectamine™ 2000 (Invitrogen, Burlington, ON). One day prior to transfection, 6 X 10^6 Phoenix Eco cells were seeded in 10 cm cell-culture dishes (Nunclon, Roskilde, Denmark) with DMEM supplemented with 10% FBS. The next day12 µg of DNA was diluted in 1.5 ml serum free opti-MEM (Invitrogen, Burlington, ON) and 60 µl Lipofectamine and further diluted 1.5 ml with opti-MEM. The tubes were incubated for five minutes at room temperature. After five minutes, the DNA was combined with the transfection reagent, mixed gently by pipetting up and down and incubated for another 25 minutes at room temperature for the formation of

complexes. In the meantime, DMEM from Phoenix Eco cells was replaced with 15 ml of opti-MEM. After incubation, the complexes were added to the cells drop-wise by gently swirling the plate. The plates were returned to the incubator at 37 ºC with 5% CO_2 for twelve hours. The next day, serum free media from plates was removed with normal DMEM supplemented with 10% FBS and the plates were incubated at 32 ºC (since the virus are more stable at this temperature as compared to 37 ºC) with 5% CO_2. Supernatant containing virus was removed from the plates, replaced with fresh media. Supernatant was filtered with 0.45µm syringe filters (Nalgene, Rochester, NY), aliquoted in to 1 ml cryogenic vials (Nalgene, Rochester, NY), flash frozen in liquid N_2 and stored at -80 ºC. The virus harvest was done at 48, 56, 72, 80 and 96 hours.

2.14.10 Determination of Viral titre using NIH 3T3 cells

NIH3T3 cells were seeded at a density of 2 X 10^5 cells per well in six-well plates (Nunclon, Roskilde, Denmark) 24 hours prior to infection. The next day virus from 48 hour harvest was thawed on ice and 100 µl of virus was diluted with 900 µl of DMEM (supplemented with 10% FBS) and from this dilution (10^{-1}), further serial dilutions were done to obtain the dilutions *viz.* 10^{-2}, 10^{-3}, 10^{-4}, 10^{-5}, 10^{-6} and each well was infected with each dilution and one well was left untreated as a control along with 1 µl of polybrene (Sigma-Aldrich, St. Louis, MO) at a concentration of 6 mg/ml. The plates were incubated at 37 ºC with 5% CO_2 for twenty four hours and the media containing virus was removed with fresh media containing puromycin (Sigma-Aldrich, St. Louis, MO) at a concentration of 2.5 µg/ml. The selection media was replaced every other day and the colonies were counted after one week by staining with crystal violet. Number of colonies was divided by dilution factor

to determine the viral titre (TU/ml).

2.14.11 Expression of *PHDX* in E-126 and Cl-22 cells

E-126 and Cl-22 cells were split at a density of 1 X 10^6 cells per plate 24 hours prior to infection. The cells were infected with retrovirus containing pBABE Puro empty vector, pBABE mPHDX and pBABE K1PHDX at a ratio of 1:1 using polybrene (6 mg/ml). The cells were incubated for 24 hours as described above and the pooled E-126 and Cl-22 cells with both m*PHDX* and K1*PHDX* gene along with individual clones for each of the cell-lines were selected for puromycin resistance. The individual colonies were picked in the NSF biosafety cabinet under the microscope (Olympus Tokyo) and allowed to grow in media containing puromycin (2.5µg/ml). The gene expression of selected clones and pooled cells was determined by real time PCR as described in section 2.15.1 (Bustin, 2000).

2.15 Determination of Gene Expression of Cells expressing *PHDX*

2.15.1 Determination of Standard Curve for PCR Quantification

The pBABE puro plasmid with *PHDX* gene cloned into BamH1 and Sal1 sites was used to determine the copy nuber by using amount of plasmid DNA (ng) and its size (bp). The online resource was used to calculate the copy number (http://www.uri.edu/research/gsc/resources/cndna.html). The plasmid DNA was diluted to obtain copy number *viz.* 10^8, 10^7, 10^6, 10^5, 10^4, 10^3 in order to determine the standard curve. The diluted plasmid DNA (5ng each) was PCR amplified in triplicate through real time as mentioned below. Average ct Values and copy number were used to construct a standard

curve in Sigma Plot**.**

2.15.2 Absolute quantification by Real time PCR

Gene expression of Cl-22 and E-126 cells expressing *PHDX* gene was determined by Real Time PCR. To assess mRNA levels, absolute quantification method was used (Bustin, 2000).

Amplification was done in an iCyclerIQ (BioRad, ON, Canada). Each reaction mix contained SYBR Green (Sigma S9430), Fluorescein calibration dye (BioRad, 170-8780) and 200 nM of each primer and dNTP solution, 1X TaKaRa Reaction buffer and 0.5 units HS Taq Polymerase. The PCR conditions employed were 95 °C for 1 minute, 40 cycles of 95 °C for 30 seconds, 60 °C for 15 seconds and 72 °C for 20 seconds. The standard curve was constructed out of known copy numbers *viz.* 10^8, 10^7, 10^6, 10^5, 10^4, 10^3 from 185 bp long amplicon obtained from *PHDX* gene cloned into pBABE puro vector as described before. The mRNA copy number was determined from the average of triplicate ct values of different cells lines expressing *PHDX* gene from the standard curve. All ct Value calculations and graphing were performed in Microsoft Office Excel spreadsheet. The statistical analysis was done using one way Anova followed by Dunnett's post-hoc test in GraphPad Prism version 5. The products were run on 1% Agarose gel to confirm the size of the products.

2.15.3 Effect of Etoposide and Hydrogen Peroxide after the introduction of normal copy of *PHDX* gene in the mutated cell-line CHO E-126 and parental CHO Cl-22 Cells

The parental cells as well as cells expressing *PHDX* were tested for response to etoposide and hydrogen peroxide treatment by the MTT and CVS assays as previously mentioned.

CHAPTER 3 - RESULTS

3.1 Overview

This section of the thesis describes the analysis of the mutated *PHDX* gene identified from the mutated cell-line CHO E-126. The aim of my project was to test the hypothesis that the loss of the *PHDX* gene is involved in etoposide and hydrogen peroxide resistance. The analysis of *neo-PHDX* fusion product in CHO-E-126 cells was conducted followed by the analysis of the fusion protein. Next we knocked down the *PHDX* gene transiently by using small interfering RNA interference technology. The *PHDX* gene from Chinese hamster ovary cells was sequenced and subsequently *PHDX* genes from both mouse (*mPHDX*) and Chinese hamster (*K1PHDX*) were cloned into pBABE Puro retroviral vector. The constructs

were used for overexpression studies of the *PHDX* gene in CHO-Cl-22 and CHO-E-126 cells. The gene expression studies were conducted through either RT-PCR using *GAPDH* as a control or through real time PCR (absolute quantification) for the cell-lines created by using both shRNAi and siRNAi technologies and in the cell-lines overexpressing the *PHDX* gene. The cytotoxic effect of etoposide and hydrogen peroxide on all the cell-lines was determined through MTT assay and crystal violet staining colony formation assay.

3.2 Analysis of CHO E-126 Cells

3.2.1 Determination of *Neo-PHDX* fusion product and sequence analysis

Initially it was important to characterize the expression and structure of the normal and the mutated PHDX alleles, in order to determine that the E-126 cell line has the U3Neo retrovirus in it. The genomic DNA (gDNA) from these cells was used to amplify the region between ampicillin resistance gene and neophosphotransferase gene. For this the gDNA of CHO E-126 cells was amplified using primers Amp1 and Neo1. The gDNA of CHO Cl-22 was used as a negative control because this parental cell line did not have any retroviral insertion in it. The band at a position of 1.615 Kb obtained was the expected band size for this product **(Figure 7)**.

It was also important to see if *PHDX* and Neo were making a fusion transcript in CHO-E-126 cells which should be altogether absent in the parental CHO-Cl-22 cells because parental cells lack the U3Neo retrovirus insertion. Therefore, the mRNA of CHO E-126 cells was reverse transcribed and amplified using the primers cDNA L (based on 5' end of the mRNA transcript, priming at exon 2 starting at nucleotide position 153 of the *PHDX* gene)

and NeoR2 (based on U3NeoSV1 neomycin resistance gene). The two controls were used this time; cDNA of CHO Cl-22 for neo gene itself; and the water as a control for the DNA contamination because sometimes neo primers give false amplification products. The *Neo-PHDX* fusion band is slighly over 1Kb using RNA from CHO-E-126 cells, giving evidence of a fusion transcript **(Figure 7)**.

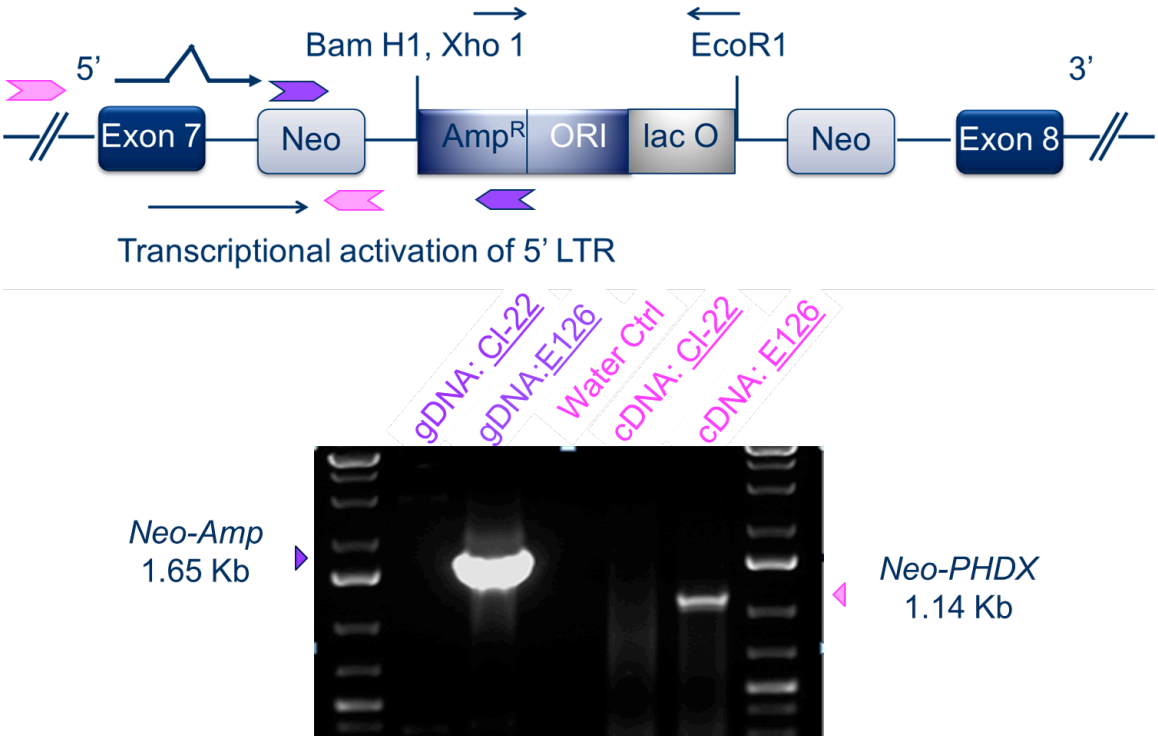

Figure 7: Verification of U3NeoSV1 contruct in E-126 cells

Upper Panel: The insertion of U3Neo retrovirus containing *Neo* and *Amp* genes is shown between exon 7 and 8 of the *PHDX* gene from 5'-3' end. Primers based on *Neo* and *Amp* genes shown in purple colour were used to amplify the gDNA of CHO-Cl-22 and CHO-E-126 cells. Primers based on 5' end of PHDX gene (forward primer) and Neo gene from the virus (reverse primer) in Pink color were used to amplify the cDNA of CHO-Cl-22 and CHO-E-126 cells.

Gel Picture: Lane 1 and 7: 1KB Plus ladder (Invitrogen); Lane 2: amplification of gDNA of CHO-Cl-22 cells by using Neo1 and Amp1 primers (-ve ctrl); Lane 3: amplification of gDNA of CHO-E-126 cells by using Neo1 and Amp1 primers; Lane 4: water control for neo primers; Lane 5: amplification of cDNA of CHO-Cl-22 cells by using cDNA L and Neo R2 primers (-ve ctrl); Lane 6: amplification of cDNA of CHO-E-126 cells by using cDNA L and Neo R2 primers (-ve ctrl)

The band obtained after cDNA amplification of CHO E-126 cells using the primers cDNA L and NeoR2 was sequenced (Robarts Research Institute, London, Ontario) **(Figure 8)**. The BlastN search was perfomed on the sequence obtained after sequencing the Neo-PHDX band. The sequence showed 92 percent sequence similarity with *PHDX* **(Figure 9)** and *neo* **(Figure 10)** genes, thus validating the construct present in CHO E-126 cells. The gaps in the blast result represent the mismatches between the two sequences blasted. The Neo-PHDX fusion protein showed the utilization of the stop codon of the *Neo* gene. The partial protein sequence (exon 2-7) showed 94.3% homology with the translated hypothetical protein sequence obtained from the database **(Figure 11)**.

```
   1 CCCCCCCCCC GGGCAGAGGA ATGGCTAAGG ACTGTGGCCC TTGGAGTAGG
  51 TCTTGCTCTG ATCACATTCC TGCTCTGGAG TAGTCTGGGG ATTGATGACG
 101 ATGTTGCTGA AGTCTTGGCC CGTCGAGGTG AGGTCCTAGA AGGCAGGTTC
 151 ATTGAGGTTC CCTGCTCTGA GGACTATGAT GGTCACCGAA AATTTGAAGG
 201 CTGCACCCCC AAGAAGTGTG GCACAGGTGT CACTGACATG GTGATCACCA
 251 GGGAGGAGGC CGAGCAGATT CGCAGAATAG CAGAGAAGGG GCTCTCCCTA
 301 GGTGGATCGG ATGGAGGGGC ATCTATCCTG GACTTGCACT CTGGGGCCCT
 351 GTCTGTTGGG AAACATTTTG TGAACCTGTA CAGATACTTT GGGGATAAAA
 401 TACAAAATAT CTTCTCTGAG GAGGACTTCC AGTTATATAG GGATGTGCGG
 451 CAGAAGGTCC AGCTCACCAT TGCTCTCCGG CCGCTTGCAA AGCTTTTGGC
 501 ATCAGTGCAT CCTTGCTGTA TCTGACAAAG CCCACATTCT TCTCCCGAAT
 551 CAATAGTACG GAAGCCCAGA CGGCTCACGA TGAGTACTGG CATGCACACG
 601 TACACAAGGT GGTGGAGAGG CTATTCCGCT ATGACTGGGC ACAACAGAAA
 651 TCGGCTGCTC TGATGCCGCC GTGTTCCGGC TGTCAGCGCA GGGGCGCCCG
 701 GTTTCTTTTT GTCAGACCGA CCTGTCCGGT GCCCTGAATG AACTGCATGA
 751 CGAGGCAACG CGCCTATCGT GGCTGGCCAC AACGGGCGTT CCTTGCCACT
 801 GTGCTCACCT TGTCCCTGAA GCGACAAGGG ACTGGCTGCT ATTTGGCAAA
 851 TGCCGGGCAG GATCTCCTGT CTTCTCCCCT TGCTCCTGCC AAAAAGTATC
 901 CATCATGGCG AAAGCAATGG GCGGCTGGCA AAACCTGGTC CCGGCTCCCC
 951 GCCCTTCCCC CCCAATCAAA ACATTGCGTT CGCGGCAACC CGTCT
```

Figure 8: CHO E-126 cDNA sequencing results reveal the junction between *PHDX*-Neo fusion gene

Unhighlighted sequence showing the *PHDX* gene (exon 2 to 7); Green highlighted -- Neophosphotransferase gene

GENE ID: 66179 1110031I02Rik | RIKEN cDNA 1110031I02 gene [Mus musculus]

Score = 645 bits (349), Expect = 0.0
Identities = 424/460 (92%), Gaps = 5/460 (1%)

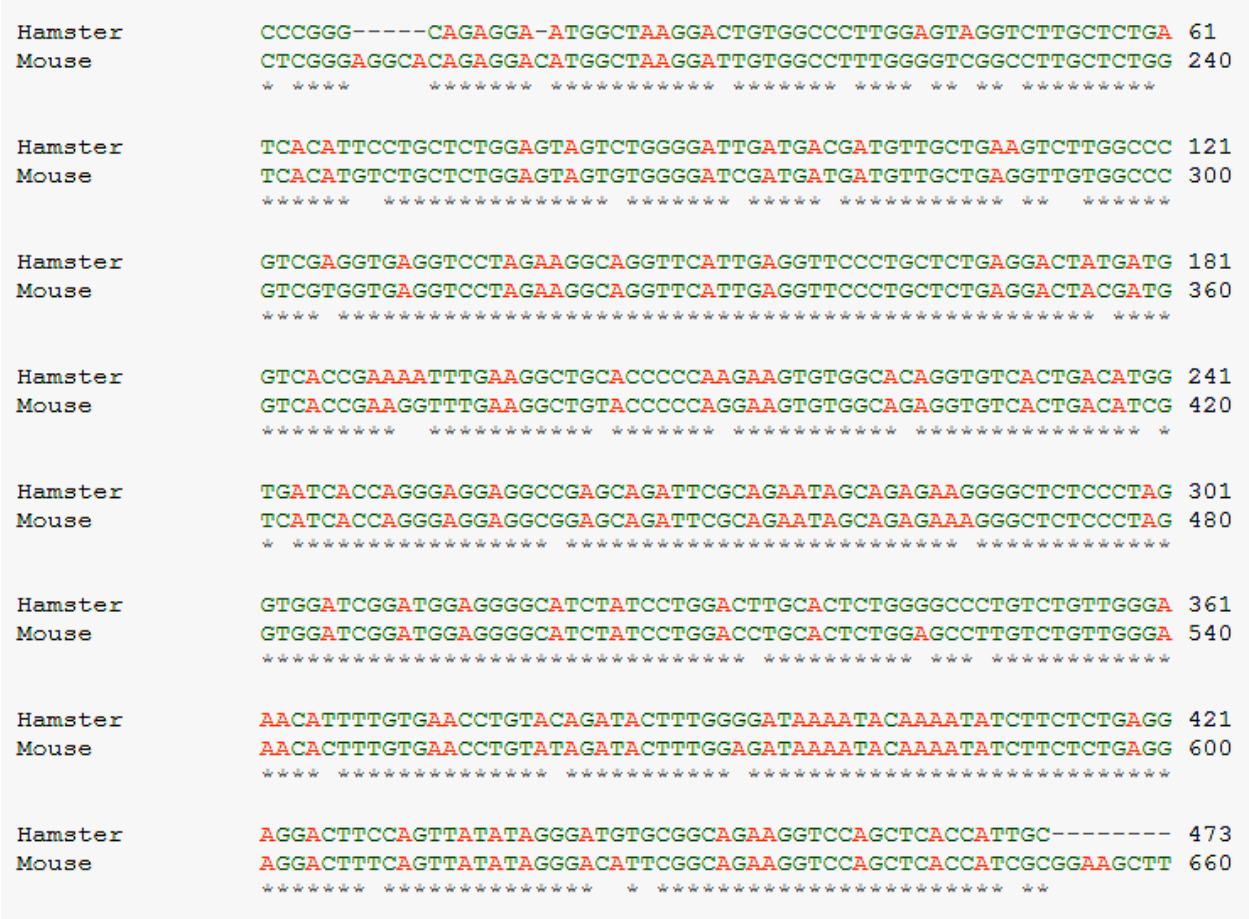

Figure 9: Blast result of *PHDX* gene from E-126.

Part of the sequence obtained from CHO-E-126 (Hamster) showing identity with the *PHDX* gene sequence obtained from Mouse (upto exon 7). Gaps represent the mismatches/insertions/deletions.

Score = 388 bits (210), Expect = 2e-111
Identities = 256/277 (92%), Gaps = 8/277 (3%)
Strand=Plus/Plus

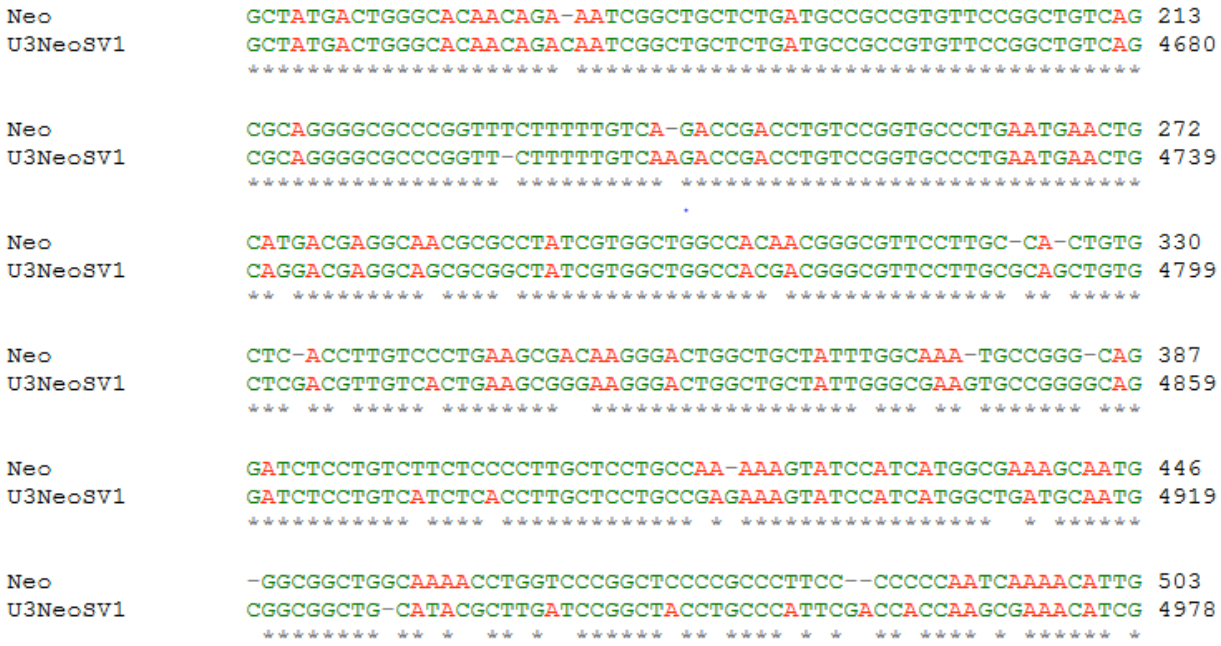

Figure 10: Blast result of *Neo* gene from E-126.

Part of the sequence obtained from CHO-E-126 showing identity with *Neophosphotransferase* gene. Gaps represent the mismatches/insertions/deletions.

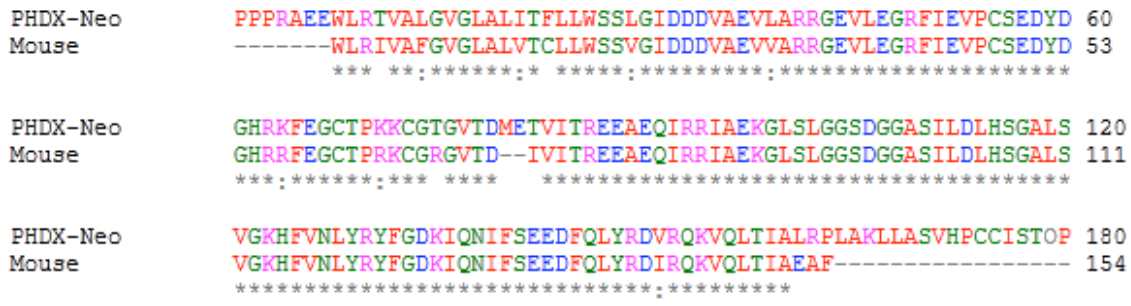

Figure 11: Blast result of Neo-PHDX fusion protein from E-126 cells with mouse PHDX hypothetical protein (from exon 1-7 obtained from database).

Gaps represent either the insertions of amino acids in PHDX-Neo (sequence translated from the database) or deletions of amino acids in mouse PHDX hypothetical protein and colons represent amino acid substitutions between the two sequences.

3.2.2 Neo-PHDX fusion protien

The sequencing of mRNA transcript from E-126 cells revealed Neo-PHDX fusion. It was of further interest to see if the fusion protein in E-126 cells. Therefore total protein was isolated from CHO-K1 and CHO- E-126. 50 μg of total protein from both cell lines was loaded and probed with neophosphotransferase polyclonal antibody. GAPDH was used as a control **(Figure 12)**. The molecular weight of Neo-PHDX fusion protein was calculated by translating the *Neo* and the *PHDX* gene sequences obtained from the database (see the details below).

Approximate Total Molecular weight of PHDX-Neo Fusion Protein:
Approximate Molecular weight of PHDX protein (Exon 1 to 7) = **25.95** kilodaltons
Approximate Molecular weight of Neophosphotransferase protein = **9.98** kilodaltons
Total approximate Molecular weight of PHDX-Neo fusion protein = **35.88** kilodaltons

The size of *Neo-PHDX* fusion protein was found to be around 35KDa which is the expected size as calculated after translating the *Neo-PHDX* gene sequence. GAPDH band was found as expected at approximately 37 KDa. The Neo-PHDX protein band was specific for E-126 cells only. The CHO-K1 protein was used as a negative control because CHO-K1 cells don't have neo cassette inserted in them. The other bands seen in the picture common to both CHO-K1 Cells and E-126 cells except for GAPDH bands are non-specific bands.

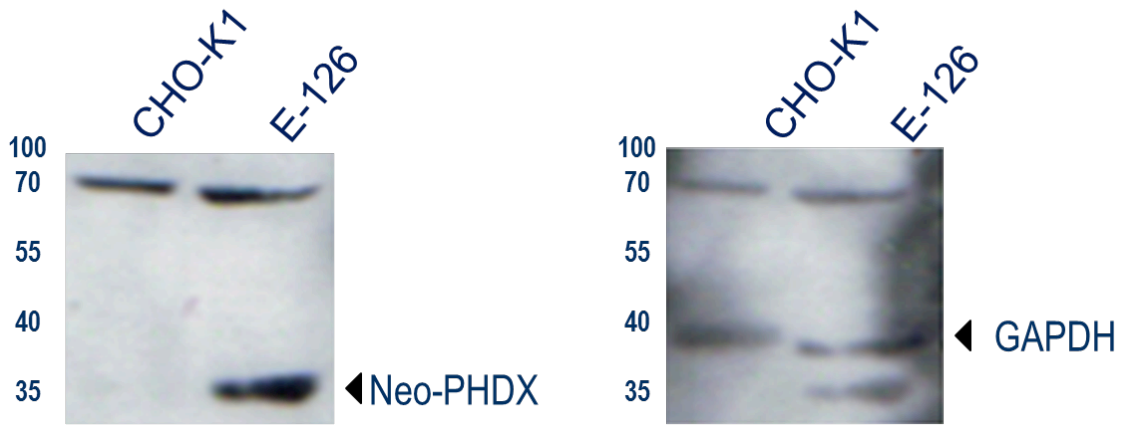

Figure 12: Western blot showing *PHDX*-Neo fusion protein.

The fusion protein is present in E-126 cells but absent in CHO-K1 cells (Left panel – band at approximately calculated from blot using markers around 35 Kda). 50 µg of total protein was loaded. The primary antibody used was Anti-Neophosphotransferase II polyclonal antibody and secondary antibody used was horse-radish peroxidase-conjugated anti-Rabbit antibody. GAPDH band is seen at approximately 37 KDa (Right panel ---PHDX-Neo band is also seen below because of incomplete stripping of the filter). The primary antibody used was GAPDH rabbit polyclonal IgG antibody and secondary antibody used was horse-radish peroxidase-conjugated anti-Rabbit antibody.

3.3 Cytotoxicity Profile of E-126 Cells

3.3.1 Etoposide and Hydrogen Peroxide MTT Assays

To confirm that the E-126 cells were resistant to etoposide and hydrogen peroxide, the MTT assays were carried out **(Figure 13 and 14)**. CHO-E-126 cells showed significant resistance to both etoposide **(Table 2)** and hydrogen peroxide **(Table 3)**.

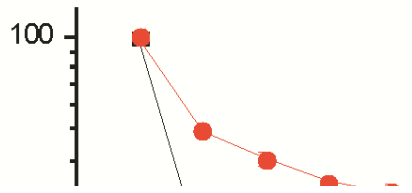

Figure 13: Effect of cytotoxicity of etoposide on CHO Cl-22 and CHO E-126 cells through MTT assay.

Cells were incubated for 48 hour with 0, 50, 100, 150, 200 and 250 μM etoposide. Cytotoxicity was determined by MTT assay and is presented as the surviving cell fraction (optical density in treated cells as a fraction of the optical density in cells treated with DMSO). Error bars represent standard error of mean of n = 4 biological replicates.

Table 2: Statistical analysis of survival curves for CHO-E-126 through MTT

etoposide assay.

Comparison of mean IC_{50} values of CHO-126 cells with that of parental CHO-Cl-22 cells by using Student's t-Test.

Cell-Line	Mean IC 50 (µM)	pValue-t-Test
Cl-22	5.649 ± 0.6021 N=4	
E-126	35.23 ± 1.125 N=4	P<0.0001

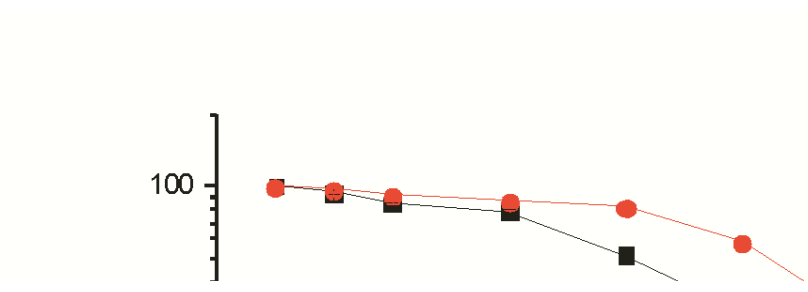

Figure 14: Effect of cytotoxicity of hydrogen peroxide on CHO-K1 and CHO E-126 cells through MTT assay.

Cells were incubated for 48 hours with 0, 50, 100, 200, 300, 400, 500 and 600µM hydrogen peroxide. Cytotoxicity was determined by MTT assay and is presented as the surviving cell fraction (optical density in treated cells as a fraction of the optical density in untreated cells). Error bars represent standard error of mean of n = 4 biological replicates.

Table 3 : Statistical analysis of survival curves for CHO-E-126 through MTT

hydrogen peroxide assay.

Comparison of mean IC_{50} values of CHO-126 cells with that of parental CHO-Cl-22 cells by using Student's t-Test.

Cell-Line	Mean IC 50 (µM)	pValue-t-Test
Cl-22	242.4 ± 3.731 N=4	
E-126	442.7 ± 24.66 N=4	0.0002

3.3.2 Results of Etoposide and Hydrogen Peroxide Crystal Violet Staining Assays

The MTT assay is a measure of mitochondrial function since the yellow coloured MTT is metabolized by mitochondria to produce purple coloured insoluble formazan crystals. The purple coloured crystals are dissolved to measure the absorbance of light.

Therefore the test is used to measure the ability of mitochondria to metabolize the MTT in the living cells.The reactive oxygen species generated by both etoposide and hydrogen peroxide might affect mitochondrial function and hence affect the assay itself. So that we could assess drug resistance accurately, we used a clonogenic assay which is not directly measuring mitochondrial function. Clonogenic assays measure the long term ability of the cells to form colonies after recovery from the drug treatment. In this way we could validate drug resistance without the limitations of the MTT assay. Therefore we used the crystal violet staining assay to determine cytotoxic effect of etoposide and hydrogen peroxide. It was found that the crystal violet staining assay after treatment with etoposide **(Figure 15)** and hydrogen peroxide **(Figure 16)** also showed resistance of the E-126 cell line compared with Cl-22 cells. The mean IC_{50} value of CHO-E-126 cells showed a significant difference compared with the parental CHO-Cl-22 cells for both etoposide **(Table 4)** and hydrogen peroxide **(Table 5)**. The results of statistical analysis validate the resistance shown by mutated CHO-E-126 cells to etoposide and hydrogen peroxide treatment.

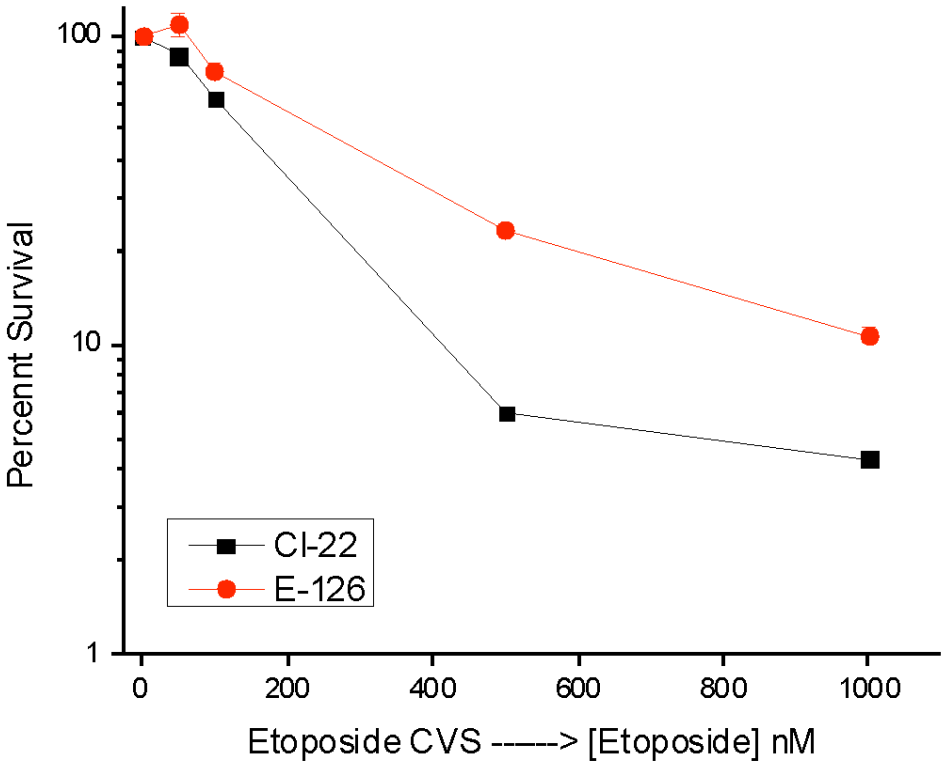

Figure 15: Effect of cytotoxicity of etoposide on CHO-K1, CHO Cl-22 and CHO E-126 cells through CVS assay.

Cells were incubated for 48 hour with 0, 50, 100, 500, and 1000 nM etoposide. Cytotoxicity was determined by CVS assay and is presented as the % surviving cell fraction (optical density in treated cells as a fraction of the optical density in cells treated with DMSO). Error bars represent standard error of mean of n= 4 biological replicates.

Table 4: Statistical analysis of survival curves for CHO-E-126 through CVS etoposide assay.

Comparison of mean IC_{50} value of CHO-126 cells with that of parental CHO-Cl-22 cells by using Student's t-Test.

Cell-Line	Mean IC 50 (nM)	pValue-t-Test
Cl-22	140.5 ± 10.31 N=4	
E-126	224.0 ± 12.93 N=4	0.0023

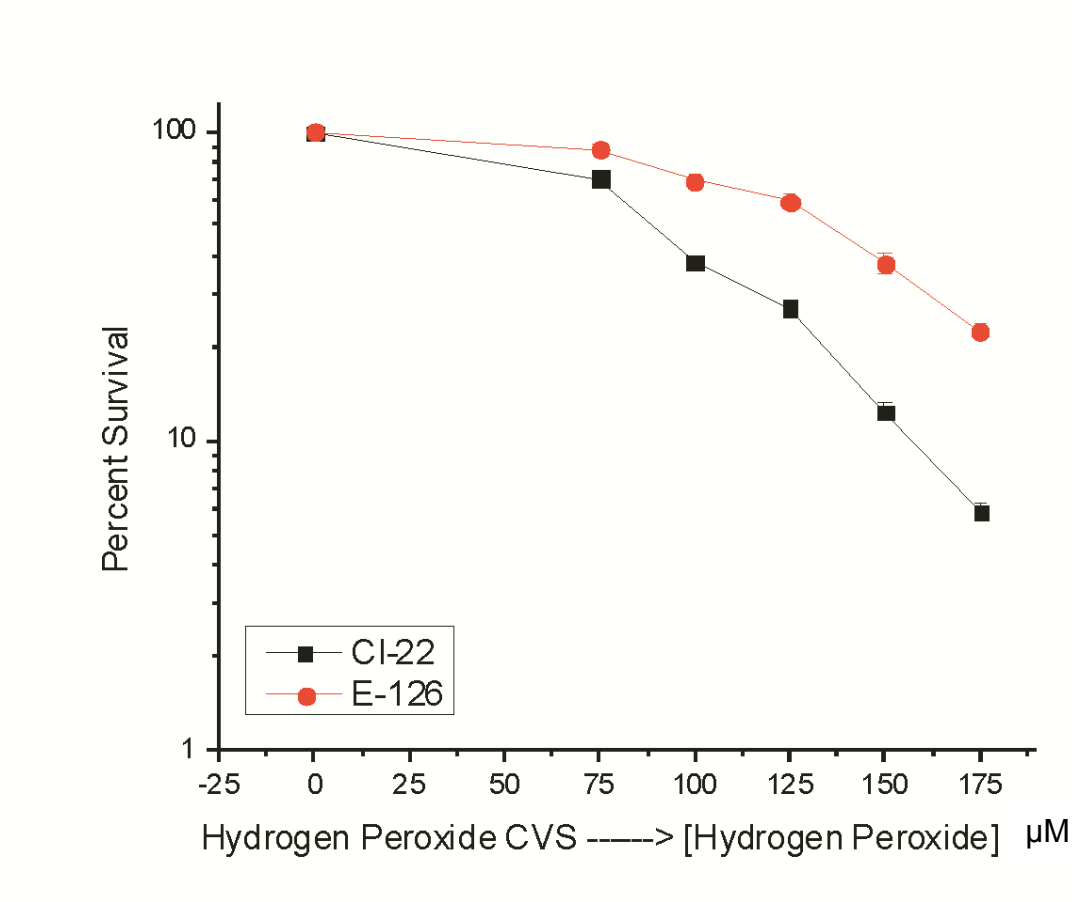

Figure 16: Effect of cytotoxicity of hydrogen peroxide on CHO-K1, CHO Cl-22 and CHO E-126 cells through CVS assay.

Cells were incubated for 48 hours with 0, 75, 100, 125, 150 and 175µM hydrogen peroxide. Cytotoxicity was determined by CVS assay and is presented as the % surviving cell fraction (optical density in treated cells as a fraction of the optical density in untreated cells). Error bars represent standard error of mean of n = 4 biological replicates.

Table 5: Statistical analysis of survival curves for CHO-E-126 through CVS hydrogen

peroxide assay.

Comparison of mean IC_{50} value of CHO-126 cells with that of parental CHO-Cl-22 cells by using Student's t-Test.

Cell-Line	Mean IC 50 (µM)	pValue-t-Test
Cl-22	56.49 ± 3.176 N=4	
E-126	149.2 ± 14.08 N=4	0.0007

3.4 Sequence Comparison of *PHDX*: CHO-K1 Vs Mouse

The sequencing of the Chinese hamster (*Cricetulus griseus*) genome has yet to be completed. Therefore in order to know the sequence of the *PHDX* mRNA from Chinese

hamster ovary (CHO-K1) cells, total RNA from CHO-K1 cells was reverse transcribed and amplified using the primers (based on mouse *PHDX* gene) pBABE F (forward primer) and cDNA R (reverse primer). The cDNA was sequenced (Robarts Research Institute, London, Ontario) using the same primers (**Figure 17)**. The sequence analysis revealed 98% sequence similarity for *PHDX* gene between cDNA from CHO-K1 and mouse **(Figure 18)**.

Sequence of PHDX gene from CHO-K1 cells

>C**hinese hamster (*Cricetulus griseus*)**

```
  1 GGGGGGGTTT TGCCTGCGAG GCTGGGCCGA TGGCGCCTCA GCGGAGGGGA
 51 CCACCCAGAA TTCCCGAGGG AAGTAGTGCT GCAGAGCGCC GGCGCGCGAC
```

```
 101 CAGTACCAAG AAGGACCGGC TGCCTCGGGA GGCACAGAGG ACATGGCTAA
 151 GGATTGTGGC CTTTGGGGTC GGCCTTGCTC TGGTCACATG TCTGCTCTGG
 201 AGTAGTGTGG GGATCGATGA TGATGTTGCT GAGGTTGTGG CCCGTCGTGG
 251 TGAGGTCCTA GAAGGCAGGT TCATTGAGGT TCCCTGCTCT GAGGACTACG
 301 ATGGTCACCG AAGGTTTGAA GGCTGTACCC CCAGGAAGTG TGGCAGAGGT
 351 GTCACTGACA TCGTCATCAC CAGGGAGGAG GCGGAGCAGA TTCGCAGAAT
 401 AGCAGAGAAA GGGCTCTCCC TAGGTGGATC GGATGGAGGG GCATCTATCC
 451 TGGACCTGCA CTCTGGAGCC TTGTCTGTTG GGAAACACTT TGTGAACCTG
 501 TATAGATACT TTGGAGATAA AATACAAAAT ATCTTCTCTG AGGAGGACTT
 551 TCAGTTATAT AGGGACATTC GGCAGAAGGT CCAGCTCACC ATCGCGGAAG
 601 CTTTCGGCAT CAGTGCATCC TTGCTGTACC TGACGAAGCC CACATTTTTC
 651 TCGCGAATAA ATAGCACAGA AGCCCGGACA GCTCATGATG AGTACTGGCA
 701 CGCACACGTG GACAAGGTGA CCTACGGCTC TTTTGACTAC ACTTCGCTGC
 751 TTTACCTATC GGATTACTTA GAGGACTTCG GTGGAGGGCG CTTTGTGTTC
 801 ATGGAAGAAG GGTCCAACAA GACAGTGGAG CCCAGAGCTG GTCGAGTCTC
 851 ATTCTTTACC TCAGCTCTGA GAACCTGCAC CGAGTGGAAA AGTCCTCTGG
 901 GGCACCCGCT ACGCCATCAC CATCGCTTTC ACCTGCAACC CGGACCACGG
 951 CATCGAGGAA CCAGTACTCA CGTGACCAAC TAGGTCAGGT CCTGAGTACC
1001 ATGTCCTGTC AAAAAGCACT CCTAGGCCGG GGGGGAGGGG GGTCCATTTC
1051 TCCCCCTTCG GGGCATTGCT GCTGCTCAAT GTGGCCTAAA
```

Figure 17: cDNA Sequence of *PHDX* gene obtained from Chinese hamster ovary cells.

GENE ID: 66179 1110031I02Rik | RIKEN cDNA 1110031I02 gene [Mus musculus]

Score = 1882 bits (1019), Expect = 0.0

Identities = 1062/1081 (98%), Gaps = 9/1081 (1%)
Strand=Plus/Plus

```
Hamster         CTGCGA-GGCTGGG-CCGATGGCGCCTCAGCGGAGGGGACCACCCAGAATTCCCGAGGGA 58
Mouse           CTGCGACGGCTGGGCCCGATGGCGCCTCAGCGGAGGGGACCACCCAGAATTCCCGAGGGA 60
                ****** ******* ************************************************

Hamster         AGTAGTGCTGCAGAGCGCCGGCGCGCGACCAGTACCAAGAAGGACCGGCTGCCTCGGGAG 118
Mouse           AGTAGTGCTGCAGAGCGCCGGCGCGCGACCAGTACCAAGAAGGACCGGCTGCCTCGGGAG 120
                ************************************************************

Hamster         GCACAGAGGACATGGCTAAGGATTGTGGCCTTTGGGGTCGGCCTTGCTCTGGTCACATGT 178
Mouse           GCACAGAGGACATGGCTAAGGATTGTGGCCTTTGGGGTCGGCCTTGCTCTGGTCACATGT 180
                ************************************************************

Hamster         CTGCTCTGGAGTAGTGTGGGGATCGATGATGATGTTGCTGAGGTTGTGGCCCGTCGTGGT 238
Mouse           CTGCTCTGGAGTAGTGTGGGGATCGATGATGATGTTGCTGAGGTTGTGGCCCGTCGTGGT 240
                ************************************************************

Hamster         GAGGTCCTAGAAGGCAGGTTCATTGAGGTTCCCTGCTCTGAGGACTACGATGGTCACCGA 298
Mouse           GAGGTCCTAGAAGGCAGGTTCATTGAGGTTCCCTGCTCTGAGGACTACGATGGTCACCGA 300
                ************************************************************

Hamster         AGGTTTGAAGGCTGTACCCCCAGGAAGTGTGGCAGAGGTGTCACTGACATCGTCATCACC 358
Mouse           AGGTTTGAAGGCTGTACCCCCAGGAAGTGTGGCAGAGGTGTCACTGACATCGTCATCACC 360
                ************************************************************

Hamster         AGGGAGGAGGCGGAGCAGATTCGCAGAATAGCAGAGAAAGGGCTCTCCCTAGGTGGATCG 418
Mouse           AGGGAGGAGGCGGAGCAGATTCGCAGAATAGCAGAGAAAGGGCTCTCCCTAGGTGGATCG 420
                ************************************************************

Hamster         GATGGAGGGGCATCTATCCTGGACCTGCACTCTGGAGCCTTGTCTGTTGGGAAACACTTT 478
Mouse           GATGGAGGGGCATCTATCCTGGACCTGCACTCTGGAGCCTTGTCTGTTGGGAAACACTTT 480
                ************************************************************

Hamster         GTGAACCTGTATAGATACTTTGGAGATAAAATACAAAATATCTTCTCTGAGGAGGACTTT 538
Mouse           GTGAACCTGTATAGATACTTTGGAGATAAAATACAAAATATCTTCTCTGAGGAGGACTTT 540
                ************************************************************

Hamster         CAGTTATATAGGGACATTCGGCAGAAGGTCCAGCTCACCATCGCGGAAGCTTTCGGCATC 598
Mouse           CAGTTATATAGGGACATTCGGCAGAAGGTCCAGCTCACCATCGCGGAAGCTTTCGGCATC 600
                ************************************************************
```

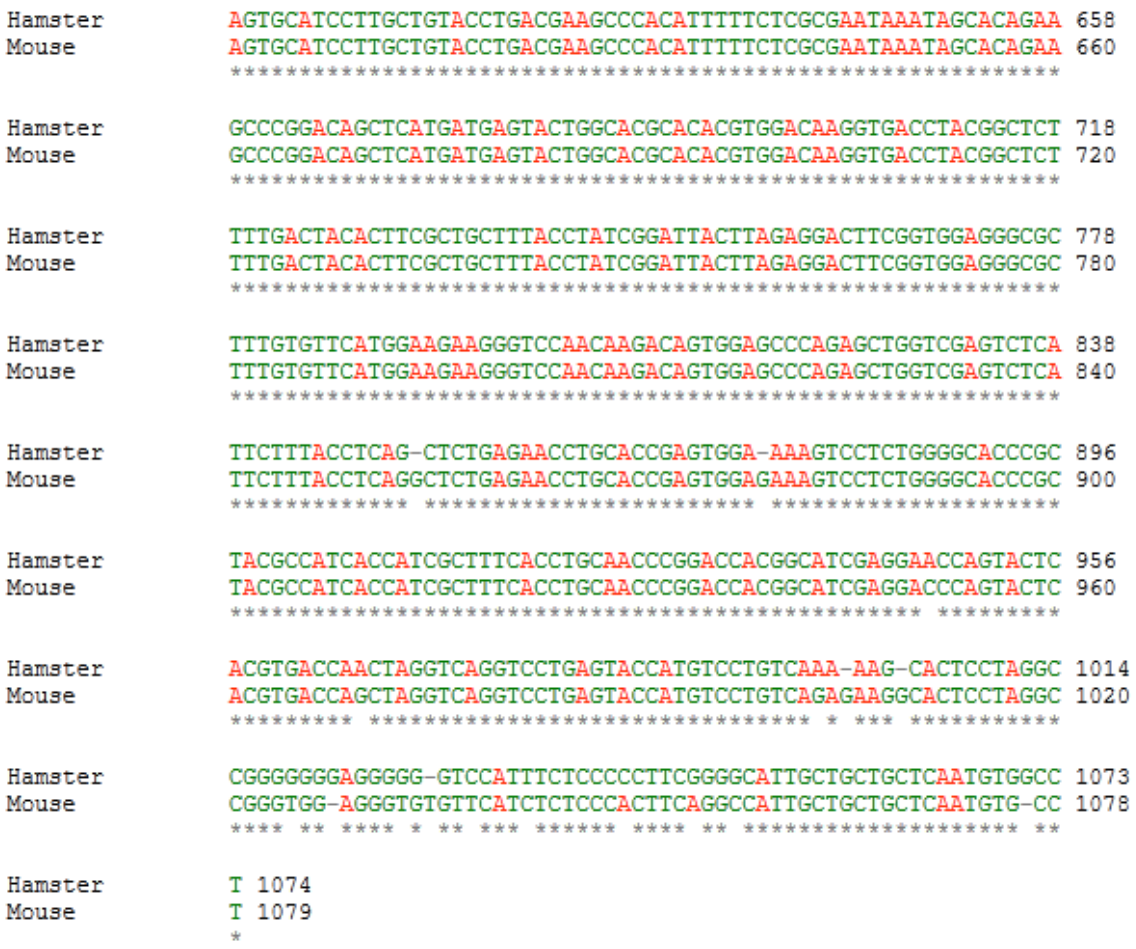

Figure 18: cDNA Sequence Comparison: CHO-K1 (Hamster) Vs Mouse for *PHDX* gene showing 98% similarity. The gaps represent the mismatches/insertions/deletions.

3.5 siRNA Knockdown of *PHDX* gene

3.5.1 Determination of Knockdown of *PHDX* gene

In previous work, we could not determine the involvement of *PHDX* gene through shRNA interference because of the off target effects of short hairpin RNA for etoposide resistance (data not shown). Therefore to try to overcome the off target effects of shRNA, the PHDX gene in CHO-K1 cells was knocked down transiently using small interfering RNAs. A pool of four siRNA targeting the open reading frame and 3' UTR of the *PHDX* gene were designed and used for these experiments. The gene expression was determined through RT-PCR using GAPDH as a control. The mock transfected CHO-K1 cells were used as a positive control for transfection and scrambled control was used as control for both types of siRNA **(Figure 19)**.

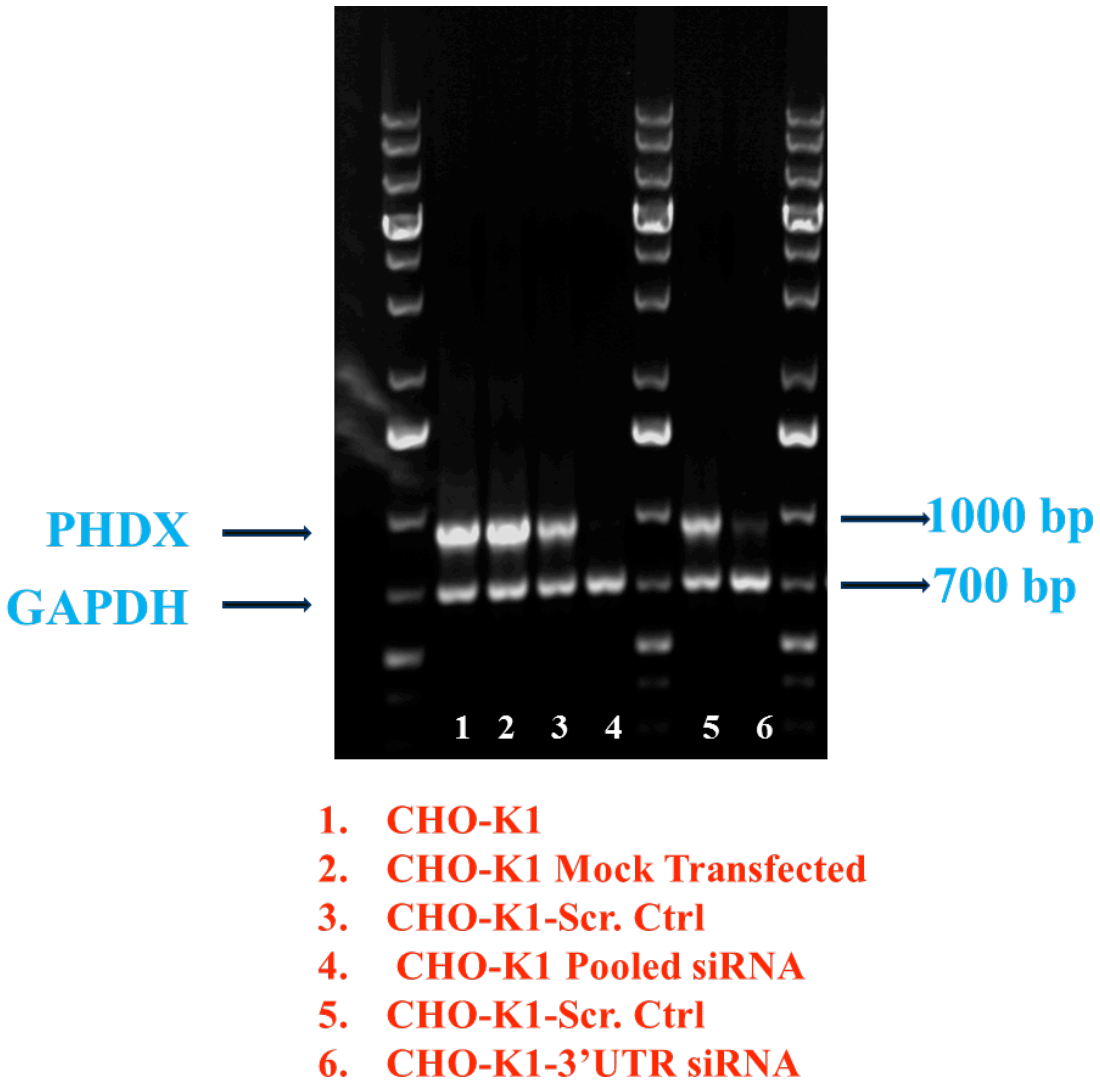

Figure 19: RT-PCR showing siRNA knockdown of the *PHDX* gene in CHO-K1 cells.

Lane 1: CHO-K1 untransfected cells; Lane 2: CHO-K1 mock transfected cells; Lane 3 and 5: CHO-K1 cells treated with scrambled control siRNA; Lane 4: CHO-K1 treated with a pool of four siRNAs designed to target open reading frame of *PHDX* gene (Pooled siRNA - Rik 1-4); Lane 6: CHO-K1 cells treated with siRNA designed to target 3' untranslated region of *PHDX* gene. 1KB plus marker from Genelute is shown at corners and in the centre.

3.5.2 Determination of Cytotoxic effect of Etoposide and Hydrogen peroxide on CHO-K1 cells knocked down of *PHDX* gene expression through siRNA

The Chinese hamster ovary cells were treated with different concentrations of etoposide **(Figure 20)** after treatment with scrambled control siRNA and both the siRNAs (targeted to knock down the *PHDX* gene). The scrambled control siRNA treated cells showed sensitivity at lower concentrations of etoposide but at the highest concentration it didn't show much difference as compared to parental CHO-K1 cells. This correlates well to the gene expression of both cells treated with the scrambled control and parental CHO-K1 cells suggesting some off target effects of siRNA. The cells having knocked down *PHDX* expression through different siRNAs clearly show resistance to etoposide at a highly significant pValue as compared to the CHO-K1 cells treated with the scramble control siRNA **(Table 6)**.

The effect of hydrogen peroxide was also determined through crystal violet staining assay by treating the control and knocked down cells with various concentration of hydrogen peroxide **(Figure 21)**. The parental and scrambled control treated CHO-K1 cells were not found to be significantly different. However CHO-K1 cells treated with both pooled and 3'UTR siRNA showed resistance at a high significance when compared with the scrambled RNAi control cells **(Table 7)**.

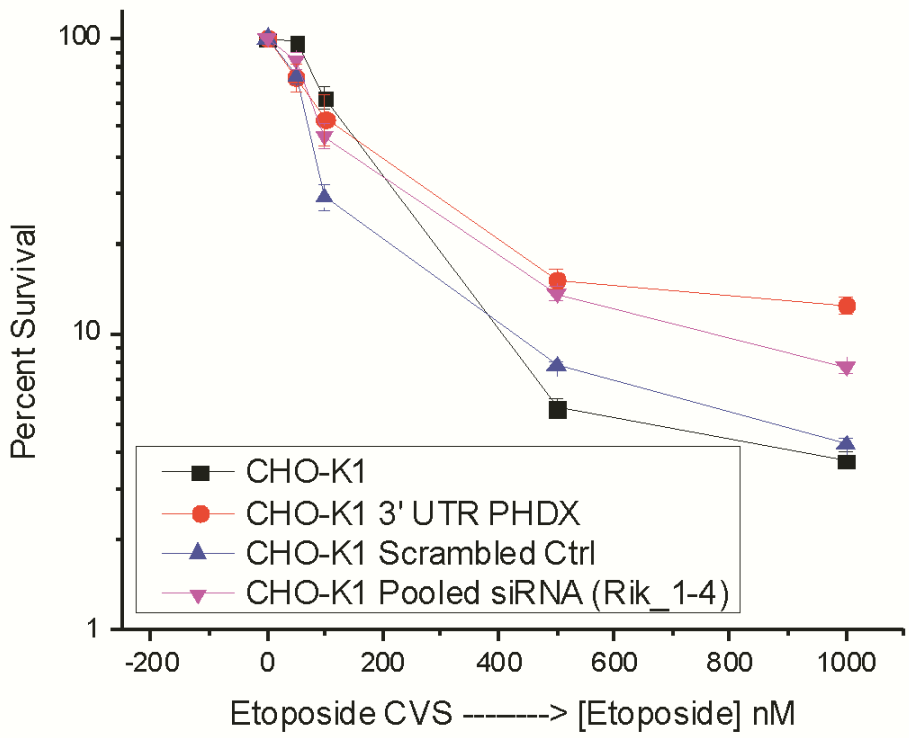

Figure 20: Effect of cytotoxicity of etoposide on CHO-K1, siRNA scrambled control and siRNA knockdowns through CVS assay.

Cells were incubated for 48 hour with 0, 50, 100, 500, and 1000 nM etoposide. Cytotoxicity was determined by CVS assay and is presented as the % surviving cell fraction (optical density in treated cells as a fraction of the optical density in cells treated with DMSO). Error bars represent standard error of mean of

n = 4 biological replicates.

Table 6 Statistical analysis of survival curves for siRNA knockdown of CHO-K1 cells

through CVS etoposide assay.

Comparison of mean IC_{50} value of CHO-K1 scrambled control cells with that of parental CHO-K1 cells; CHO-K1 3' UTR PHDX cells with that of CHO-K1 scrambled control cells and CHO-K1 Pooled siRNA (Rik 1-4) with that of CHO-K1 scrambled control cells by using Student's t-Test.

Cell-Line	Mean IC 50 (nM)	pValue-t-Test
CHO-K1	155.5 ± 12.01 N=4	
CHO-K1 Scrambled Ctrl	48.02 ± 2.022 N=4	0.0001
CHO-K1 Pooled siRNA (Rik 1-4)	95.21 ± 7.476 N=4	0.0009
CHO-K1 3'UTR PHDX siRNA	91.95 ± 9.750 N=4	0.0045

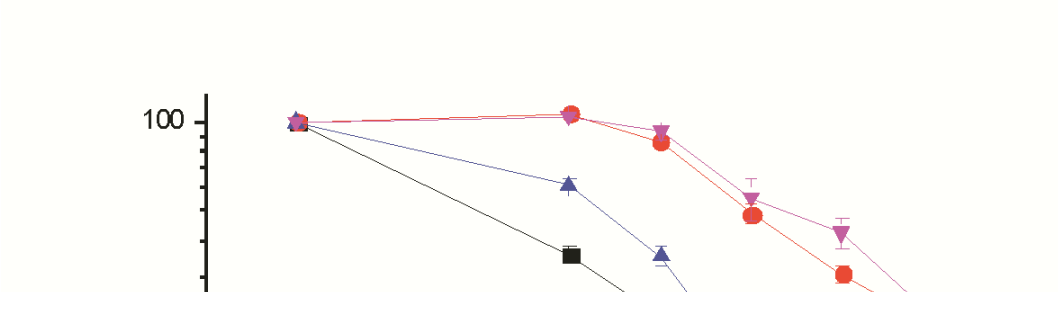

Figure 21: Effect of cytotoxicity of Hydrogen Peroxide on CHO-K1, siRNA scrambled control and siRNA knockdowns through CVS assay.

Cells were incubated for 48 hours with 0, 75, 100, 125, 150 and 175μM hydrogen peroxide. Cytotoxicity was determined by CVS assay and is presented as the % surviving cell fraction (optical density in treated cells as a fraction of the optical density in untreated cells). Error bars represent standard error of mean of n = 4 biological replicates.

Table 7: Statistical analysis of survival curves for siRNA knockdown of CHO-K1

through CVS hydrogen peroxide assay.

Comparison of mean IC_{50} value of CHO-K1 scrambled control cells with that of parental CHO-K1 cells; CHO-K1 3' UTR PHDX cells with that of CHO-K1 scrambled control cells and CHO-K1 Pooled siRNA (Rik 1-4) with that of CHO-K1 scrambled control cells by using Student's t-Test.

Cell-Line	Mean IC 50 (µM)	pValue-t-Test
CHO-K1	28.77 ± 2.667 N=4	
CHO-K1 Scrambled Ctrl	34.43 ± 4.418 N=4	0.3148
CHO-K1 Pooled siRNA (Rik 1-4)	205.9 ± 32.59 N=4	0.002
CHO-K1 3'UTR PHDX siRNA	162.5 ± 5.621 N=4	< 0.0001

3.6 Overexpression of *PHDX* gene

The small interfering RNA interference studies revealed an association of *PHDX* gene loss in etoposide and hydrogen peroxide resistance. The overexpression studies were conducted in both CHO-Cl-22 and CHO-E-126 cells for further functional study of this gene.

The *PHDX* genes from mouse (*mPHDX*) as well as Chinese hamster ovary cells (*K1PHDX*) were cloned into pBABE puro retroviral vector. CHO-Cl-22 and CHO-E-126 cells were infected separately with both constructs and stable cell-lines through puromycin selection were created by taking pooled cells and individual clones. CHO-Cl-22 and CHO-E-126 cells were also infected with the empty vector to serve as control for both types of overexpression studies. The gene expression was determined by real time RT-PCR through absolute quantification.

3.6.1 Overexpression of *PHDX* gene in CHO-Cl-22 cells

The expression levels of the transfected *PHDX* gene was determined by real time RT-PCR using the absolute quantification method **(Figure 22)**.The statistical significance of the gene expression levels between cell lines was done by one way Anova analysis (Dunnett's post-hoc test) GraphPad Prism 5.

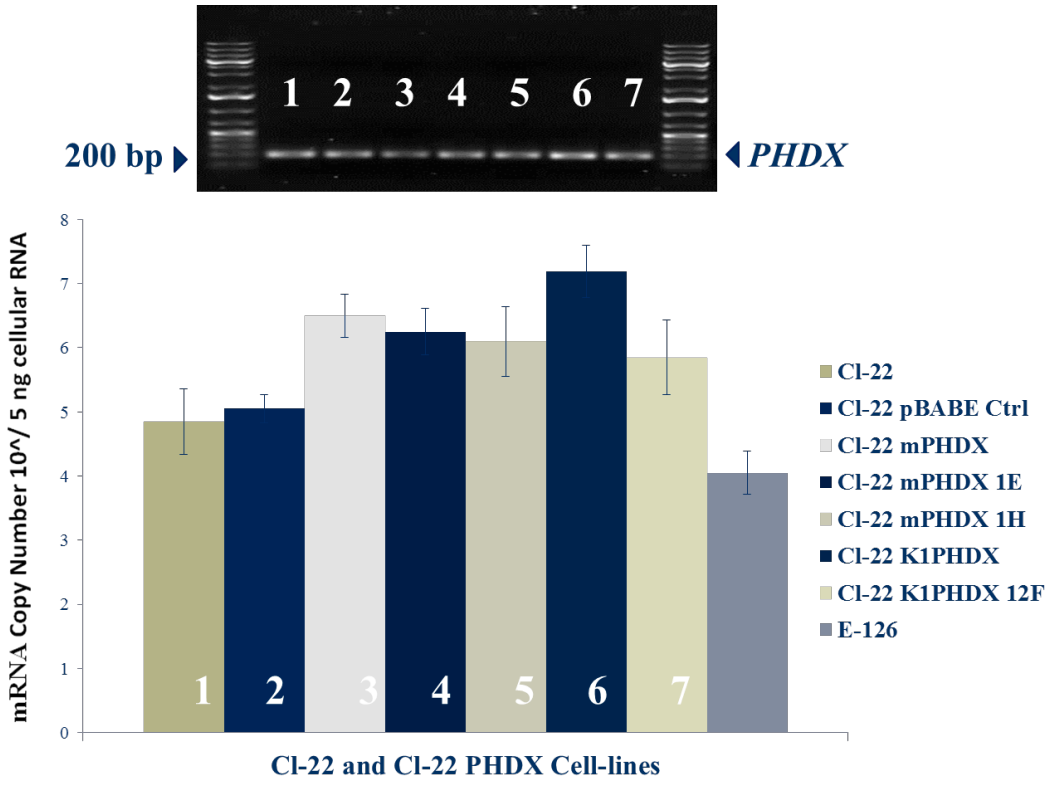

Figure 22: Overexpression of *PHDX* in CHO-Cl-22 cells as determined by real time RT-PCR and absolute quantification.

Gel Picture: Lane 1: Cl-22; Lane 2: Cl-22-pBABE Ctrl; Lane 3: Cl-22 mPHDX (pooled cells); Lane 4: Cl-22 mPHDX 1E (clone 1); Lane 5: Cl-22 mPHDX 1H (clone 2); Lane 6: Cl-22 K1PHDX (pooled cells); Lane 7: Cl-22 K1PHDX 8C (individual clone).

Bar Graph: The mean value of mRNA copy number of Cl-22 pBABE Ctrl is compared with Cl-22 cells and Cl-22 cells over expressing *PHDX* gene. Anova significance at pValue < 0.05 level is denoted by (*), pValue < 0.001 is denoted by (**) and pValue < 0.0001 is

denoted by (***). *PHDX* expression in E-126 cells which is significantly different from Cl-22 cells (pValue < 0.0001) is also shown to compare the expression level in E-126 cells. Error bars represent the standard error of mean of n = 3 replicates.

3.6.2 Effect of *PHDX* overexpression in CHO-Cl-22 cells by using Crystal Violet

staining assay

CHO-Cl-22 cells, CHO-Cl-22 cells having both *mPHDX* and *K1PHDX* genes and CHO-Cl-22 cells containing pBABE puro vector were tested through crystal violet staining assay. To determine the cytotoxicity of etoposide and hydrogen peroxide, these cells were treated with various concentrations of both the cytotoxic agents. The experiment yielded similar results for the both *mPHDX* and *K1PHDX* genes. The results for only *mPHDX* genes have been shown for the sake of simplicity **(Figure 23)**. The overexpression studies using crystal violet staining assay after etoposide treatment did not yield any statistically significant differences among parental Cl-22, Cl-22 pBABE ctrl and Cl-22 cells overexpressing *PHDX* gene **(Table 8)**. Similarly treatment with hydrogen peroxide **(Figure 24)** also didn't show any statistically significant difference between Cl-22 pBABE ctrl cells and Cl-22 cells overexpressing *PHDX* gene. However the Cl-22 pBABE control cells showed some resistance to hydrogen peroxide treatment as compared to parental Cl-22 cells suggesting the effect of vector itself **(Table 9)**.

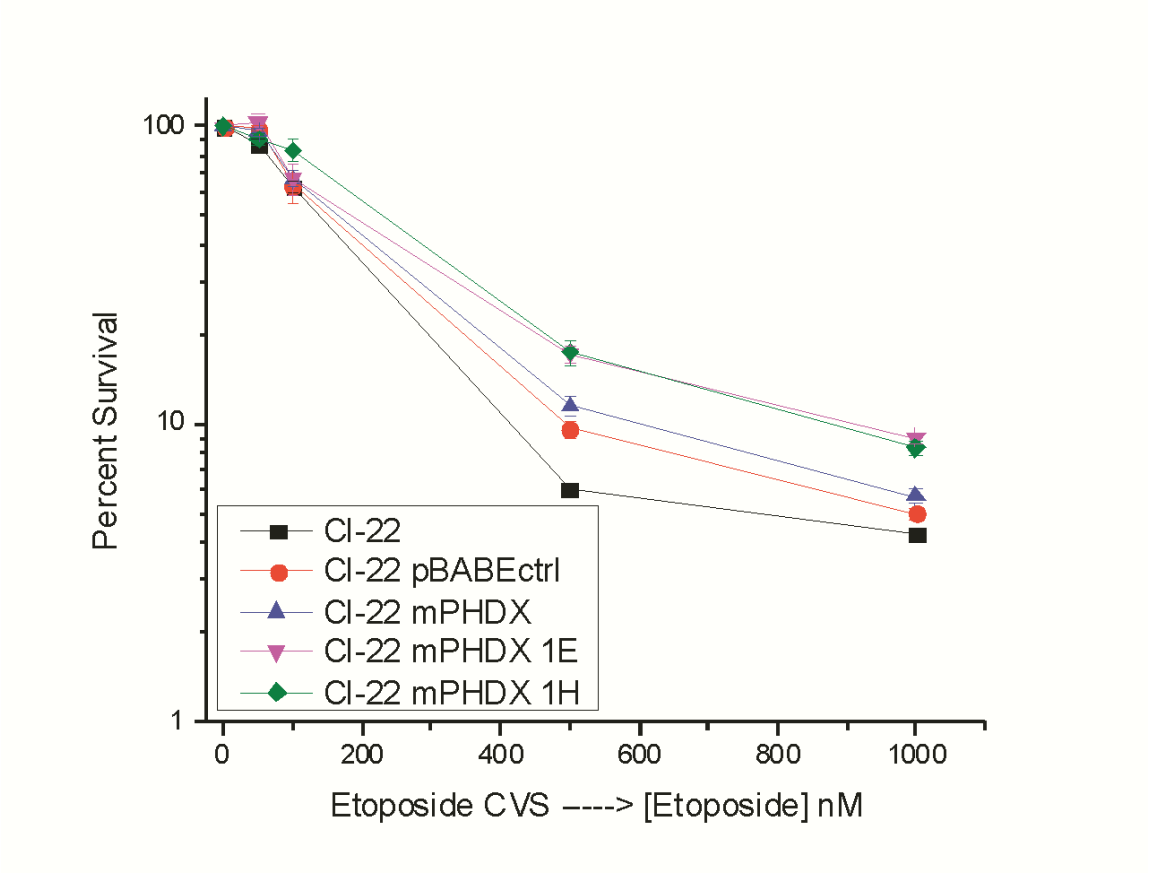

Figure 23: Effect of cytotoxicity of etoposide on Cl-22, Cl-22 pBABE ctrl, Cl-22 mPHDX (pooled cells), Cl-22 mPHDX 1E (clone 1) and Cl-22 mPHDX 1H (clone 2) through CVS assay.

Cells were incubated for 48 hour with 0, 50, 100, 500, and 1000 nM etoposide. Cytotoxicity was determined by CVS assay and is presented as the % surviving cell fraction (optical density in treated cells as a fraction of the optical density in cells treated with DMSO). Error bars represent standard error of mean of n = 4 biological replicates.

Table 8: Statistical analysis of survival curves for overexpression of *PHDX* in Cl-22 through CVS etoposide assay.

Comparison of mean IC_{50} value of Cl-22 pBABE ctrl cells with that of parental Cl-22 cells; Cl-22 pBABE ctrl cells with that of Cl-22 mPHDX cells; Cl-22 pBABE ctrl cells with that of Cl-22 mPHDX 1Ecells and Cl-22 pBABE ctrl cells with that of Cl-22 mPHDX 1H cells by using Student's t-Test.

Cell-Line	Mean IC 50 (nM)	pValue-t-Test
Cl-22	140.5 ± 10.31 N=4	
Cl-22 pBABE Ctrl	168.7 ± 18.62 N=4	0.2327
Cl-22 mPHDX	175.3 ± 16.74 N=4	0.8017
Cl-22 mPHDX 1E	202.9 ± 17.91 N=4	0.2338
Cl-22 mPHDX 1H	225.5 ± 30.94 N=4	0.1666

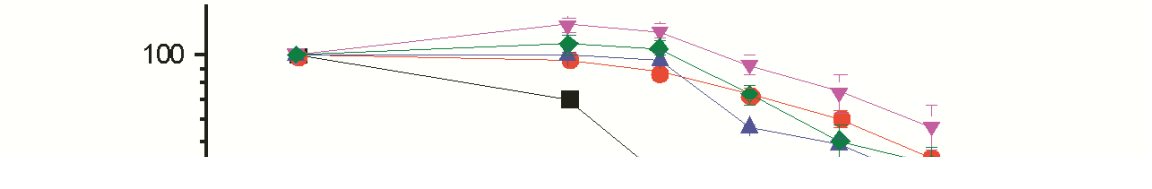

Figure 24: Effect of cytotoxicity of hydrogen peroxide on Cl-22, Cl-22 pBABE ctrl, Cl-22 mPHDX (pooled cells), Cl-22 mPHDX 1E (clone 1) and Cl-22 mPHDX 1H (clone 2) through CVS assay.

Cells were incubated for 48 hours with 0, 75, 100, 125, 150 and 175μM hydrogen peroxide. Cytotoxicity was determined by CVS assay and is presented as the surviving cell fraction (optical density in treated cells as a fraction of the optical density in untreated cells). Error bars represent standard error of mean of n = 4 biological replicates.

Table 9: Statistical analysis of survival curves for overexpression of *PHDX* in Cl-22 through CVS hydrogen peroxide assay

Comparison of mean IC_{50} value of Cl-22 pBABE ctrl cells with that of parental Cl-22 cells; Cl-22 pBABE ctrl cells with that of Cl-22 mPHDX cells; Cl-22 pBABE ctrl cells with that of Cl-22 mPHDX 1E cells and Cl-22 pBABE ctrl cells with that of Cl-22 mPHDX 1H cells by using Student's t-Test.

Cell-Line	Mean IC 50 (µM)	pValue-t-Test
Cl-22	56.49 ± 3.176 N=4	
Cl-22 pBABE Ctrl	299.9 ± 32.13 N=4	0.0003
Cl-22 mPHDX	234.0 ± 19.80 N=4	0.1313
Cl-22 mPHDX 1E	914.9 ± 339.6 N=4	0.1215
Cl-22 mPHDX 1H	371.7 ± 98.48 N=4	0.5143

3.6.3 Effect of *PHDX* overexpression in CHO-Cl-22 cells by using MTT assay

CHO-Cl-22 cells, CHO-Cl-22 cells having both *mPHDX* and *K1PHDX* genes and the cells containing pBABE puro vector were tested again for the effect of etoposide **(Figure 25)** and hydrogen peroxide **(Figure 26)** through the MTT assay. The effect of etoposide on Cl-22 pBABE control cells and Cl-22 cells was not significantly different but pooled Cl-22 mPHDX and both the individually picked clones 1E and 1H showed high level of resistance to etoposide treatment **(Table 10)**. The treatment with hydrogen peroxide revealed that Cl-22 pBABE control cells were more sensitive than parental Cl-22 cells. However no difference was observed between pooled Cl-22 mPHDX and Cl-22 pBABE control cells. Although both the individual clones 1E and 1H showed significant resistance to hydrogen peroxide treatment however, a large variation (standard deviation) in the data was observed **(Table 11)**.

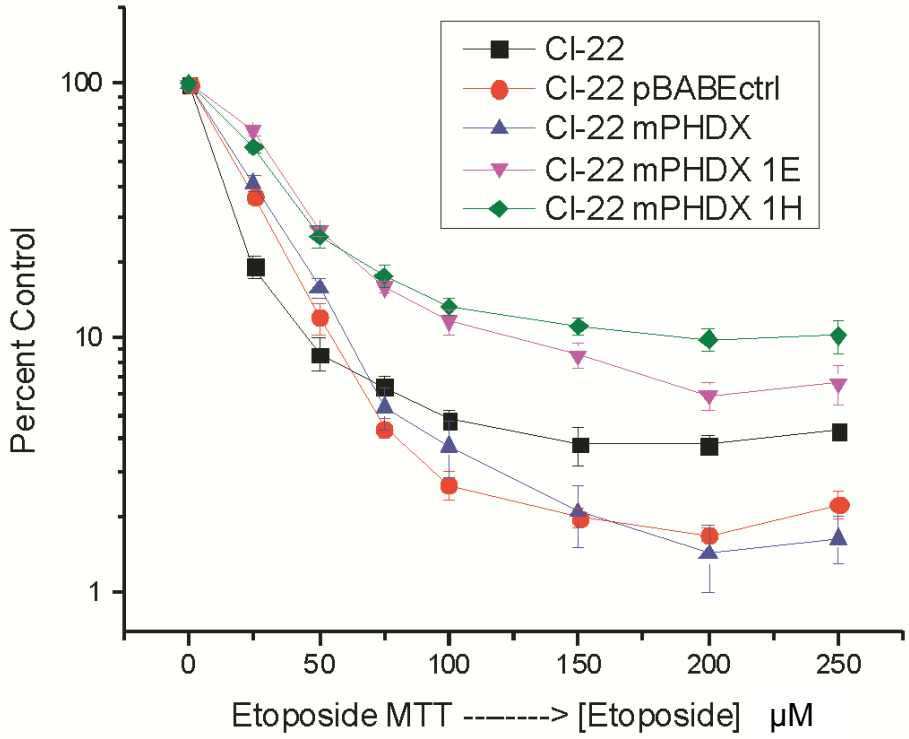

Figure 25: Effect of cytotoxicity of etoposide on Cl-22, Cl-22 pBABE ctrl, Cl-22 mPHDX (pooled cells), Cl-22 mPHDX 1E (clone 1) and Cl-22 mPHDX 1H (clone 2) through MTT assay.

Cells were incubated for 48 hour with 0, 50, 100, 150, 200 and 250 µM etoposide. Cytotoxicity was determined by the MTT assay and is presented as the % surviving cell fraction (optical density in treated cells as a fraction of the optical density in cells treated with DMSO). Error bars represent standard error of mean of n = 4 biological replicates.

Table 10: Statistical analysis of survival curves for overexpression of *PHDX* in Cl-22 through MTT etoposide assay

Comparison of mean IC_{50} value of Cl-22 pBABE ctrl cells with that of parental Cl-22 cells; Cl-22 pBABE ctrl cells with that of Cl-22 mPHDX cells; Cl-22 pBABE ctrl cells with that of Cl-22 mPHDX 1E cells and Cl-22 pBABE ctrl cells with that of Cl-22 mPHDX 1H cells by using Student's t-Test.

Cell-Line	Mean IC 50 (µM)	pValue-t-Test
Cl-22	5.649 ± 0.6021 N=4	
Cl-22 pBABE Ctrl	4.983 ± 0.6015 N=4	0.4633
Cl-22 mPHDX	11.54 ± 1.077 N=4	0.0018
Cl-22 mPHDX 1E	16.23 ± 0.8429 N=4	< 0.0001
Cl-22 mPHDX 1H	21.82 ± 0.9507 N=4	< 0.0001

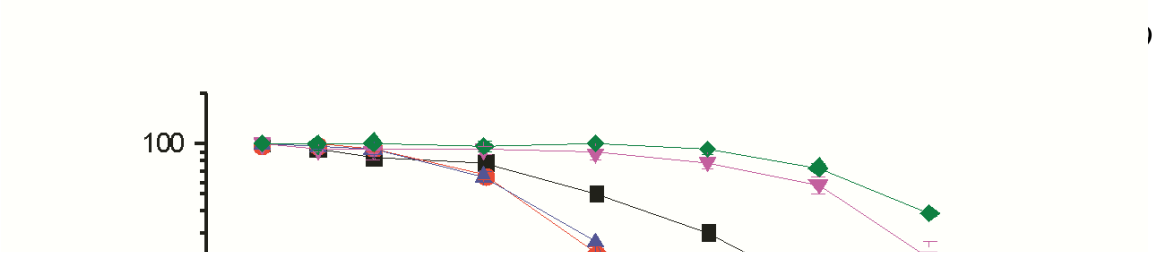

Figure 26: Effect of cytotoxicity of hydrogen peroxide on Cl-22, Cl-22 pBABE ctrl, Cl-22 mPHDX (pooled cells), Cl-22 mPHDX 1E (clone 1) and Cl-22 mPHDX 1H (clone 2) through MTT assay

Cells were incubated for 48 hours with 0, 50, 100, 200, 300, 400, 500 and 600µM hydrogen peroxide. Cytotoxicity was determined by MTT assay and is presented as the % surviving cell fraction (optical density in treated cells as a fraction of the optical density in untreated cells). Error bars represent standard error of mean of n = 4 biological replicates.

Table 11: Statistical analysis of survival curves for overexpression of *PHDX* in Cl-22

through MTT hydrogen peroxide assay.

Comparison of mean IC_{50} value of Cl-22 pBABE ctrl cells with that of parental Cl-22 cells; Cl-22 pBABE ctrl cells with that of Cl-22 mPHDX cells; Cl-22 pBABE ctrl cells with that of Cl-22 mPHDX 1E cells and Cl-22 pBABE ctrl cells with that of Cl-22 mPHDX 1H cells by using Student's t-Test.

Cell-Line	Mean IC 50 (µM)	pValue-t-Test
Cl-22	242.4 ± 3.731 N=4	
Cl-22 pBABE Ctrl	163.8 ± 10.53 N=4	0.0004
Cl-22 mPHDX	163.1 ± 11.25 N=4	0.9665
Cl-22 mPHDX 1E	697.6 ± 131.2 N=4	0.0067
Cl-22 mPHDX 1H	1945 ± 87.56 N=4	< 0.0001

3.6.4 Overexpression of *PHDX* gene in CHO E-126 cells

Overexpression studies in CHO-Cl-22 did not provide a clear picture regarding the function of this gene in relation to drug resistance. The clonogenic assay did not show any effect of etoposide and hydrogen peroxide in Cl-22 cells overexpressing the *PHDX* gene. An effect of puromycin vector was observed. The siRNA knockdown studies of *PHDX* supported an association of the loss of gene function in drug resistance. To verify further the involvement of *PHDX* in resistance, the normal *PHDX* gene was introduced into CHO-E-126 cells. It was believed that introducing *PHDX* gene in E-126 cells might rescue the phenotype by restoring the sensitivity of mutant clone CHO-E-126. The constructs containing *PHDX* gene from mouse (m*PHDX*) as well as Chinese hamster ovary cells (K1*PHDX*) were used again to infect CHO-E-126 cells this time. Stable cell-lines through puromycin selection were created by taking pooled cells and individual clones in the same way as clones were created after infecting CHO-Cl-22 cells with pBABE puro construct. The gene expression was determined by real time RT-PCR through absolute quantification. The gene expression of E-126 pBABE control cells was compared with parental CHO-E-126 cells; and E-126 mPHDX, E-126 mPHDX 4C, E-126 K1PHDX, E-126 K1PHDX 8C by using one way Anova (Dunnett's post-hoc test) in GraphPad Prism 5 **(Figure 27)**.

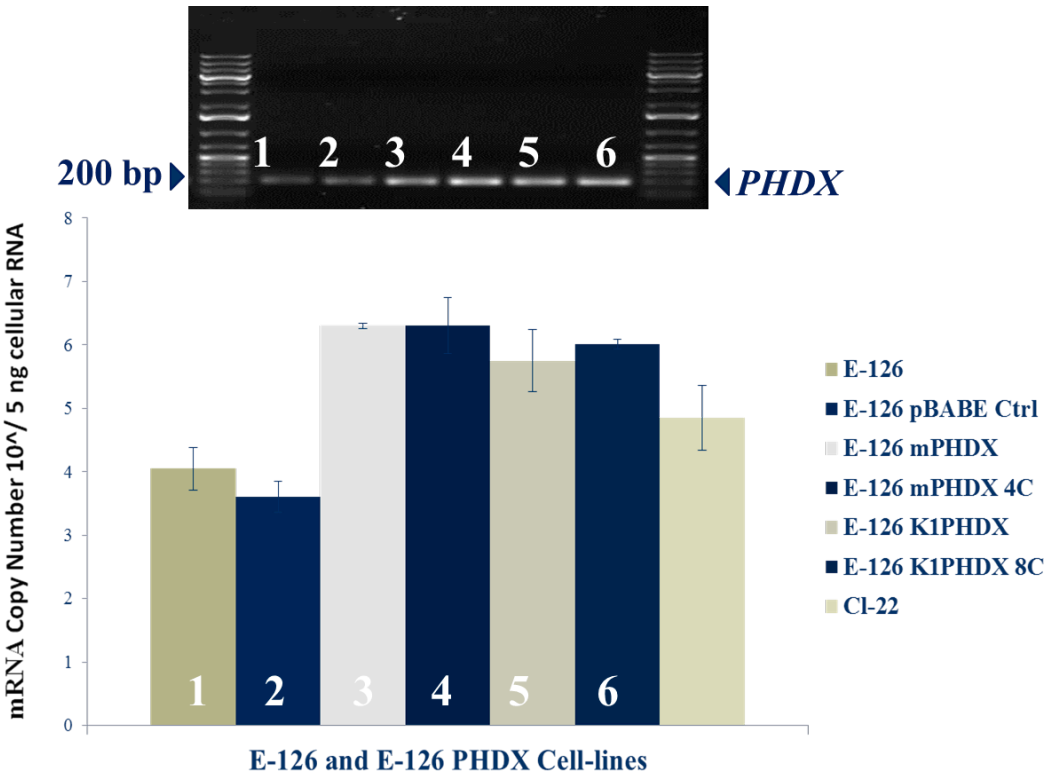

Figure 27: Overexpression of *PHDX* in CHO-E-126 cells as determined by real time RT-PCR and by absolute quantification.

Gel Picture: Lane 1: E-126; Lane 2: E-126-pBABE Ctrl; Lane 3: E-126 mPHDX (pooled cells); Lane 4: E-126 mPHDX 4C (individual clone); Lane 5: E-126 K1PHDX (pooled cells); Lane 4: E-126 K1PHDX 8C (individual clone).

Bar Graph: The mean value of mRNA copy number of E-126 pBABE Ctrl is compared with E-126 cells and E-126 cells over expressing *PHDX* gene. Anova significance at pValue < 0.05 level is denoted by (*), pValue < 0.001 is denoted by (**) and pValue < 0.0001 is denoted by (***). *PHDX* expression in Cl-22 cells which is significantly different from E-

126 cells (pValue < 0.0001) is also shown to compare the expression level of *PHDX* in Cl-22 cells. Error bars represent the standard error of mean of n = 3 replicates.

3.6.5 Effect of *PHDX* overexpression in CHO-E-126 cells through Crystal Violet

staining assay

CHO-E-126 cells, CHO-E-126 cells having both *mPHDX* and *K1PHDX* genes and the CHO-E-126 cells containing pBABE puro vector were tested for drug sensitivity through the crystal violet staining assay. To determine the cytotoxicity of etoposide and hydrogen peroxide, these cells were treated with various concentrations of both the cytotoxic agents. The experiments yielded similar results for both *mPHDX* and *K1PHDX* genes. Again, the results for only *mPHDX* genes have been shown for the sake of simplicity **(Figure 28)**. The overexpression studies using crystal violet staining assay for etoposide on E-126 cells showed the mPHDX pooled cells and individual clone 4C to be more resistant as compared to E-126 pBABE ctrl cells. We observed that the vector had made E-126 pBABE ctrl cells more sensitive to etoposide treatment as compared to parental E-126. The results obtained had high statistical significance **(Table 12)**. The treatment with hydrogen peroxide **(Figure 29)** didn't show any statistically significant difference among E-126 cells, E-126 pBABE ctrl cells and the individual clone 4C. The pooled E-126 cells overexpressing *PHDX* gene were more resistant to hydrogen peroxide treatment than E-126 pBABE ctrl cells. However a large amount of statistical variance was observed in case of both pooled E-126 mPHDX and E-126 mPHDX 4C cells **(Table 13)**.

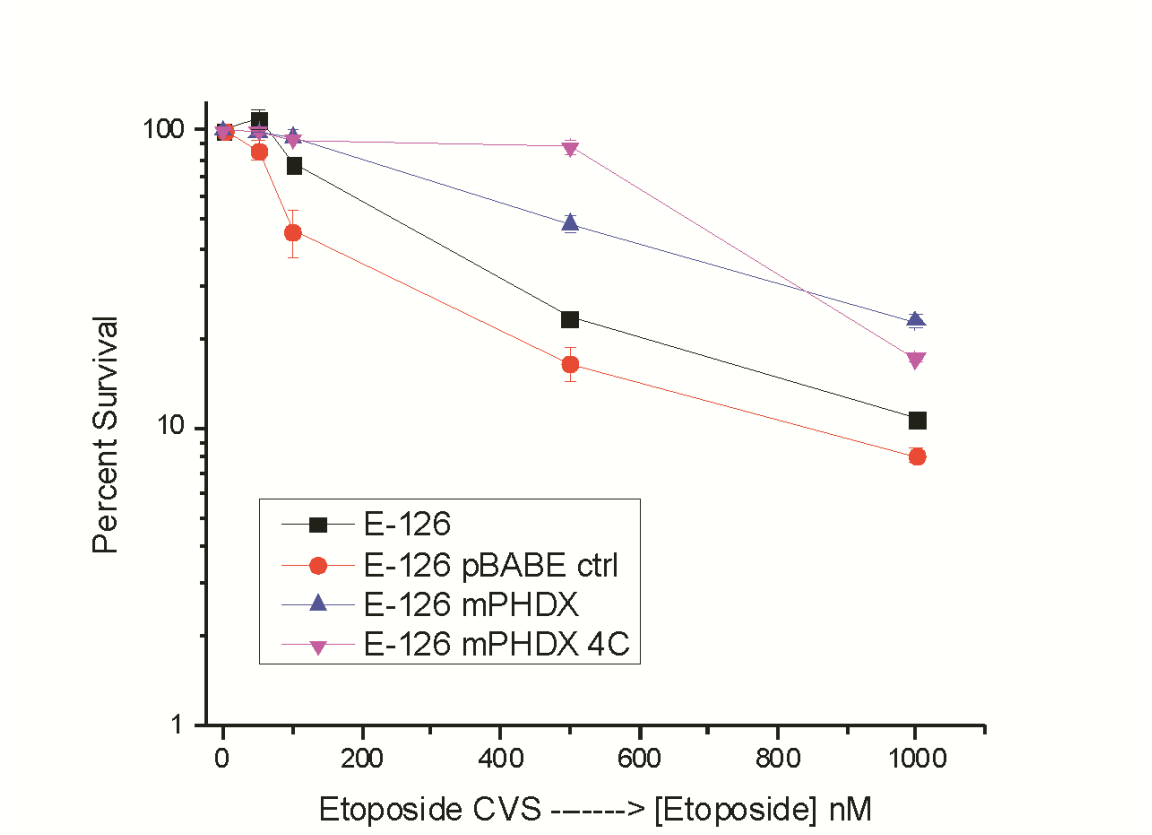

Figure 28: Effect of cytotoxicity of etoposide on E-126, E-126 pBABE ctrl, E-126 mPHDX (pooled cells) and E-126 mPHDX 4C (individual clone) through CVS assay. Cells were incubated for 48 hour with 0, 50, 100, 500, and 1000 nM etoposide. Cytotoxicity was determined by CVS assay and is presented as the % surviving cell fraction (optical density in treated cells as a fraction of the optical density in cells treated with DMSO). Error bars represent standard error of mean of n = 4 biological replicates.

Table 12: Statistical analysis of survival curves for overexpression of *PHDX* in E-126 through CVS etoposide assay.

Comparison of mean IC_{50} value of E-126 pBABE ctrl cells with that of parental E-126 cells; E-126 pBABE ctrl cells with that of E-126 mPHDX cells and E-126 pBABE ctrl cells with that of E-126 mPHDX 4C cells by using Student's t-Test.

Cell-Line	Mean IC 50 (nM)	pValue-t-Test
E-126	224.0 ± 12.93 N=4	
E-126 pBABE Ctrl	128.7 ± 15.38 N=4	0.0032
E-126 mPHDX	487.5 ± 47.04 N=4	0.0003
E-126 mPHDX 4C	813.3 ± 65.91 N=4	P<0.0001

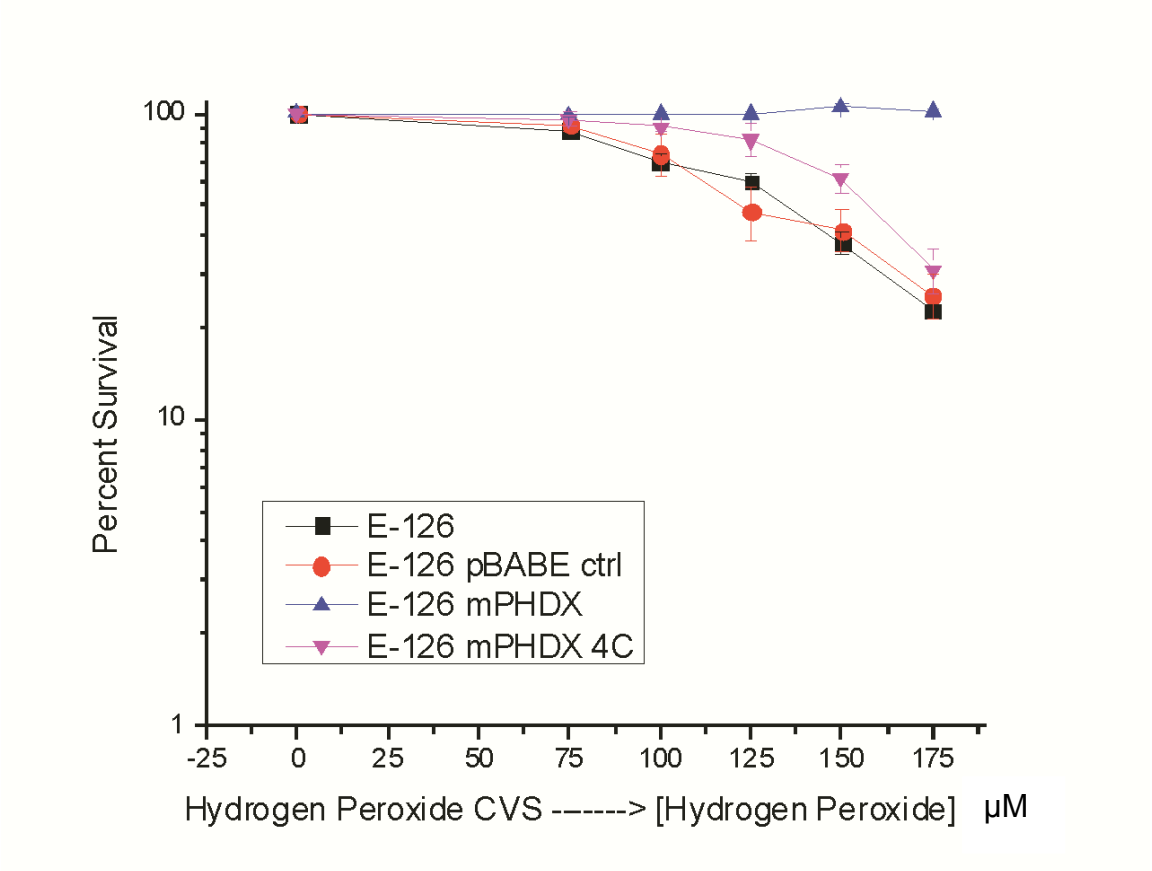

Figure 29: Effect of cytotoxicity of hydrogen peroxide on E-126, E-126 pBABE ctrl, E-126 mPHDX (pooled cells) and E-126 mPHDX 4C (individual clone) through CVS assay.

Cells were incubated for 48 hours with 0, 75, 100, 125, 150 and 175µM hydrogen peroxide. Cytotoxicity was determined by CVS assay and is presented as the % surviving cell fraction (optical density in treated cells as a fraction of the optical density in untreated cells). Error bars represent standard error of mean of n = 4 replicates.

Table 13: Statistical analysis of survival curves for overexpression of *PHDX* in E-126 through CVS hydrogen peroxide assay.

Comparison of mean IC_{50} value of E-126 pBABE ctrl cells with that of parental E-126 cells; E-126 pBABE ctrl cells with that of E-126 mPHDX cells and E-126 pBABE ctrl cells with that of E-126 mPHDX 4C cells by using Student's t-Test.

Cell-Line	Mean IC 50 (µ M)	pValue-t-Test
E-126	149.2 ± 14.08 N=4	
E-126 pBABE Ctrl	158.9 ± 27.58 N=4	0.7637
E-126 mPHDX	9351 ± 2743 N=3	0.0103
E-126 mPHDX 4C	328.5 ± 89.19 N=4	0.1193

3.6.6 Effect of of *PHDX* overexpression in CHO-E-126 cells through MTT assay

CHO-E-126 cells, CHO-E-126 cells having both *mPHDX* and *K1PHDX* genes and E-126 cells containing pBABE puro vector were tested again for the effect of etoposide

(Figure 30) and hydrogen peroxide **(Figure 31)** through the MTT assay. E-126 pBABE control cells were more sensitive than parental E-126 cells. The E-126 mPHDX (pooled cells) were not significantly different from the pBABE control cells but E-126 mPHDX 4C (individual clone) cells were significantly sensitive than the pBABE control cells **(Table 14)**. The treatment with hydrogen peroxide made E-126 pBABE control cells more sensitive than parental E-126 cells. As compared to E-126 pBABE ctrl cells, E-126 mPHDX (pooled cells) and E-126 mPHDX 4C showed significant resistance. Athough the data for E-126 cells overexpressing the *PHDX* gene cells showed large variation (standard deviations) **(Table 15)**.

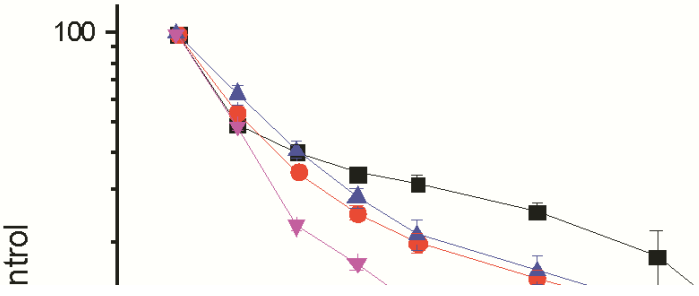

Figure 30: Effect of cytotoxicity of etoposide on E-126, E-126 pBABE ctrl, E-126 mPHDX (pooled cells) and E-126 mPHDX 4C (individual clone) through MTT assay. Cells were incubated for 48 hour with 0, 50, 100, 150, 200 and 250 μM etoposide. Cytotoxicity was determined by MTT assay and is presented as the surviving cell fraction (optical density in treated cells as a fraction of the optical density in cells treated with DMSO). Error bars represent standard error of mean of n = 4 replicates.

Table 14: Statistical analysis of survival curves for overexpression of *PHDX* in E-126 through MTT etoposide assay.

Comparison of mean IC_{50} value of E-126 pBABE ctrl cells with that of parental E-126 cells; E-126 pBABE ctrl cells with that of E-126 mPHDX cells and E-126 pBABE ctrl cells with that of E-126 mPHDX 4C cells by using Student's t-Test.

Cell-Line	Mean IC 50 (µM)	pValue-t-Test
E-126	35.23 ± 1.125 N=4	
E-126 pBABE Ctrl	27.27 ± 1.258 N=4	0.0033
E-126 mPHDX	32.51 ± 3.264 N=4	0.1846
E-126 mPHDX 3D	21.55 ± 1.343 N=4	0.0209
E-126 mPHDX 4C	18.66 ± 0.8724 N=4	0.0013

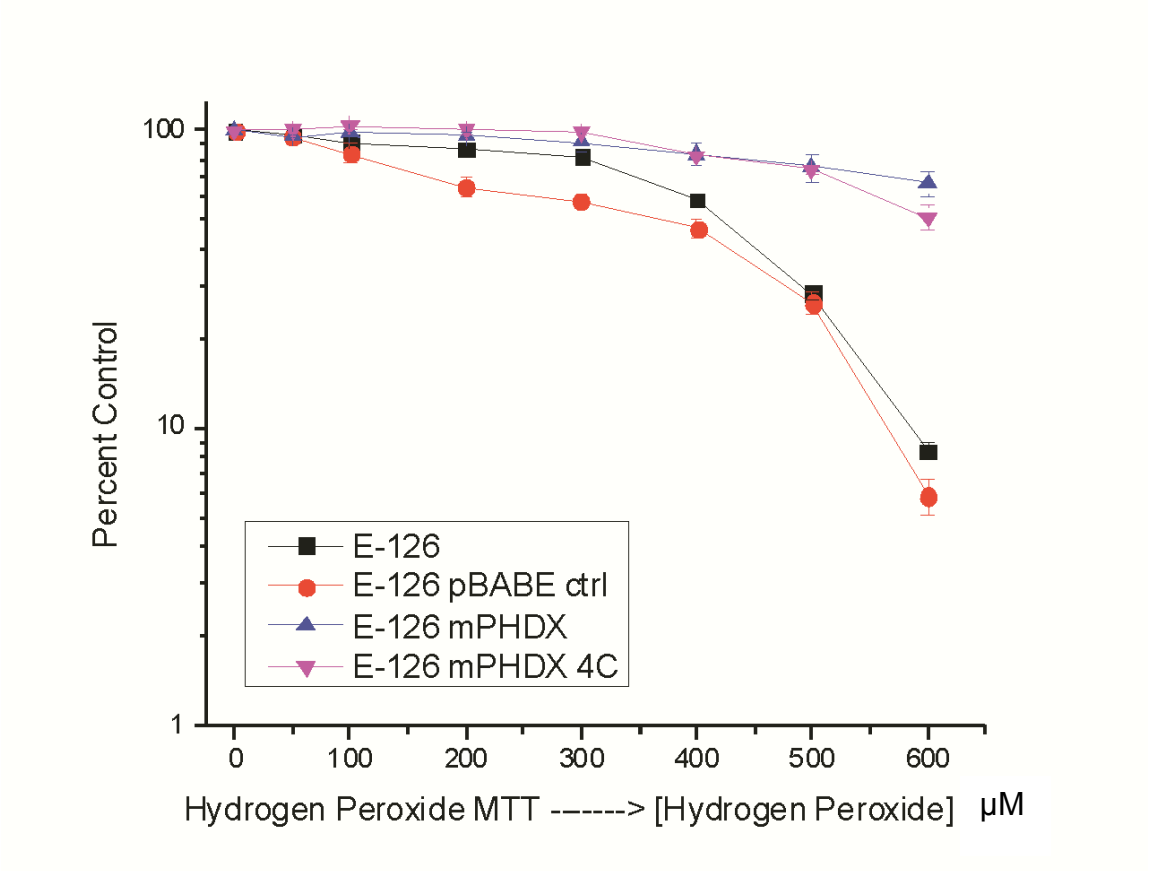

Figure 31: Effect of cytotoxicity of etoposide on E-126, E-126 pBABE ctrl, E-126 mPHDX (pooled cells) and E-126 mPHDX 4C (individual clone) through MTT assay. Cells were incubated for 48 hours with 0, 50, 100, 200, 300, 400, 500 and 600µM hydrogen peroxide. Cytotoxicity was determined by MTT assay and is presented as the surviving cell fraction (optical density in treated cells as a fraction of the optical density in untreated cells). Error bars represent standard error of mean of n = 4 replicates.

Table 15: Statistical analysis of survival curves for overexpression of *PHDX* in E-126 through MTT hydrogen peroxide assay.

Comparison of mean IC_{50} value of E-126 pBABE ctrl cells with that of parental E-126 cells; E-126 pBABE ctrl cells with that of E-126 mPHDX cells and E-126 pBABE ctrl cells with that of E-126 mPHDX 4C cells by using Student's t-Test.

Cell-Line	Mean IC 50 (µM)	pValue-t-Test
E-126	442.7 ± 24.66 N=4	
E-126 pBABE Ctrl	288.5 ± 31.73 N=4	0.0086
E-126 mPHDX	2296 ± 700.0 N=4	0.0286
E-126 mPHDX 3D	1691 ± 142.1 N=4	< 0.0001
E-126 mPHDX 4C	1817 ± 243.7 N=4	0.0008

Table 16: Summary Table of results for cytotoxic assays

cell-line	Etoposide	Hydrogen Peroxide
CHO-K1	**Sensitive**	**Sensitive**
Cl-22	**Sensitive**	**Sensitive**
E-126	**Resistant**	**Resistant**
siRNA Knock-down of PHDX	**Resistant**	**Resistant**
PHDX Overexpression in Cl-22	CVS – **Sensitive - - (similar to Cl-22)** MTT - **Resistant**	CVS – **Sensitive - (similar to Cl-22)** MTT - **Resistant**
PHDX Overexpression in E-126	CVS – **Resistant** MTT - Resistant **(Clone 4C –Sensitive)**	CVS – **Resistant** MTT - **Resistant**

CHAPTER 4 - DISCUSSION

4.1 Summary and Significance of Results

Through characterization of etoposide and hydrogen peroxide resistant cell-line CHO-E-126, I was able to establish that there was an association of a novel prolyl hydroxylase gene *PHDX* with resistance. It was hypothesized that the inactivation of this gene by insertional mutagenesis conferred resistance to etoposide and hydrogen peroxide. It was found that knocking down of this gene transiently in CHO-K1 cells caused significant resistance to etoposide and hydrogen peroxide treatment. However the overexpression of the gene in Cl-22 cells through clonogenic assays did not show an effect on etoposide and hydrogen peroxide response. Interestingly, the overexpression of this gene in E-126 cells failed to render the cells sensitive to etoposide and hydrogen peroxide treatment except in the MTT assay. In the following sections we discuss the experimental results of the functional analyis of the *PHDX* gene through knockdown and overexpression studies.

Initially to address the involvement of the *PHDX* gene in drug resistance, the gene was knocked down through shRNAi. In these experiments, no conclusive results could be obtained because of the off target effects of shRNA observed in the control cells (results not shown). The introduction of ds RNA longer than 29-30 nucleotides can elicit an interferon response and siRNA off-target effects can be controlled to some extent by keeping the length of the dsRNA to 21-nt (Rao *et al.*, 2009b). The shortcoming of using long double stranded hairpin RNA to avoid interferon response can be overcome by transiently knocking down the

gene using short dsRNA. Therefore, short RNAi molecules were used to knockdown the gene.

The knocked down cells from both pooled and 3'UTR siRNA showed significant resistance to etoposide and hydrogen peroxide treatment as compared to scrambled control cells **(Figure 20 and 21)**. Therefore the resistance shown by CHO-K1 cells with a knockdown of the *PHDX* gene supports our hypothesis for the loss of the gene function in E-126 cells. The transient knock down of this gene in E-126 cells (already having reduced expression of the *PHDX* gene) were treated with scrambled control siRNA and pooled siRNA (results not shown) and tested for etoposide and hydrogen peroxide treatment. The further knock down of the *PHDX* gene in E-126 cells with a disruption in the *PHDX* gene, did not affect the siRNA treated cells after etoposide and hydrogen peroxide treatment. This further suggests that the *PHDX* gene might have a role in drug resistance.

We observed in our preliminary experiments that the transient overexpression of the *PHDX* gene in CHO-K1 cells was toxic and compromised with the cell viability. Our logical hypothesis based on the observation of mutated E-126 cells and siRNA knockdown of CHO-K1 cells showing etoposide and hydrogen peroxide resistance suggests that the overexpression of the *PHDX* gene should render the cells more sensitive to the treatment. Based on our previous preliminary studies, overexpression of the gene results in cellular toxicity. However, contrary to our hypothesis, we observed that when the Cl-22 cells and E-126 cells were stably infected with the retroviral vector pBABE puro having the *PHDX* gene, no toxicity and loss of cell viability was observed. Taken together, it suggests that puromycin selection in Cl-22 and E-126 cells overexpressing the *PHDX* gene seems to overcome the

toxicity of the gene. Moreover, cytotoxicity of etoposide and hydrogen peroxide was not observed in the overexpression studies of the gene in Cl-22 and E-126 cells through clonogenic assays. Although the advantage of cell survival with puromycin selection exists, yet the effect of puromycin resistant gene in the constructs itself seems to override the overexpression of the *PHDX* gene in both Cl-22 (two normal copies) and E-126 cells (one normal copy). This overriding effect is thus more evident in E-126 cells overexpressing the gene, which became resistant as compared to the Cl-22 cells overexpressing the gene where there was no change in survival compared to empty vector control. In the CVS assay, the effect of hydrogen peroxide treatment on Cl-22 cells overexpressing the *PHDX* gene and the Cl-22 empty vector control cells was absent, which again suggested that there is no effect of this cytotoxic agent in cells overexpressing the prolyl hydroxylase gene. Moreover, a comparison of the parental Cl-22 and E-126 cells with Cl-22 and E-126 cells having the empty vector demonstrated the effect of puromycin vector.

Conversely, it is also possible that during puromycin selection the transgene might have mutated into a dominant negative allele. This might have made the cells unable to revert to the sensitive phenotype. A similar phenomon has been reported earlier in the loss of *p53* functions (Hicks *et al.*, 1991). The loss of wild type activity of the tumor suppressor *p53* gene resulted in a dominant negative phenotype due to mutations which conferred survival advantage to the REF 52 cells (*ibid.*). However, DNA sequencing of the transgene for possible mutations in the previously mentioned stable *PHDX* transgene transfected cell lines will provide evidence for the possibility of dominant negative effect of the *PHDX* gene.

The effect of puromycin resistance gene as a drug marker has been studied before, and it has been reported that puromycin vectors generate high levels of ROS which resulted in the fomation of protein aggregates of the promyelocytic leukemia (PML) protein. The PML protein is reported to regulate cell-cycle and DNA damage response (Moran *et al.*, 2009). The puromycin selection in overexpression studies in Cl-22 and E-126 cells might have conferred some intracellular changes, which is consistent with the fact that repeated passaging is known to produce alterations in the genetic makeup of transformed cells (Wang and Wang, 2010). There is thus a possibility that the cells overexpressing the *PHDX* gene might have acquired survival/growth advantage. It may be suggested that puromycin selection might have created some mutations in cells which subsequently led them to overcome the toxicity of the overexpressed gene. Despite these disadvantages of this vector, this particular vector system was used since the E-126 cells already have a neomycin and hygromycin selection markers and hence the only other choice of an additional marker was puromycin.

Our results with the MTT assay varied from the crystal violet staining assay with the Cl-22 and E-126 cells, overexpressing the *PHDX* gene, treated with etoposide and hydrogen peroxide treatment. Both these cell types overexpressing the gene showed resistance to the treatment and this was not in agreement with the results obtained in the CVS assay. Both these assays have certain advantages and thus it has been argued that different types of assays might be required to obtain a reliable measurement of the cytotoxicity of different drugs (Ulukaya *et al.*, 2008). The advantage of the MTT assay is that the assay offers speedy measurements of growth stimulation and drug sensitivity even though the assay has some

limitations (Alley *et al.*, 1988). One of the problems with the MTT assay is that the cells are kept in the culture for less than six cell doubling times, which is an insufficient time to detect delayed cell death. This phenomenon has been reported for treatment of cells with certain chemotherapeutic agents. However unlike MTT assay, a long term clonogenic assay would be less likely to miss such delayed response and not underestimate the cell killing (Weisenthal *et al.*, 1983).

The crystal violet assay generally measures the capacity of the cells to form colonies after treatment with cytotoxic agents whereas the MTT assay correlates with the metabolic state of the cells and is a measure of the mitochondrial function of the living cells. The effect of etoposide and paclitaxel on the lung cancer cell line A549 was found to be 10-30 fold less inhibitory in the MTT assay as compared to ATP assay, which measures the ATP levels of the cells because there is a reduction in the ATP level in the dying cells. The ATP assay quantitates the mitochondrial ATP levels (Ulukaya *et al.*, 2008) unlike the MTT assay which is dependent on the activity of mitochondria to metabolize the formazan crystals (Mosmann, 1983). There is evidence of increased resistance to etoposide treatment in MTT assay in A549 cells (Ulukaya *et al.*, 2008) and this correlates well with the overexpression studies in Cl-22 and E-126 cells when the results of both MTT and crystal violet staining assays were compared. Dicumarol, a mitochondrial uncoupler and ROS generator has been reported to disrupt the MTT assay in CHO and EMT6 cell lines (Collier and Pritsos, 2003). Compounds such as doxorubicin, etoposide and hydrogen peroxide generate ROS and are expected to interfere with MTT oxidation thereby making the MTT assay unreliable (Collier and Pritsos, 2003; Droge, 2002; Sawada *et al.*, 2001; van Maanen *et al.*, 1988). Therefore resistance to

etoposide and hydrogen peroxide in the MTT assay also suggests an interference of the mitochondrial function because of the excessive generation of ROS. Therefore it further supports the notion that as a result of ROS generation, it is reasonable to accept the results of the CVS assay better than the MTT assay. It seems that excessive generation of ROS might have compromised the effect of the cytotoxic agents in both Cl-22 and E-126 cells overexpressing the gene in the MTT assay. In the MTT assay there is also the likelihood of the disruption of mitochondrial function due to etoposide and hydrogen peroxide treatment and it is all the more applicable in this case because the assay itself measures the mitochondrial function (Ulukaya *et al.*, 2008). Therefore it is highly likely that the true assessment of the cytotoxicity of these agents could not be done with considerable clarity using the MTT assay. However one of the E-126 clones overexpressing the gene showed sensitivity to etoposide in the MTT assay which actually supports our hypothesis. But based on the limitations of this assay as discussed, we can argue that the sensitivity could be the result of clonal variation. Moreover we did not see the sensitivity with other individually picked clones (results not shown). Overall, the crystal violet staining assay results following etoposide and hydrogen peroxide treatment appears to be a better approach to assess the cytotoxic response of both the cell types in this study.

Prolyl hydroxylases are involved in post translational hydroxylation of proline to form hydroxyproline (Freeman *et al.*, 2003). This post-translational modification leads to the rapid degradation of HIF-1α (Benizri *et al.*, 2008). In our studies, we do not have any direct evidence of such function for the gene (*PHDX*), nevertheless, this function may be a possibility that needs further study. When we analysed the results of clonogenic assay for the

overexpression studies, we observed that the overexpression of this gene neither reversed the resistance of E-126 cells nor increased the sensitivity of Cl-22 cells to either etoposide or hydrogen peroxide treatment. A very likely possibility is that the effect of overexpression of the prolyl hydroxylase gene in both the cell types may have been inhibited by the excessive generation of ROS (Berra *et al.*, 2006) due to etoposide and hydrogen peroxide treatment (Droge, 2002; Sawada *et al.*, 2001; van Maanen *et al.*, 1988). A possible outcome is that the consequent activation of HIF-1α; it is well known that HIF-1α activation is directly associated with proproliferative effects such as resistance to apoptosis, invasion/metastasis, angiogenesis and immortalization (Lopez-Lazaro, 2006; Nishi *et al.*, 2004; Semenza, 2003; Semenza, 2006). The resultant effect was that we were unable to demonstrate the expected senitivity to both drugs due to the overexpression of this gene in the cell lines under study. Also, knocking this prolyl hydroxylase gene down might have affected the function of gene and have activated HIF-1α as mentioned above and thus provided the knocked down cells with an advantage to escape cell-death (Figure 1). It would be interesting to quantify and compare the levels of HIF-1α in the parental cells, *PHDX* knocked down cells and cells overexpressing the *PHDX* gene.

4.2 Conclusions

The results from the *PHDX* gene knock down experiments supported our hypothesis that loss of this gene results in resistance to the cytotoxic agents, etoposide and hydrogen peroxide. This supports a possible role of this unknown prolyl hydroxylase gene in drug resistance. Based on literature evidence regarding the shortcomings of the MTT assay and in

view of the results (in particular, the overexpression studies) presented in this study, we conclude that the clonogenic crystal violet staining assay gave us more interpretable results in comparison with the MTT assay. Therefore I conclude that overexpression of the *PHDX* gene in Cl-22 and E-126 cells did not make the cells sensitive to the treatment as was expected. In support of these arguments, I also showed that the overexpression of the mouse *PHDX* (*mPHDX*) and the Chinese hamster *PHDX* (*K1PHDX*) gene in both CHO-Cl-22 and CHO-E-126 cells showed resistance suggesting the homology between hamster and mouse *PHDX* genes.

4.3 Future Directions

In the present work, I studied the effects of knock down of a novel prolyl hydroxylase or the *PHDX* gene for its ability to confer resistance to two cytotoxic agents, namely etoposide and hydrogen peroxide respectively. While the design and the experimental approaches used in this study followed a sequential pattern, I found that during the course of this study, there were some experimental challenges. I therefore feel that to further this study, we need to focus on the removal of these hurdles. The work is interesting as we have been able to show through functional studies that the novel *PHDX* gene confers resistance to the cytotoxic agents, etoposide and hydrogen peroxide in *in vitro* cell line models (Chinese hamster ovary cell lines). I will discuss the experimental challenges here and the possible suggestions for future studies.

I observed that the shRNA knock down of the gene showed off target effects of shRNAi. Between the two knock down strategies that I tried, the most successful was the

siRNA (pooled and 3'UTR siRNA) induced knock down of the gene, which resulted in drug resistance. An important control for these experiments is to rescue the phenotype in the knocked down cells by transfecting a cDNA that is not targeted by the 3'UTR RNAi. Since the 3'UTR siRNA is targeted against the 3' untranslated region of the gene, it would not be effective to knock down the *PHDX* transgene (cloned *PHDX* mRNA devoid of 3' UTR region). We did not have much success with the 3'UTR targeted siRNA knockdown experiments. The rescue experiment can be repeated with 3'UTR siRNA.

I have argued that the *PHDX* gene is a contributor of drug resistance through its inactivation under certain conditions within the cellular environment, such as the activation of the HIF-1α gene (we have discussed the possible connection of HIF-1α to prolyl hydroxylases). If this is the case, then we see an interesting future direction to this study where we can do a quantitative anlaysis of HIF-1α in cells with the knock down of the *PHDX* gene versus cells having normal copy of the gene.

I also propose cloning of the *Neo-PHDX* fusion product in the CHO-K1 cells and by the utilization of this *in vitro* system, we could perform detailed experiments to study the effects of etoposide and hydrogen peroxide to obtain further insights to the function of the fusion *PHDX* gene. Moreover, to study the PHDX protein, I suggest cloning the gene with a tag of choice (examples include Flag, GFP) in a suitable vector. This has not been done initially because we wanted to see the knockdown effect of the *PHDX* gene. The tagged protein will be helpful to see the intracellular localization of the protein and also to find out its possible binding partners.

Overall I envision that all future experiments may be directed towards the further

functional characterization of the *PHDX* gene and as such I suggest that *in vitro* studies should be culminated into *in vivo* studies. I suggest *in vivo* functional study involving the use of transgenic mice with conditional or genetrap allele of the *PHDX* gene. The *in vivo* model may provide a more specific solution for knocking the gene and then studying its effect in the mice. Moreover, it is also possible to develop *in vivo* tumours in the *PHDX* knockout mouse and then those tumours or tumour derived cell lines could be tested for chemotherapeutic drug sensitivity.

CHAPTER 5 - References

Abuin, A. *et al.* (2007). Gene trap mutagenesis. *Handb Exp Pharmacol* 129-147.

Adams, J. M., Cory, S. (2001). Life-or-death decisions by the Bcl-2 protein family. *Trends Biochem Sci* 26, 61-66.

Aebi, S. *et al.* (1997). Resistance to cytotoxic drugs in DNA mismatch repair-deficient cells. *Clin Cancer Res* 3, 1763-1767.

Agrawal, N. *et al.* (2003). RNA interference: biology, mechanism, and applications. *Microbiol Mol Biol Rev* 67, 657-685.

Alley, M. C. *et al.* (1988). Feasibility of drug screening with panels of human tumor cell lines using a microculture tetrazolium assay. *Cancer Res* 48, 589-601.

Amati, B. *et al.* (1993). The c-Myc protein induces cell cycle progression and apoptosis through dimerization with Max. *EMBO J* 12, 5083-5087.

Annunen, P. *et al.* (1997). Cloning of the human prolyl 4-hydroxylase alpha subunit isoform alpha(II) and characterization of the type II enzyme tetramer. The alpha(I) and alpha(II) subunits do not form a mixed alpha(I)alpha(II)beta2 tetramer. *J Biol Chem* 272, 17342-17348.

Apel, K., Hirt, H. (2004). Reactive oxygen species: metabolism, oxidative stress, and signal transduction. *Annu Rev Plant Biol* 55, 373-399.

Araki, M. *et al.* (2009). International Gene Trap Project: towards gene-driven saturation mutagenesis in mice. *Curr Pharm Biotechnol* 10, 221-229.

Bartlett, D. W., Davis, M. E. (2006). Insights into the kinetics of siRNA-mediated gene silencing from live-cell and live-animal bioluminescent imaging. *Nucleic Acids Res* 34, 322-333.

Bartlett, D. W., Davis, M. E. (2007). Effect of siRNA nuclease stability on the in vitro and in vivo kinetics of siRNA-mediated gene silencing. *Biotechnol Bioeng* 97, 909-921.

Beck, W. T. *et al.* (1999). Tumor cell resistance to DNA topoisomerase II inhibitors: new developments. *Drug Resist Updat* 2, 382-389.

Benizri, E. *et al.* (2008). The magic of the hypoxia-signaling cascade. *Cell Mol Life Sci* 65, 1133-1149.

Berra, E. *et al.* (2003). HIF prolyl-hydroxylase 2 is the key oxygen sensor setting low steady-state levels of HIF-1alpha in normoxia. *EMBO J* 22, 4082-4090.

Berra, E. *et al.* (2006). The hypoxia-inducible-factor hydroxylases bring fresh air into hypoxia signalling. *EMBO Rep* 7, 41-45.

Bromberg, K. D. *et al.* (2003). A two-drug model for etoposide action against human topoisomerase IIalpha. *J Biol Chem* 278, 7406-7412.

Bruick, R. K., McKnight, S. L. (2001). A conserved family of prolyl-4-hydroxylases that modify HIF. *Science* 294, 1337-1340.

Bustin, S. A. (2000). Absolute quantification of mRNA using real-time reverse transcription polymerase chain reaction assays. *J Mol Endocrinol* 25, 169-193.

Cai, H. (2005). Hydrogen peroxide regulation of endothelial function: origins, mechanisms, and consequences. *Cardiovasc Res* 68, 26-36.

Chang, W. *et al.* (1993). Enrichment of insertional mutants following retrovirus gene trap selection. *Virology* 193, 737-747.

Chaudhary, P. M., Roninson, I. B. (1993). Induction of multidrug resistance in human cells by transient exposure to different chemotherapeutic drugs. *J Natl Cancer Inst* 85, 632-639.

Chiou, S. K. *et al.* (1994). Bcl-2 blocks p53-dependent apoptosis. *Mol Cell Biol* 14, 2556-2563.

Cioffi, C. L. *et al.* (2003). Differential regulation of HIF-1 alpha prolyl-4-hydroxylase genes by hypoxia in human cardiovascular cells. *Biochem Biophys Res Commun* 303, 947-953.

Clarke, A. R. *et al.* (1993). Thymocyte apoptosis induced by p53-dependent and independent pathways. *Nature* 362, 849-852.

Collier, A. C., Pritsos, C. A. (2003). The mitochondrial uncoupler dicumarol disrupts the MTT assay. *Biochem Pharmacol* 66, 281-287.

Cooper, S. K. *et al.* (2008). A novel function for hydroxyproline oxidase in apoptosis through generation of reactive oxygen species. *J Biol Chem* 283, 10485-10492.

Corcoran, G. B. *et al.* (1994). Apoptosis: molecular control point in toxicity. *Toxicol Appl Pharmacol* 128, 169-181.

Corpas, F. J. *et al.* (2001). Peroxisomes as a source of reactive oxygen species and nitric oxide signal molecules in plant cells. *Trends Plant Sci* 6, 145-150.

Cory, S., Adams, J. M. (2002). The Bcl2 family: regulators of the cellular life-or-death switch. *Nat Rev Cancer* 2, 647-656.

D'Arpa, P. *et al.* (1990). Involvement of nucleic acid synthesis in cell killing mechanisms of topoisomerase poisons. *Cancer Res* 50, 6919-6924.

Danks, M. K. *et al.* (1993). Single-strand conformational polymorphism analysis of the M(r) 170,000 isozyme of DNA topoisomerase II in human tumor cells. *Cancer Res* 53, 1373-1379.

Datta, S. R. *et al.* (1997). Akt phosphorylation of BAD couples survival signals to the cell-intrinsic death machinery. *Cell* 91, 231-241.

de Murcia, G. *et al.* (1986). Modulation of chromatin superstructure induced by poly(ADP-ribose) synthesis and degradation. *J Biol Chem* 261, 7011-7017.

DiCiommo, D. P. *et al.* (2004). Retinoblastoma protein purification and transduction of retina and retinoblastoma cells using improved alphavirus vectors. *Invest Ophthalmol Vis Sci* 45, 3320-3329.

Doench, J. G. *et al.* (2003). siRNAs can function as miRNAs. *Genes Dev* 17, 438-442.

Donze, O., Picard, D. (2002). RNA interference in mammalian cells using siRNAs synthesized with T7 RNA polymerase. *Nucleic Acids Res* 30, e46.

Droge, W. (2002). Free radicals in the physiological control of cell function. *Physiol Rev* 82, 47-95.

Dykxhoorn, D. M. *et al.* (2003). Killing the messenger: short RNAs that silence gene expression. *Nat Rev Mol Cell Biol* 4, 457-467.

Ekoff, M., Nilsson, G. (2011). Mast cell apoptosis and survival. *Adv Exp Med Biol* 716, 47-60.

Elbashir, S. M. *et al.* (2001). Duplexes of 21-nucleotide RNAs mediate RNA interference in cultured mammalian cells. *Nature* 411, 494-498.

Epstein, A. C. *et al.* (2001). C. elegans EGL-9 and mammalian homologs define a family of dioxygenases that regulate HIF by prolyl hydroxylation. *Cell* 107, 43-54.

Evan, G. I., Littlewood, T. D. (1993). The role of c-myc in cell growth. *Curr Opin Genet Dev* 3, 44-49.

Fink, D. *et al.* (1998). The role of DNA mismatch repair in drug resistance. *Clin Cancer Res* 4, 1-6.

Foreman, J. *et al.* (2003). Reactive oxygen species produced by NADPH oxidase regulate plant cell growth. *Nature* 422, 442-446.

Foyer, C. H., Noctor, G. (2005). Redox homeostasis and antioxidant signaling: a metabolic interface between stress perception and physiological responses. *Plant Cell* 17, 1866-1875.

Freeman, R. S. *et al.* (2003). SM-20, EGL-9, and the EGLN family of hypoxia-inducible factor prolyl hydroxylases. *Mol Cells* 16, 1-12.

Friedrich, G., Soriano, P. (1991). Promoter traps in embryonic stem cells: a genetic screen to identify and mutate developmental genes in mice. *Genes Dev* 5, 1513-1523.

Frohman, M. A. *et al.* (1988). Rapid production of full-length cDNAs from rare transcripts: amplification using a single gene-specific oligonucleotide primer. *Proc Natl Acad Sci U S A* 85, 8998-9002.

Garcia-Ruiz, C. *et al.* (1997). Direct effect of ceramide on the mitochondrial electron transport chain leads to generation of reactive oxygen species. Role of mitochondrial glutathione. *J Biol Chem* 272, 11369-11377.

Garrido, C. *et al.* (1999). HSP27 inhibits cytochrome c-dependent activation of procaspase-9. *FASEB J* 13, 2061-2070.

Gechev, T. S., Hille, J. (2005). Hydrogen peroxide as a signal controlling plant programmed cell death. *J Cell Biol* 168, 17-20.

Geiszt, M., Leto, T. L. (2004). The Nox family of NAD(P)H oxidases: host defense and beyond. *J Biol Chem* 279, 51715-51718.

Gorman, A. *et al.* (1997). Role of peroxide and superoxide anion during tumour cell apoptosis. *FEBS Lett* 404, 27-33.

Gossen, J. A. *et al.* (1993). Plasmid rescue from transgenic mouse DNA using LacI repressor protein conjugated to magnetic beads. *Biotechniques* 14, 624-629.

Gossler, A. *et al.* (1989). Mouse embryonic stem cells and reporter constructs to detect developmentally regulated genes. *Science* 244, 463-465.

Green, D. R., Reed, J. C. (1998). Mitochondria and apoptosis. *Science* 281, 1309-1312.

Guan, C. *et al.* (2010). A review of current large-scale mouse knockout efforts. *Genesis* 48, 73-85.

Gupta, R. S. (1983). Genetic, biochemical, and cross-resistance studies with mutants of Chinese hamster ovary cells resistant to the anticancer drugs, VM-26 and VP16-213. *Cancer Res* 43, 1568-1574.

Hannon, G. J. (2002). RNA interference. *Nature* 418, 244-251.

Harris, C. C., Hollstein, M. (1993). Clinical implications of the p53 tumor-suppressor gene. *N Engl J Med* 329, 1318-1327.

Helaakoski, T. *et al.* (1995). Cloning, baculovirus expression, and characterization of a second mouse prolyl 4-hydroxylase alpha-subunit isoform: formation of an alpha 2 beta 2 tetramer with the protein disulfide-isomerase/beta subunit. *Proc Natl Acad Sci U S A* 92, 4427-4431.

Helmbach, H. *et al.* (2002). Drug resistance towards etoposide and cisplatin in human melanoma cells is associated with drug-dependent apoptosis deficiency. *J Invest Dermatol* 118, 923-932.

Hengartner, M. O., Horvitz, H. R. (1994a). C. elegans cell survival gene ced-9 encodes a functional homolog of the mammalian proto-oncogene bcl-2. *Cell* 76, 665-676.

Hengartner, M. O., Horvitz, H. R. (1994b). Programmed cell death in Caenorhabditis elegans. *Curr Opin Genet Dev* 4, 581-586.

Henle, E. S., Linn, S. (1997). Formation, prevention, and repair of DNA damage by iron/hydrogen peroxide. *J Biol Chem* 272, 19095-19098.

Hicks, G. G. *et al.* (1991). Mutant p53 tumor suppressor alleles release ras-induced cell cycle growth arrest. *Mol Cell Biol* 11, 1344-1352.

Hicks, G. G. *et al.* (1995). Retrovirus gene traps. *Methods Enzymol* 254, 263-275.

Hicks, G. G. *et al.* (1997). Functional genomics in mice by tagged sequence mutagenesis. *Nat Genet* 16, 338-344.

Holliday, R., Ho, T. (1990). Evidence for allelic exclusion in Chinese hamster ovary cells. *New Biol* 2, 719-726.

Horvitz, H. R. *et al.* (1994). The genetics of programmed cell death in the nematode Caenorhabditis elegans. *Cold Spring Harb Symp Quant Biol* 59, 377-385.

Huang, D. C., Strasser, A. (2000). BH3-Only proteins-essential initiators of apoptotic cell death. *Cell* 103, 839-842.

Hubbard, S. C. *et al.* (1994). Generation of Chinese hamster ovary cell glycosylation mutants by retroviral insertional mutagenesis. Integration into a discrete locus generates mutants expressing high levels of N-glycolylneuraminic acid. *J Biol Chem* 269, 3717-3724.

Hunt, C. R. *et al.* (1998). Genomic instability and catalase gene amplification induced by chronic exposure to oxidative stress. *Cancer Res* 58, 3986-3992.

Hutcheson, D. A., Kardon, G. (2009). Genetic manipulations reveal dynamic cell and gene functions: Cre-ating a new view of myogenesis. *Cell Cycle* 8, 3675-3678.

Imlay, J. A., Linn, S. (1988). DNA damage and oxygen radical toxicity. *Science* 240, 1302-1309.

Ivan, M. *et al.* (2001). HIFalpha targeted for VHL-mediated destruction by proline hydroxylation: implications for O2 sensing. *Science* 292, 464-468.

Jaakkola, P. *et al.* (2001). Targeting of HIF-alpha to the von Hippel-Lindau ubiquitylation complex by O2-regulated prolyl hydroxylation. *Science* 292, 468-472.

Jackson, A. L., Loeb, L. A. (2000). Microsatellite instability induced by hydrogen peroxide in Escherichia coli. *Mutat Res* 447, 187-198.

Jackson, S. P. (1996). DNA damage detection by DNA dependent protein kinase and related enzymes. *Cancer Surv* 28, 261-279.

Jainchill, J. L. *et al.* (1969). Murine sarcoma and leukemia viruses: assay using clonal lines of contact-inhibited mouse cells. *J Virol* 4, 549-553.

Jao, L. E. *et al.* (2008). Using retroviruses as a mutagenesis tool to explore the zebrafish genome. *Brief Funct Genomic Proteomic* 7, 427-443.

Jeffers, J. R. *et al.* (2003). Puma is an essential mediator of p53-dependent and -independent apoptotic pathways. *Cancer Cell* 4, 321-328.

Kaelin, W. G. (2005). Proline hydroxylation and gene expression. *Annu Rev Biochem* 74, 115-128.

Kam, P. C., Ferch, N. I. (2000). Apoptosis: mechanisms and clinical implications. *Anaesthesia* 55, 1081-1093.

Karagiannis, T. C., El Osta, A. (2004). siRNAs: mechanism of RNA interference, in vivo and potential clinical applications. *Cancer Biol Ther* 3, 1069-1074.

Karpinich, N. O. *et al.* (2002). The course of etoposide-induced apoptosis from damage to DNA and p53 activation to mitochondrial release of cytochrome c. *J Biol Chem* 277, 16547-16552.

Keith, C. T., Schreiber, S. L. (1995). PIK-related kinases: DNA repair, recombination, and cell cycle checkpoints. *Science* 270, 50-51.

Keon, J. *et al.* (2003). A genomics approach to crop pest and disease research. *Pest Manag Sci* 59, 143-148.

Kivirikko, K. I., Myllyharju, J. (1998). Prolyl 4-hydroxylases and their protein disulfide isomerase subunit. *Matrix Biol* 16, 357-368.

Kivirikko, K. I., Pihlajaniemi, T. (1998). Collagen hydroxylases and the protein disulfide isomerase subunit of prolyl 4-hydroxylases. *Adv Enzymol Relat Areas Mol Biol* 72, 325-398.

Koike, K. *et al.* (1996). Overexpression of multidrug resistance protein gene in human cancer cell lines selected for drug resistance to epipodophyllotoxins. *Jpn J Cancer Res* 87, 765-772.

Kruman, I. *et al.* (1997). Evidence that 4-hydroxynonenal mediates oxidative stress-induced neuronal apoptosis. *J Neurosci* 17, 5089-5100.

Lage, H. *et al.* (1999). Expression of DNA repair proteins hMSH2, hMSH6, hMLH1, O6-methylguanine-DNA methyltransferase and N-methylpurine-DNA glycosylase in melanoma cells with acquired drug resistance. *Int J Cancer* 80, 744-750.

Lage, H. *et al.* (2000). Modulation of DNA topoisomerase II activity and expression in melanoma cells with acquired drug resistance. *Br J Cancer* 82, 488-491.

Lapierre, J. *et al.* (2011a). Potent and systematic RNAi mediated silencing with single oligonucleotide compounds. *RNA* 17, 1032-1037.

Lapierre, J. *et al.* (2011b). Potent and systematic RNAi mediated silencing with single oligonucleotide compounds. *RNA* 17, 1032-1037.

Lee, R. C. *et al.* (1993). The C. elegans heterochronic gene lin-4 encodes small RNAs with antisense complementarity to lin-14. *Cell* 75, 843-854.

Lewandoski, M. (2001). Conditional control of gene expression in the mouse. *Nat Rev Genet* 2, 743-755.

Li, J. *et al.* (2006). The NADPH oxidase NOX4 drives cardiac differentiation: Role in regulating cardiac transcription factors and MAP kinase activation. *Mol Biol Cell* 17, 3978-3988.

Loike, J. D., Horwitz, S. B. (1976). Effect of VP-16-213 on the intracellular degradation of DNA in HeLa cells. *Biochemistry* 15, 5443-5448.

Lopez-Lazaro, M. (2006). HIF-1: hypoxia-inducible factor or dysoxia-inducible factor? *FASEB J* 20, 828-832.

Lopez-Lazaro, M. (2007). Dual role of hydrogen peroxide in cancer: possible relevance to cancer chemoprevention and therapy. *Cancer Lett* 252, 1-8.

Maehara, Y. *et al.* (2000). Overexpression of the heat shock protein HSP70 family and p53 protein and prognosis for patients with gastric cancer. *Oncology* 58, 144-151.

Marks, D. I., Fox, R. M. (1991). DNA damage, poly (ADP-ribosyl)ation and apoptotic cell death as a potential common pathway of cytotoxic drug action. *Biochem Pharmacol* 42, 1859-1867.

Maury, J. J. *et al.* (2011). Technical advances to genetically engineering human embryonic stem cells. *Integr Biol (Camb)* 3, 717-723.

McClive, P. *et al.* (1998). Gene trap integrations expressed in the developing heart: insertion site affects splicing of the PT1-ATG vector. *Dev Dyn* 212, 267-276.

Meister, G., Tuschl, T. (2004). Mechanisms of gene silencing by double-stranded RNA. *Nature* 431, 343-349.

Mevorach, D. (2003). [Apoptosis: death is part of life]. *Harefuah* 142, 832-3, 878.

Mizumoto, K. *et al.* (1994). Programmed cell death (apoptosis) of mouse fibroblasts is induced by the topoisomerase II inhibitor etoposide. *Mol Pharmacol* 46, 890-895.

Montecucco, A., Biamonti, G. (2007). Cellular response to etoposide treatment. *Cancer Lett* 252, 9-18.

Moran, D. M. *et al.* (2009). Puromycin-based vectors promote a ROS-dependent recruitment of PML to nuclear inclusions enriched with HSP70 and Proteasomes. *BMC Cell Biol* 10, 32.

Mosmann, T. (1983). Rapid colorimetric assay for cellular growth and survival: application to proliferation and cytotoxicity assays. *J Immunol Methods* 65, 55-63.

Motulsky HJ. Regression Guide. 1-294. 2007.

Ref Type: Generic

Motuslky HJ. Statistics Guide. 1-255. 2007.

Ref Type: Generic

Munster, P. N. *et al.* (2001). Modulation of Hsp90 function by ansamycins sensitizes breast cancer cells to chemotherapy-induced apoptosis in an RB- and schedule-dependent manner. See: E. A. Sausville, Combining cytotoxics and 17-allylamino, 17-demethoxygeldanamycin: sequence and tumor biology matters, Clin. Cancer Res., 7: 2155-2158, 2001. *Clin Cancer Res* 7, 2228-2236.

Myllyharju, J. (2003). Prolyl 4-hydroxylases, the key enzymes of collagen biosynthesis. *Matrix Biol* 22, 15-24.

Myllyharju, J., Kivirikko, K. I. (2001). Collagens and collagen-related diseases. *Ann Med* 33, 7-21.

Nieminen, A. L. *et al.* (1997). Mitochondrial permeability transition in hepatocytes induced by t-BuOOH: NAD(P)H and reactive oxygen species. *Am J Physiol* 272, C1286-C1294.

Nishi, H. *et al.* (2004). Hypoxia-inducible factor 1 mediates upregulation of telomerase (hTERT). *Mol Cell Biol* 24, 6076-6083.

Niwa, H. *et al.* (1993). An efficient gene-trap method using poly A trap vectors and characterization of gene-trap events. *J Biochem* 113, 343-349.

Nyaho JKC. Characterization Of The Etoposide-Resistant Cell Line CHO E-126. M.Sc.Thesis , 1-103. 8-20-2003.

Ref Type: Generic

O'Kane, C. J., Gehring, W. J. (1987). Detection in situ of genomic regulatory elements in Drosophila. *Proc Natl Acad Sci U S A* 84, 9123-9127.

Oltvai, Z. N., Korsmeyer, S. J. (1994). Checkpoints of dueling dimers foil death wishes. *Cell* 79, 189-192.

Osipovich, A. B. *et al.* (2004). Activation of cryptic 3' splice sites within introns of cellular genes following gene entrapment. *Nucleic Acids Res* 32, 2912-2924.

Park, H. S. *et al.* (2004). Sequential activation of phosphatidylinositol 3-kinase, beta Pix, Rac1, and Nox1 in growth factor-induced production of H2O2. *Mol Cell Biol* 24, 4384-4394.

Park, S. *et al.* (2005). Substantial DNA damage from submicromolar intracellular hydrogen peroxide detected in Hpx- mutants of Escherichia coli. *Proc Natl Acad Sci U S A* 102, 9317-9322.

Pathak, V. K., Temin, H. M. (1990). Broad spectrum of in vivo forward mutations, hypermutations, and mutational hotspots in a retroviral shuttle vector after a single replication cycle: substitutions, frameshifts, and hypermutations. *Proc Natl Acad Sci U S A* 87, 6019-6023.

Pericone, C. D. *et al.* (2002). Short-sequence tandem and nontandem DNA repeats and endogenous hydrogen peroxide production contribute to genetic instability of Streptococcus pneumoniae. *J Bacteriol* 184, 4392-4399.

Persengiev, S. P. *et al.* (2004). Nonspecific, concentration-dependent stimulation and repression of mammalian gene expression by small interfering RNAs (siRNAs). *RNA* 10, 12-18.

Rao, D. D. *et al.* (2009a). Comparative assessment of siRNA and shRNA off target effects: what is slowing clinical development. *Cancer Gene Ther* 16, 807-809.

Rao, D. D. *et al.* (2009b). siRNA vs. shRNA: similarities and differences. *Adv Drug Deliv Rev* 61, 746-759.

Realini, C. A., Althaus, F. R. (1992). Histone shuttling by poly(ADP-ribosylation). *J Biol Chem* 267, 18858-18865.

Roshon, M. *et al.* (2003). Gene trap mutagenesis of hnRNP A2/B1: a cryptic 3' splice site in the neomycin resistance gene allows continued expression of the disrupted cellular gene. *BMC Genomics* 4, 2.

Ross, J. S. *et al.* (2007). miRNA: the new gene silencer. *Am J Clin Pathol* 128, 830-836.

Sablina, A. A. *et al.* (2005). The antioxidant function of the p53 tumor suppressor. *Nat Med* 11, 1306-1313.

Saintigny, Y. *et al.* (2002). Homologous recombination resolution defect in werner syndrome. *Mol Cell Biol* 22, 6971-6978.

Salvesen, G. S., Duckett, C. S. (2002). IAP proteins: blocking the road to death's door. *Nat Rev Mol Cell Biol* 3, 401-410.

Sambrook J, Russell DW. *Molecular cloning*

a laboratory manual, 3rd ed Edition, Cold Spring Harbor, N.Y: Cold Spring Harbor Laboratory Press, 2001.

Sauer, H. *et al.* (2000). Role of reactive oxygen species and phosphatidylinositol 3-kinase in cardiomyocyte differentiation of embryonic stem cells. *FEBS Lett* 476, 218-223.

Sawada, M. *et al.* (2001). p53 regulates ceramide formation by neutral sphingomyelinase through reactive oxygen species in human glioma cells. *Oncogene* 20, 1368-1378.

Semenza, G. L. (2003). Targeting HIF-1 for cancer therapy. *Nat Rev Cancer* 3, 721-732.

Semenza, G. L. (2006). Development of novel therapeutic strategies that target HIF-1. *Expert Opin Ther Targets* 10, 267-280.

Semizarov, D. *et al.* (2003). Specificity of short interfering RNA determined through gene expression signatures. *Proc Natl Acad Sci U S A* 100, 6347-6352.

Shiozaki, E. N., Shi, Y. (2004). Caspases, IAPs and Smac/DIABLO: mechanisms from structural biology. *Trends Biochem Sci* 29, 486-494.

Silver, J., Keerikatte, V. (1989). Novel use of polymerase chain reaction to amplify cellular DNA adjacent to an integrated provirus. *J Virol* 63, 1924-1928.

Siminovitch, L. (1976). On the nature of hereditable variation in cultured somatic cells. *Cell* 7, 1-11.

Slevin, M. L. (1991). The clinical pharmacology of etoposide. *Cancer* 67, 319-329.

Sliva, K., Schnierle, B. S. (2010). Selective gene silencing by viral delivery of short hairpin RNA. *Virol J* 7, 248.

Sordet, O. *et al.* (2003). Apoptosis induced by topoisomerase inhibitors. *Curr Med Chem Anticancer Agents* 3, 271-290.

Stanford, W. L. *et al.* (2001). Gene-trap mutagenesis: past, present and beyond. *Nat Rev Genet* 2, 756-768.

Stewart, B. W. (1994). Mechanisms of apoptosis: integration of genetic, biochemical, and cellular indicators. *J Natl Cancer Inst* 86, 1286-1296.

Strasser, A. *et al.* (1995). Bcl-2 and Fas/APO-1 regulate distinct pathways to lymphocyte apoptosis. *EMBO J* 14, 6136-6147.

Straub, J. A. *et al.* (2003). Induction of SM-20 in PC12 cells leads to increased cytochrome c levels, accumulation of cytochrome c in the cytosol, and caspase-dependent cell death. *J Neurochem* 85, 318-328.

Takano, H. *et al.* (1991). Increased phosphorylation of DNA topoisomerase II in etoposide-resistant mutants of human cancer KB cells. *Cancer Res* 51, 3951-3957.

Tanaka, T. *et al.* (2007). Induction of ATM activation, histone H2AX phosphorylation and apoptosis by etoposide: relation to cell cycle phase. *Cell Cycle* 6, 371-376.

Theard, D. *et al.* (2001). Etoposide and adriamycin but not genistein can activate the checkpoint kinase Chk2 independently of ATM/ATR. *Biochem Biophys Res Commun* 289, 1199-1204.

Toman, R. E. *et al.* (2002). Ceramide-induced cell death in primary neuronal cultures: upregulation of ceramide levels during neuronal apoptosis. *J Neurosci Res* 68, 323-330.

Tyurina, Y. Y. *et al.* (2004). Lipid antioxidant, etoposide, inhibits phosphatidylserine externalization and macrophage clearance of apoptotic cells by preventing phosphatidylserine oxidation. *J Biol Chem* 279, 6056-6064.

Ulukaya, E. *et al.* (2008). The MTT assay yields a relatively lower result of growth inhibition than the ATP assay depending on the chemotherapeutic drugs tested. *Toxicol In Vitro* 22, 232-239.

Ushio-Fukai, M. (2006). Redox signaling in angiogenesis: role of NADPH oxidase. *Cardiovasc Res* 71, 226-235.

van Maanen, J. M. *et al.* (1988). Mechanism of action of antitumor drug etoposide: a review. *J Natl Cancer Inst* 80, 1526-1533.

Veal, E. A. *et al.* (2007). Hydrogen peroxide sensing and signaling. *Mol Cell* 26, 1-14.

Vilain, N. *et al.* (2003). Modulation of drug sensitivity in yeast cells by the ATP-binding domain of human DNA topoisomerase IIalpha. *Nucleic Acids Res* 31, 5714-5722.

Wang, J. C. (1996). DNA topoisomerases. *Annu Rev Biochem* 65, 635-692.

Wang, L., Wang, Z. Y. (2010). The Wilms' tumor suppressor WT1 induces estrogen-independent growth and anti-estrogen insensitivity in ER-positive breast cancer MCF7 cells. *Oncol Rep* 23, 1109-1117.

Wataba, K. *et al.* (2001). Over-expression of heat shock proteins in carcinogenic endometrium. *Int J Cancer* 91, 448-456.

Weisenthal, L. M. *et al.* (1983). Comparison of dye exclusion assays with a clonogenic assay in the determination of drug-induced cytotoxicity. *Cancer Res* 43, 258-264.

Wiles, M. V. *et al.* (2000). Establishment of a gene-trap sequence tag library to generate mutant mice from embryonic stem cells. *Nat Genet* 24, 13-14.

Wilson, C. *et al.* (1989). P-element-mediated enhancer detection: an efficient method for isolating and characterizing developmentally regulated genes in Drosophila. *Genes Dev* 3, 1301-1313.

Winter, A. D., Page, A. P. (2000). Prolyl 4-hydroxylase is an essential procollagen-modifying enzyme required for exoskeleton formation and the maintenance of body shape in the nematode Caenorhabditis elegans. *Mol Cell Biol* 20, 4084-4093.

Withers-Ward, E. S. *et al.* (1994). Distribution of targets for avian retrovirus DNA integration in vivo. *Genes Dev* 8, 1473-1487.

Wyllie, A. H. (1997). Apoptosis: an overview. *Br Med Bull* 53, 451-465.

Yang, D. *et al.* (2002). Short RNA duplexes produced by hydrolysis with Escherichia coli RNase III mediate effective RNA interference in mammalian cells. *Proc Natl Acad Sci U S A* 99, 9942-9947.

Yonish-Rouach, E. *et al.* (1991). Wild-type p53 induces apoptosis of myeloid leukaemic cells that is inhibited by interleukin-6. *Nature* 352, 345-347.

Yu, J. Y. *et al.* (2002). RNA interference by expression of short-interfering RNAs and hairpin RNAs in mammalian cells. *Proc Natl Acad Sci U S A* 99, 6047-6052.

Zakian, V. A. (1995). ATM-related genes: what do they tell us about functions of the human gene? *Cell* 82, 685-687.

Zambrowicz, B. P. *et al.* (1998). Disruption and sequence identification of 2,000 genes in mouse embryonic stem cells. *Nature* 392, 608-611.

Zamore, P. D. *et al.* (2000). RNAi: double-stranded RNA directs the ATP-dependent cleavage of mRNA at 21 to 23 nucleotide intervals. *Cell* 101, 25-33.

Zhang, H. *et al.* (1990). A model for tumor cell killing by topoisomerase poisons. *Cancer Cells* 2, 23-27.

Zhang, X. L. *et al.* (2011). Activation of hypoxia-inducible factor-1 ameliorates postischemic renal injury via inducible nitric oxide synthase. *Mol Cell Biochem* .

Zuryn, S. *et al.* (2010). A strategy for direct mapping and identification of mutations by whole-genome sequencing. *Genetics* 186, 427-430.